



# Detection and counting of Powered Two Wheelers in traffic using a single-plane Laser Scanner

Yadu Prabhakar

## ► To cite this version:

Yadu Prabhakar. Detection and counting of Powered Two Wheelers in traffic using a single-plane Laser Scanner. Computer Science [cs]. INSA de Rouen, 2013. English. NNT : 2013ISAM0033 . tel-00973472

**HAL Id: tel-00973472**

**<https://theses.hal.science/tel-00973472>**

Submitted on 4 Apr 2014

**HAL** is a multi-disciplinary open access archive for the deposit and dissemination of scientific research documents, whether they are published or not. The documents may come from teaching and research institutions in France or abroad, or from public or private research centers.

L'archive ouverte pluridisciplinaire **HAL**, est destinée au dépôt et à la diffusion de documents scientifiques de niveau recherche, publiés ou non, émanant des établissements d'enseignement et de recherche français ou étrangers, des laboratoires publics ou privés.



**Normandy University**  
**National Institute of Applied Sciences of Rouen**  
**Computer Science, Information Processing and Systems Laboratory**

Doctorate Thesis  
Major: Signal and Image Processing

A Dissertation Presented by  
**Yadu PRABHAKAR**

Submitted for the fulfilment to obtain the degree of  
DOCTOR of Normandy University  
INSA of Rouen

**Detection and counting of Powered Two Wheelers in traffic using a single-plane Laser Scanner**

<b>François Goulette</b>	Professor, MINES ParisTech, CAOR	<b>Reviewer</b>
<b>Jack-Gérard Postaire</b>	Emeritus Professor, University of Lille1, LAGIS	<b>Reviewer</b>
<b>Fawzi Nashashibi</b>	Researcher HDR, INRIA-IMARA	<b>Examiner</b>
<b>Jean-Philippe Tarel</b>	Researcher, IFSTTAR, COSYS	<b>Examiner</b>
<b>Abdelaziz Bensrhair</b>	Professor, INSA of Rouen, LITIS	<b>Thesis Director</b>
<b>Christèle Lecomte</b>	Assistant Professor, University of Rouen, LITIS	<b>Supervisor</b>
<b>Peggy Subirats</b>	Doctor Engineer, CETE NC, ERA34	<b>Supervisor</b>
<b>Eric Violette</b>	Road safety expert, CETE NC, ERA34	<b>Guest</b>





# Glossary

---

PTW: Powered Two Wheelers

LV: Light Vehicle

HV: Heavy Vehicle

ANR: National Research Agency (*In French*: Agence Nationale de la Recherche)

METRAMoto: Powered Two Wheeler traffic measurement for road safety and risk assessment (*In French*: **ME**sure du **TRA**fic de deux roues **MOTO**risés) website: [www.project-metromoto.fr](http://www.project-metromoto.fr)

ONISR: National Joint Ministerial Road Safety Observatory, (*In French*: Observatoire National Interministériel de la Sécurité Routière)

CERTU: Centre d'Etudes sur les Réseaux, les Transports, l'Urbanisme et les constructions

CETE: Public Works Centre for Technical Studies (*In French*: Centre d'étude techniques et l'équipement)

SETRA: Study Center for Transports and Roads (*In French*: Service d'Etudes sur les Transports, les Routes et leurs Aménagements)

ALS: Airborne Laser Scanning

SLAM: Simultaneous Localisation and Mapping

LMS: Laser Measurement System

SVM: Support Vector Machine

LLC: Last Line Check

*a*: All symbols in italics are the variables used in the equations

[#]: Reference to bibliography

(#): Reference to equation





# Detection and counting of Powered two wheelers in traffic using a single-plane Laser Scanner

By  
Yadu PRABHAKAR

---

## Abstract:

The safety of Powered Two Wheelers (PTWs) is important for public authorities and road administrators around the world. Recent official figures show that PTWs are estimated to represent only 2% of the total traffic but represent 30% of total deaths on French roads. However, as these estimated figures are obtained by simply counting the number plates registered, they do not give a true picture of the PTWs on the road at any given moment. To date, there is no overall solution to this problem that uses a single sensor capable of detecting PTWs and taking into consideration their interaction with the other vehicles on the road (for example: Inter-lane traffic, when PTWs travel between two lanes on a highway), and no state-of-the-art technical solutions can be adapted to measure this category of vehicle in traffic (unlike Light Vehicles (LVs) and Heavy Vehicles (HVs)). The research work in this domain has not, therefore, been greatly developed.

This is an issue of concern and gave rise to the launch of the ANR Project METRAMOTO (**ME**sure du **TRA**fic des deux roues **MOTO**risés pour la sécurité routière et l'évaluation des risques / Powered Two Wheeler traffic measurement for road safety and risk assessment). This project started in November 2010 and explores four technologies to measure the PTW traffic: Intrusive technology with piezo-electric sensors and magnetometers and Non Intrusive technology with a vision camera and a laser scanner. For this research work, a non-intrusive technology, particularly a laser scanner has been chosen. Hence the title "Detection and counting of PTWs in real time traffic using a single-plane laser scanner".

This dissertation is a technical applied research work and deals with two problems: detection of PTWs and the use of a laser scanner to count PTWs in the traffic. These two problems have not often been explored. Traffic generally contains random vehicles of unknown nature and behaviour such as speed, vehicle interaction with other users on the road etc. Even though there are several technologies that can measure traffic, for example radars, cameras, magnetometers etc, as the PTWs are small-sized vehicles, they often move in between lanes and at quite a high speed compared to the vehicles moving in the adjacent lanes. This makes them difficult to detect.

The main objective of this technical research work is to propose a prototype that can detect and count the PTWs in the traffic. This prototype is meant to be integrated into a system that can be easily installed on a highway and is able to detect and count PTWs in real-time. Ideally the system should be self-calibrating with respect to the installation site and be able to work autonomously on road for a long duration of time.

Moreover, laser scanner technology has not often been explored independently for the detection and counting of traffic on a highway. Usually this technology is used at automatic toll plazas to classify vehicles that are travelling slowly. At each lane, one laser scanner is installed and to make this technology more effective, it is combined with another technology such as cameras or other laser

scanners. Our goal is to detect PTWs from a single-plane laser scanner placed on a pole or a gantry at a certain height, with the vehicles passing at various speeds on the road below it.

In the framework of METRAMOTO, the proposed solution in this research work is intended to be installed on a highway to detect, extract, classify and count PTWs in real time under all traffic conditions (traffic at normal speeds, dense traffic and even traffic jams). Hence, the final system must be as automatic as possible so that the road administrators can simply install it on any road (motorway, expressway) with a very little intervention.

The developed method is composed of the following parts: a configuration to install the laser scanner on the road is chosen and a data coherence method is introduced so that the system is able to detect the road verges and its own height above the road surface. This is validated by simulator. Then the raw data obtained is pre-processed and is transform into the spatial temporal domain. Following this, an extraction algorithm called the Last Line Check (LLC) method is proposed. Once extracted, the object is classified using one of the two classifiers either the Support Vector Machine (SVM) or the k-Nearest Neighbour (KNN). At the end, the results given by each of the two classifiers are compared and presented in this research work. For the present research work a prototype has been developed and tested on real traffic of unknown behaviour.

# Détection des deux roues motorisés par télémétrie laser à balayage

Auteur:

Yadu PRABHAKAR

---

Résumé:

La sécurité des deux-roues motorisés (2RM) constitue un enjeu essentiel pour les pouvoirs publics et les gestionnaires routiers. Si globalement, l'insécurité routière diminue sensiblement depuis 2002, la part relative des accidents impliquant les 2RM a tendance à augmenter. Ce constat est résumé par les chiffres suivants : les 2RM représentent environ 2 % du trafic et 30 % des tués sur les routes. Le risque d'être tué en moto est 24 fois supérieur à celui des automobilistes. On observe depuis plusieurs années une augmentation du parc des 2RM et pourtant il manque des données et des informations sur ce mode de transport, ainsi que sur les interactions des 2RM avec les autres usagers et l'infrastructure routière. Un état de l'art effectué en 2009 a montré qu'il n'existe pas de solution technique adaptée à la mesure du trafic de cette catégorie de véhicule (contrairement aux véhicules légers et aux poids lourds) et la recherche/développement dans ce domaine est peu active.

A partir des données précédentes, le projet **ANR METRAMOTO (ME**sure des **TRA**ffics des deux roues **MOTO**risés) qui est labellisé Move'o a été lancé en Novembre 2010. Ce projet explore quatre technologies : la technologie intrusive avec les capteurs hybride et magnétomètres ; la technologie non-intrusive avec les capteurs vidéo et un scanner laser. Le but de ce projet est d'une part, de développer des outils pour détecter et compter les 2RM dans le trafic afin de produire des mesures pouvant être utilisées pour établir des statistiques relatives à la circulation des 2RM et d'autre part d'identifier les trajectoires des 2RM pour analyser les interactions avec les autres véhicules. Ces objectifs concernent à la fois la mobilité, l'exploitation de la route et la sécurité routière. Pour ces travaux de thèse, j'ai choisi un télémètre laser à balayage (scanner laser). Donc l'intitulé de cette recherche est « La détection des deux roues motorisés par télémétrie laser à balayage ».

Ce travail de recherche effectué dans cette thèse appliquée est divisé en deux parties : la détection des 2RM et la détection des objets routiers par scanner laser. Le trafic routier en général contient des véhicules de nature et comportement inconnus, par exemple leurs vitesses, leurs trajectoires et leurs interactions avec les autres usagers de la route. Malgré plusieurs technologies pour mesurer le trafic, par exemple les radars ou les boucles électromagnétiques, on est incapable de détecter les 2RM à cause de leurs petits gabarits leur permettant de circuler à vitesse élevée et ce même en interfile.

De plus, la technologie scanner laser n'est pas beaucoup explorée indépendamment pour détecter et compter les véhicules sur les routes urbaines ou autoroutes. On peut souvent trouver cette technologie sur les péages automatiques, lieu où la vitesse des véhicules n'est pas élevée. La plupart du temps, un scanner laser est fusionné avec une camera (ou un autre scanner laser) et le système est installé sur chaque voie de circulation, ce qui rend l'ensemble très cher. Notre but est de détecter et compter les 2RM en utilisant un scanner laser mono nappe qui peut être installé sur un poteau ou sous un pont d'une hauteur quelconque.

Dans le cadre du projet METRAMOTO, la solution proposée peut être intégrée dans un système qui serait installé sur une route au trafic aléatoire (dense, fluide, bouchons) pour détecter et compter des

2RM en temps réel. Donc le système doit être le plus autonome possible pour que les gestionnaires de route puissent le poser en toute simplicité sur la route.

La méthode développée est composée de plusieurs sous-parties: Choisir une configuration optimale du scanner laser afin de l'installer sur la route. Ensuite une méthode de mise en correspondance est proposée pour trouver la hauteur et les bords de la route. Le choix d'installation est validé par un simulateur. A ces données brutes, la méthode de prétraitement est implémentée et une transformation de ces données dans le domaine spatio-temporel est faite. Après cette étape de prétraitement, la méthode d'extraction nommée 'Last Line Check (LLC)' est appliquée. Une fois que le véhicule est extrait, il est classifié avec un SVM et un KNN. Ensuite un compteur est mis en œuvre pour compter les véhicules classifiés. A la fin, une comparaison de la performance de chacun de ces deux classifieurs est réalisée. La méthode proposée reste un prototype et est testée sur les données télématiques du trafic réel.

*This dissertation is dedicated to my family whom I owe  
everything and my beautiful wife, Néha*

*I love you all*



# Acknowledgements

---

I would like to express my gratitude to a lot of people without whom this dissertation would not be possible. Some were there since the beginning while some joined me during this journey. My first and the foremost thanks to my parents Arun Kumar Prabhakar and Rekha Prabhakar, my sister Raagini Prabhakar, who stood beside me every single day, made me feel that nothing is impossible.

I feel myself lucky and wish to thank Pr. Abdelaziz Bensrhair for being my thesis director, for guiding me at every path and for sharing his experience that gave me a new vision to see, understand and dig further during my PhD life at LITIS of INSA of Rouen. My special thanks, Dr. Christèle Lecomte, my PhD guide, who always supported me, at every moment during these 3 years and guided me through it. This research work gave me an opportunity to equally understand the technical world. I would thank Mr. Eric Violette, who is also the team leader of ERA34, for guiding me and sharing his invaluable expertises thereby enriching my work.

I would like to warmly thank Pr. Jack-G  rald Postaire and Pr. Fran  ois Goulette who accepted to review my thesis report as well as Dr. Fawzi Nashashibi and Dr. Jean-Philippe Tarel to be examiners for this work.

I wish to extend my sincere thanks Dr. Damien Vivet who really helped me during this work by sharing his experience and knowledge thus giving a new outlook to my work. You were really my second guide for this PhD work. My sincere thanks to Ms. Dilys Mascoto who helped me in putting my ideas in a better way during all my written work and yes, I did need your guidance to express myself better. My special gratitude to Pr. Didier Aubert, Pr. Laurent Trassoudiane and Dr. Nicolas Hautiere for being present and for sharing their invaluable experiences.

My special thanks to the Region of Upper Normandy and the IFSTTAR for trusting me and financing my work. I would like to acknowledge other members of the consortium of project METRAMOTO, especially to Ms. Christina BURAGA of CETE M  diterran   for being present and organising all the experimental evaluations for my research work. All these experimentations and tests would not have been possible without the help of Mr. David Doucet and Mr. Lucien Di Giacomo. A special thanks to Ms. Peggy Subirats for organizing these experimentations with the other members of METRAMOTO.

I shared good moments working at LITIS and CETE NC. My special thanks to Dr. Samia Ainouz, Dr. Katherine Romeo, Ms. Elsa Planterose, Pr. Pascal Vasseur, Dr. Stephane Mousset, Dr. Sebastain Kramm for listening and advising me whenever I needed.

I cannot forget all the joyful moments that I shared with all the members of CETE NC. My thanks to Mr. Jean-Yves Lebourg, Ms. Lucie Groult, Ms. Francine Gigon, Mr. Cyrille Lelez, Mr. Olivier Bisson and Mr. Alexandre Hublert for their kind support and for being present for all this time.

My special thanks with no goodbye, having unforgettable joyful memories with all my friends and pals Amnir Hadachi, Alina Miron, Laura Guilani, Amelie Dewlie, Romain Desormeaux, Julien Legallic, Ovidius Serban, Nadine Salameh, Nawal Alioua, Zakariae Bram, Rawia Mhiri and Fan Wang.

All my thanks to the administrative and technical staff of LITIS-INSA of Rouen and CETE NC, Especially Ms. Brigitte Diarra, Ms. Sandra Hauges, Ms. Marie-Christine Corniere, Mr. Jean-Fran  ois Brulard and Mr. Fabrice Hertel for their availabilities during all these years.





## Index

General Introduction .....	1
CHAPTER 1: Motivation and Overview .....	5
Introduction .....	7
1.1. Problem statement .....	7
1.1.1. Evolution in the number of PTWs .....	7
1.1.2. PTW Accidents .....	8
1.1.3. Difficulties in detecting PTWs.....	9
1.2. Projects related to PTW safety .....	10
1.3. METRAMOTO .....	11
1.3.1. Comparison of technologies .....	13
1.3.2. Choice of the technology .....	14
1.4. Research work done for the detection of PTWs .....	14
1.4.1. Definition of a PTW.....	14
1.4.2. Existing solutions.....	15
1.5. Research work done to date for laser scanners.....	18
1.5.1. Principles and techniques.....	18
1.5.2. Applications .....	22
Conclusion.....	27
CHAPTER 2: Data Acquisition .....	29
Introduction .....	31
2.1. Simulator .....	31
2.1.1. Problem statement.....	32
2.1.2. Different configurations.....	33
2.1.3. Description.....	34
2.1.4. Discussion.....	37
2.1.5. Demonstration.....	38
2.1.6. Solution proposed .....	41
2.2. Choice of a laser scanner .....	41
2.3. Road profile .....	44
2.4. Different positions for the laser scanner.....	45
2.5. Data coherence method .....	49
2.5.1. Height.....	49
2.5.2. Road verges.....	50

2.6. Databases .....	51
2.6.1. Controlled site .....	51
2.6.2. Real sites .....	53
Conclusion .....	57
CHAPTER 3: Extraction and classification .....	59
Introduction .....	61
3.1. Pre-processing .....	62
3.1.1. Signal rectification .....	62
3.1.2. Transformation into a spatio-temporal domain.....	68
3.2. Extraction process.....	71
3.2.1. Last Line Check .....	71
3.2.2. Vehicle counter .....	73
3.3. Classification .....	74
3.3.1. Choice of parameters .....	77
3.3.2. Support Vector Machine (SVM).....	81
3.3.3. K Nearest Neighbour (KNN) .....	81
3.3.4. Learning data set .....	82
3.4. Implementation of the method.....	83
Conclusion .....	86
CHAPTER 4: Results and discussions .....	89
Introduction .....	91
4.1. Controlled site.....	91
4.2. Real Site SUDIII.....	96
4.2.1. SVM Results .....	96
4.2.2. KNN Results .....	102
4.3. Real Site Motor way A13 .....	107
4.3.1. SVM.....	108
4.3.2. KNN.....	108
Conclusion .....	110
Conclusion and Perspectives .....	113
List of Publications.....	117
ANNEX 1 .....	119
Bibliography.....	121

## Figures

Figure 1: Overview of the thesis by chapters .....	3
Figure 2: Increase in the number of PTWs (>50cm3) [ONSIR11] .....	7
Figure 3: The death rate and the traffic of each category of vehicle [ONSIR11].....	8
Figure 4: PTW mortality rate: relation with the climate and accident rate .....	9
Figure 5: Time of Flight principle. $d$ is the distance [COLV11].....	19
Figure 6: Different acquisition applications [BERG04][FUMA11].....	20
Figure 7: Example of classical PTW inter-lane traffic .....	31
Figure 8: Occlusion of a PTW by an HV .....	32
Figure 9: Calculation of shadow.....	33
Figure 10: Simulated carriageway (Left) 2-lane and (Right) 3-lane .....	33
Figure 11: Example of different possible ways to mount a single laser scanner on a gantry when we have 3 lanes .....	34
Figure 12: Simulated example of the segment .....	36
Figure 13: An example of the cases simulated. (Above) Laser scanner position represented in red box. (Below) corresponding simulator scenes.....	37
Figure 14: Simulator.....	37
Figure 15: Two lanes simulation with inter-lane traffic .....	39
Figure 16: Case 3 simulated data.....	40
Figure 17: Optimal solution for two and three lanes.....	41
Figure 18: Relationship between speed (0km/h to 150 km/h) of PTW and number of scans. Red line corresponds to the limit of the data acquisition (2 scans) for a PTW with a length of 2m. ....	42
Figure 19: LMS SICK 111(Left). Installation of the laser scanner on the experimental site (Right) ...	43
Figure 20: Distance between measured points [SICK08] .....	44
Figure 21: A simulated scene. Laser scanner installed at height $h$ and above the centre point between two lanes. Each lane measures $L$ metres. ....	44
Figure 23: Possible configuration: 1. Roadside mast-mounted 2. Gantry or under the bridge 3. Cross-fire .....	45
Figure 22: Empty scan.....	45
Figure 24: (Left) System installed on the site of IFSTTAR Nantes. (Right) A close up of the system (Gantry configuration).....	46
Figure 25: Configured images. (Left) Roadside mast-mounted: Laser scanner installed at the roadside. (Right) Gantry: Laser scanner placed above the traffic.....	46
Figure 26: Three different projection angles. From left to right: $0^\circ$ , $60^\circ$ and $77^\circ$ .....	47
Figure 27: Configuration $60^\circ$ (Left). Configuration $77^\circ$ (Right).....	48
Figure 28: Mixed pixels [DIET01].....	48
Figure 29: Empty scan.....	49
Figure 30: Beam projection.....	50
Figure 31: Beam diameter and distance between two measured points [BENJ08] .....	50
Figure 32: Our controlled experimental site.....	52
Figure 33: A visual example of the cases discussed above and used create the database. ....	52
Figure 34: SUDIII: A view of the Highway.....	53
Figure 35: The installation site. Pink arrow, the insertion path; Blue arrow, the deceleration lane. Zoom: Green line, at a right angle to the road; Red line, the bridge. (Google Maps). ....	54
Figure 36: Reconstructed scene of the site. The laser scanner is installed at 6.3m above the second lane .....	54
Figure 37: Distribution of vehicles of different colour present in the scene. <i>Others</i> corresponds to orange, green, yellow etc.....	55

Figure 38: Experimental Site A13 .....	56
Figure 39: An overview of our system .....	61
Figure 40: (Left) An example of the scene when a vehicle passes below the laser scanner. (Right).The raw data in polar coordinates with the vehicle shown in green and the environment (trees, pole etc.) in red.....	62
Figure 41: Example of a data array (scan).....	63
Figure 42: (Left) Image representing a motorbike passing below a unit (Middle) An example of accumulation of data. in 2D. (Right) The reconstructed data in 3D; X_axis: Accumulation of scans, Y_axis: height of the vehicle and Z_axis: Scan points representing the road (Hidden).....	64
Figure 43: Principle of checking the neighbourhood. In blue are the values representing a vehicle while in grey are the non-observed values. Extreme points in black. ....	65
Figure 44: 'fill' filter (w.r.t : with respect to).....	66
Figure 45: Deformed information at the corner. $\alpha$ is the transversal inclination angle of the road.....	67
Figure 46: Pre-processing of the raw data. ....	68
Figure 47: Spatio-temporal domain: accumulation of p scans, a 2D reconstruction and the view from above. ....	68
Figure 48: Inverted image, Shadows (non observed zones) in dark red around the vehicles.....	69
Figure 50: When the object is exactly below the laser scanner (Left). Zone 1 and Zone 2 correspond to the 'shadowy' zones. When the objects are at border of the region of interest (Right), complete shadow or partial shadow is cast outside this zone. Hence the exact length of the non-observed zone cannot be estimated.....	70
Figure 49: Shadows .....	70
Figure 51: Laser scanner partially falling on the object. E is the error. ....	70
Figure 52: (Left) Vehicle entering the scene. (Right) Intensity (height) representation of the scan. ....	72
Figure 53: Illustration of the LLC method: (Left): 2 vehicles entering the scene. (Right) One vehicle completely entered and extracted boxed in red. ....	72
Figure 54: Flowchart describing the LLC method's working principle at an instant t .....	73
Figure 55: Example of a decision tree over five objects a,b,c,d,e. The points m,n,p,q are the nodes of the tree. The discontinuous line indicated the level below which we can define three classes [FLAM11] .....	75
Figure 56: A PTW at different speeds varying from 20km/h up to 90 km/h.....	77
Figure 57: Left: LV at 50 km/h with a Height sum of 8.89e5. Right: PTW with a Height sum of 1.92e5. ....	78
Figure 58: Left: An LV raw image, after filtering and the region growing. Right: a PTW: similar processing.....	79
Figure 59: Height normalized by Nbx.....	79
Figure 60: Comparison plots of different parameters.....	80
Figure 61: Final overview of the system.....	83
Figure 62: Empty scan on the left and the corresponding image on the right.....	84
Figure 63: Empty scan with the interval of values were probability to find the correct height is maximum.....	84
Figure 64: Image formed by the accumulation of scans.....	85
Figure 65: (Left) After applying the fill filter. (Right) After changing the coordinate system. ....	85
Figure 66: Vehicles extracted through LLC and their corresponding real images .....	86
Figure 67: Scenes recorded with a camera installed next to the laser scanner, and results obtained after application of our method to these different scenes. ....	92
Figure 68: Scenes recorded with a camera installed next to the laser scanner, and results obtained after application of our method to these different scenes .....	93

Figure 69: 3D and 2D views of the semi-Cartesian coordinates .....	94
Figure 70: Cartesian coordinates .....	95
Figure 71: Site SUDIII .....	96
Figure 72: Missed LVs due to occlusion.....	97
Figure 73: The original scene and the vehicle passed under the scanner. The red dot is where the laser scanner is placed. Yellow line is the line of tolerance.....	99
Figure 74: Width .....	99
Figure 75: Vehicles passing through the zone of confidence (SVM (width)). .....	100
Figure 76: Linear separation: Width to Height to number of scans. PTW in green and others in Red. ....	101
Figure 77: Vehicles passing through the zone of confidence (SVM2 (width+H_Nbx)). .....	102
Figure 78: Case when the PTW is not detected.....	103
Figure 79: False alarm cases .....	104
Figure 80: Exceptions.....	105
Figure 81: Sensor noise .....	105
Figure 82: Different PTWs detected.....	106
Figure 83: Inter-lane practice A13 .....	110
Figure 84: The false alarm cases (A13).....	110
Figure 85: Different types of laser scanner in the market .....	119



## Tables

Table 1: Accident overview in past 2 years (2010-11) depending upon areas. [Source Sécurité Routiere France: Bilan 2011]	8
Table 2: Different PTW safety projects [w3]	10
Table 3 : Recent Projects concerning PTWs	10
Table 4: Comparison of Intrusive and Non intrusive technology	13
Table 5: Different technologies using various laser scanner applications	19
Table 6: Comparison of laser scanners. *Scans in a straight line	22
Table 7: Simulator vehicle dimensions	36
Table 8: LMS 111 Laser beam expansion	43
Table 9: Comparison between roadside mast-mounted and gantry configuration	46
Table 10: Comparison between three vertical configurations	49
Table 11: Different categories of vehicles passing under the laser scanner at different heights	53
Table 12: Database table (Ground Truth)	54
Table 13: Different categories of vehicles per lanes (Ground truth)	55
Table 14: PTW traffic on the A13 motorway	56
Table 15: Overall distribution per category of vehicle on the A13	56
Table 16: Registering a vehicle	74
Table 17: Difference between SVM and KNN	81
Table 18: Learning set	83
Table 19: Comparison of the ground truth with the width found	86
Table 20: Controlled site database	94
Table 21: Results of our method: semi-Cartesian coordinate system [120 samples]	94
Table 22: Cartesian: Result of PTW detection	95
Table 23: Learning database (Controlled site + Real site)	96
Table 24: Confusion matrix of vehicles: Real site	97
Table 25: Vehicles detected on real site (1 hour data)	98
Table 26: All vehicles detected on real site (2 lanes)	98
Table 27: Traffic per lane (per category).	99
Table 28: SVM single parameter results	100
Table 29: Per lane detection rate using SVM (Width)	100
Table 30: Confusion matrix SVM2	101
Table 31: Per lane detection rate using SVM2 (Width + H_Nbx)	101
Table 32: KNN results (K=5)	102
Table 33: KNN results K=10	102
Table 34: KNN results K=20	103
Table 35: Comparative KNN and SVM performance table P1: single parameter and P2: two parameters	106
Table 36: KNN: Confusion matrix for PTW	107
Table 37: SVM: Confusion matrix for PTW	107
Table 38: Parisian traffic (Motorway A13)	108
Table 39: SVM classification results on A13	108
Table 40: KNN results for Paris A13 (K=5)	108
Table 41: KNN results for Paris A13 (K=10)	109
Table 42: KNN results for Paris A13 (K=20)	109





## General Introduction

The safety of Powered Two Wheelers (PTWs) is important for public authorities and road administrators around the world. Official figures show that PTWs represent only 2% of the total traffic on French roads (2011), but as these figures are obtained by simply counting the number plates registered, they do not give a true picture of the PTWs on the road at any given moment. To date, there is no overall solution to this problem that uses a sensor capable of detecting PTWs and taking into consideration their interaction with other vehicles on the road (for example: Inter-lane traffic, when PTWs move in between two lanes on a highway), and no state-of-the-art technical solutions can be adapted to measure this category of vehicle in traffic (unlike Light Vehicles and Heavy Vehicles). The research in this domain has not therefore been greatly developed. This is an issue of concern. For this reason, the project METRAMOTO<sup>1</sup> (Traffic Measurement of PTWs) was launched in November 2010, which is a French ANR<sup>2</sup> Project and is certified by the research pole Mov'eo<sup>3</sup>. [w4][BURA13].

This PhD comes under the project ANR METRAMOTO and was carried out in collaboration with CETE Normandie Centre (Public Works Centre for Technical Studies: ERA 34), IFSTTAR (The French institute of science and technology for transport, development and networks) and LITIS (Computer Science, Information Processing and Systems Laboratory: Intelligent Transportation Systems EA 4108) and is financed by IFSTTAR and the Upper Normandy Region, France. This PhD officially started on 1<sup>st</sup> October 2010.

Our goal is to detect PTWs using a single plane laser scanner placed on a pole at a certain height, with the vehicles passing at various speeds on the road below it. The laser scanner provides information about the scanned area over a certain period of time.

The main objective of this technical research work is to propose a prototype that is able to detect and count the PTWs in traffic. This prototype is meant to be integrated into a system that can be easily installed on a highway and can detect and count PTWs in real-time. Ideally the system should be self-calibrating with respect to the installation site and be able to work autonomously for a long-term.

To solve the problem stated above; this research work has been subdivided into several sub-problems. First and foremost in order to detect the PTW, the characteristics of this category of vehicle that may help to distinguish it from other vehicles are determined. There are several technologies that count vehicles on the road. Using a single laser scanner was a predefined constraint, but using this technology to detect, extract, classify and count PTWs is an original task. This leads us to the second problem, which is the detection of vehicles using a single laser scanner. So, this dissertation is divided as follows: <sup>1</sup>

### 1. Motivation and Overview

This part focuses on the general question of why there are so many accidents involving PTWs and gives some recent figures. Then the state of research focusing on PTWs is presented. After that we introduce the METRAMOTO project and the different technologies involved. This part also justifies our choice of a laser scanner over other technologies for the detection of PTWs. After that we define

---

<sup>1</sup> Agence Nationale de Recherche : [www.agence-nationale-recherche.fr](http://www.agence-nationale-recherche.fr)

<sup>2</sup> METRAMOTO : [www.projet-metramoto.fr](http://www.projet-metramoto.fr)

<sup>3</sup> Mov'eo : Pôle de compétitivité : [www.pole-moveo.org](http://www.pole-moveo.org)

the PTW and present the research work done to date for the detection of this category of vehicle. As we detect the PTW using a laser scanner, we present the state-of-the-art for the detection of objects on the road using a laser scanner. Once the object is extracted it must be classified by the different types of methods used. At the end, the technical and theoretical state-of-the-art for counting objects is presented.

## **2. Data acquisition**

In this chapter all the steps followed to acquire the laser scanner data are described. To begin with, a justification is given for the choice of the laser scanner used for this research work. Then different ways to mount a laser scanner are presented and an optimal installation position is chosen taking into consideration the traffic of PTWs.

To theoretically justify this choice of installation, a simulator has been implemented that shows the possible cases of occlusion of PTW in different traffic scenes.

Once a laser scanner is chosen and an optimal position for its installation is determined, a method is applied, enabling the system to find the road verges and find its own height.

For the data acquisition, the first database was constructed on a controlled site (controlled traffic behaviour). The main aim of this database was to understand the laser scanner data and validate our first approach. Then, the other database sets were constructed on different uncontrolled sites (expressway and motorway).

## **3. Extraction and classification**

In this part, the procedure to extract information from the data is explained as follows:

- **Extraction:** In this part a filter is created that is capable of minimizing noise linked to the artefacts and filling up the non measured data. Then a general pre-processing is done, i.e. changing the coordinate system and introducing an angle that compensates the possible slope of the road. The data obtained is then concatenated during a certain period of time in order to transform it into a spatial temporal domain. To this accumulated information a new extraction method is applied. This method is rapid and is made for the detection of PTWs in real-time and is adaptable to any situation present in the scene.
- **Classification:** Once the object is extracted, the next step is to classify it. All the possible features of the object are calculated and then the invariant features are chosen as the parameters of the classifier. Once classified, we can count the vehicle according to the category found.

## **4. Results and perspectives**

The method described in the previous part is applied to the databases (one controlled and two real). The results obtained are analysed, discussed and the perspectives of the research work are given.

An overview of this research work is presented in the Figure 1.

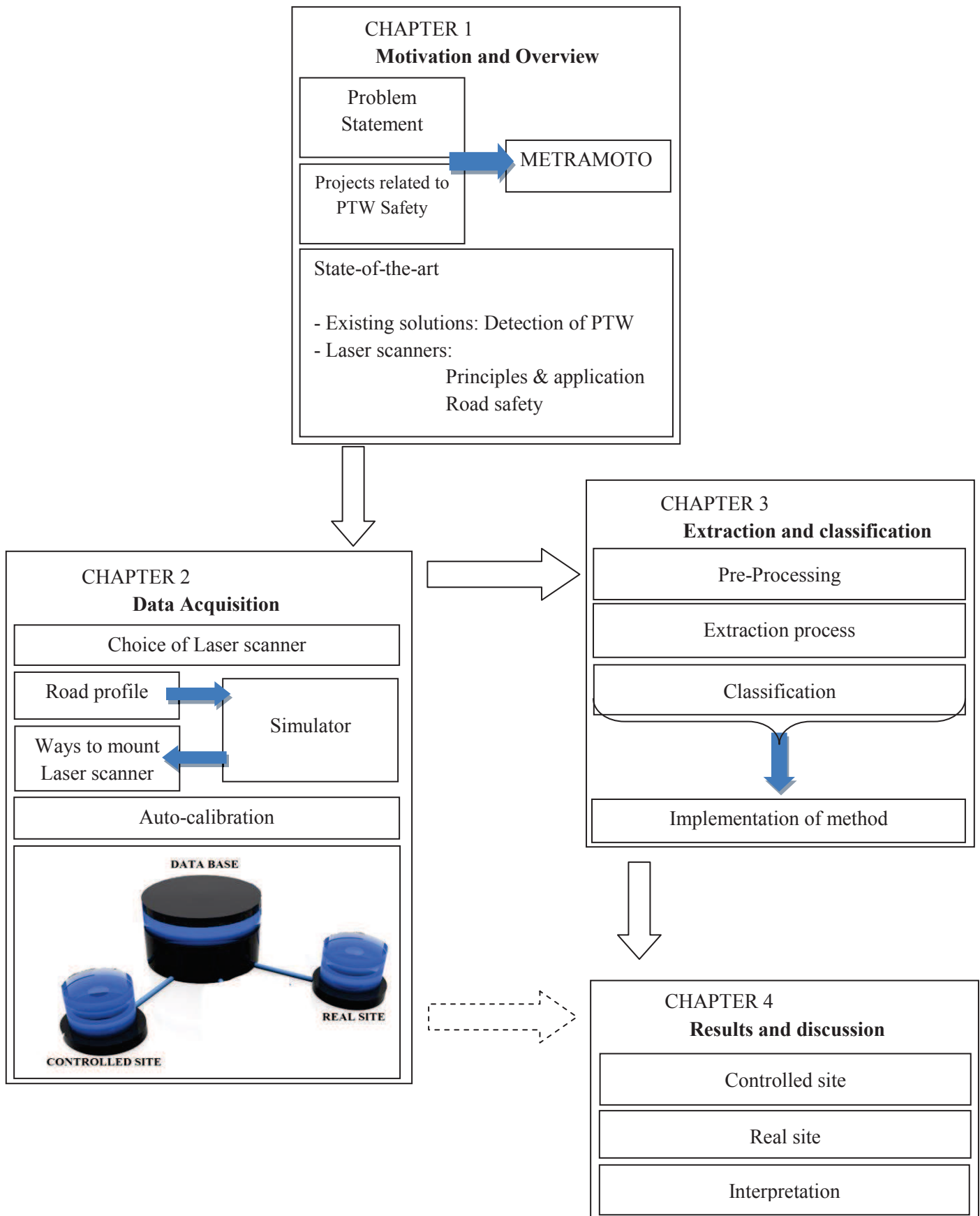


Figure 1: Overview of the thesis by chapters



## CHAPTER 1: Motivation and Overview

---

Introduction .....	7
1.1. Problem statement .....	7
1.1.1. Evolution in the number of PTWs .....	7
1.1.2. PTW Accidents .....	8
1.1.3. Difficulties in detecting PTWs.....	9
1.2. Projects related to PTW safety .....	10
1.3. METRAMOTO .....	11
1.3.1. Comparison of technologies .....	13
1.3.2. Choice of the technology .....	14
1.4. Research work done for the detection of PTWs .....	14
1.4.1. Definition of a PTW.....	14
1.4.2. Existing solutions.....	15
1.5. Research work done to date for laser scanners.....	18
1.5.1. Principles and techniques.....	18
1.5.2. Applications .....	22
Conclusion.....	27

---



## Introduction

In this chapter, an overview of the problem is given, highlighting the necessity for this research work and the work done to date for the Powered Two Wheelers (PTWs). As PTWs will be detected using a laser scanner, a brief introduction of this category of vehicle and the laser scanner will be given. This part also justifies certain choices such as the choice of the technology for this research work and the type of laser scanner chosen. The research work done to date for the detection of PTWs in traffic and the existing methods that use the laser scanner for the detection of objects on the road are presented.

### 1.1. Problem statement

The safety of Powered Two Wheelers (PTWs) is an important issue for public authorities and road managers around the world. Official figures show that PTWs are estimated to be only 2% of the total traffic on French roads, but represent 30% of deaths in road accidents [ONSIR11]. Over the past 10 years there has been a constant increase in the number of PTWs on the road.

#### 1.1.1. Evolution in the number of PTWs

For PTWs having a capacity of more than 50cm<sup>3</sup>, there is an estimated increase in their traffic by a factor of 6.7. Official figures show that the death rate of riders has increased to nearly 30% in 2011[ONSIR11] in the past 10 years.

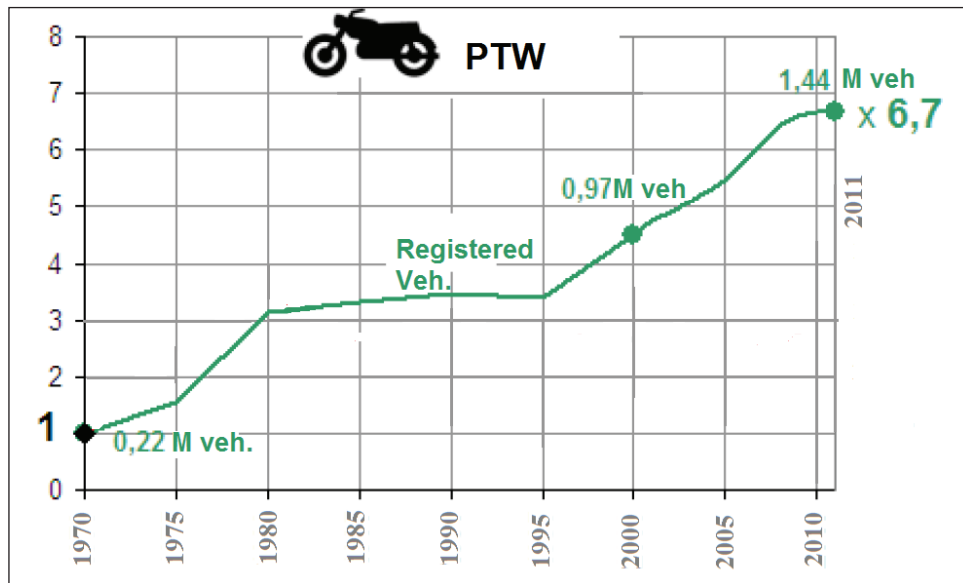


Figure 2: Increase in the number of PTWs (>50cm<sup>3</sup>) [ONSIR11]

Figure 2 shows a constant increase in the number of PTWs registered since 1970. The estimated figures cited above are obtained by simply counting the number plates registered. They do not give a true picture of the PTWs on the road at any given moment.

With an increase in the traffic of PTWs, there is an increase in the number of accidents involving this category of vehicle. The main reason is that the PTW accidents do not share the same profile as other classes of vehicles. There are many factors that provoke these PTW accidents, such as loss of control on bends, more frequent overtaking, and due to its small size, possibility to weave in and out of lanes at high speed.



### 1.1.2. PTW Accidents

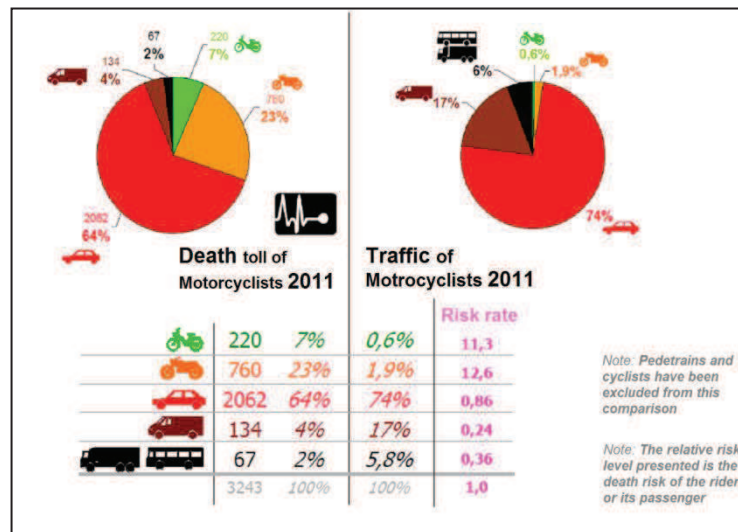


Figure 3: The death rate and the traffic of each category of vehicle [ONSIR11]

Figure 3 shows the death rate of motorcyclists when they are interacting with other categories of vehicles [ONISR11]. Here is a table that gives an overview of the accidents per category of vehicle depending where they occur during the years 2010 and 2011.

	Total			Rural Area			Urban Area		
	2010	2011	%	2010	2011	%	2010	2011	%
<b>Pedestrians</b>	485	519	13	139	169	6	346	350	32
<b>Cycle</b>	147	141	3	88	83	3	59	58	5
<b>PTW</b>	952	980	25	557	599	20	395	381	35
<b>Light Vehicles</b>	2117	2062	52	1829	1785	63	288	277	25
<b>Utility Vehicles</b>	146	134	3	127	124	4	19	19	1
<b>Heavy Vehicles</b>	69	67	2	68	64	2	1	3	0
<b>Others</b>	76	60	2	51	43	2	25	17	2
<b>Total</b>	3992	3963	100	2859	2867	100	1133	1096	100

Table 1: Accident overview in past 2 years (2010-11) depending upon areas. [Source Sécurité Routière France: Bilan 2011]

Table 1 demonstrates that in rural areas, PTW accidents represent 20% of all fatal accidents even though the number of accidents, since the past two years (2010 and 2011) has been quite stable. In urban areas this figure is even higher at 35% of the total fatal accidents. A study by ONISR in 2011 shows that the PTW fatal accident rate depends on the weather conditions and the time of day. If it is sunny, people prefer to ride a PTW. At certain times of the day, the probability of encountering a PTW is higher i.e. more probability of PTW interaction with other categories of vehicles and hence more accident risks.

This is demonstrated in Figure 4, which shows that accidents are more likely to occur during favourable weather conditions that provide good visibility and a better grip on the road, thus encouraging more motorcyclists to use the PTW. During the period from spring to autumn, a large number of convoys of PTWs can be easily seen on the highways. The higher number of interactions leads to more accidents. The graph shown in Figure 4 demonstrates the seriousness of the problem; it shows 0.09 PTW deaths/ hour, i.e. one death every 11 hours.

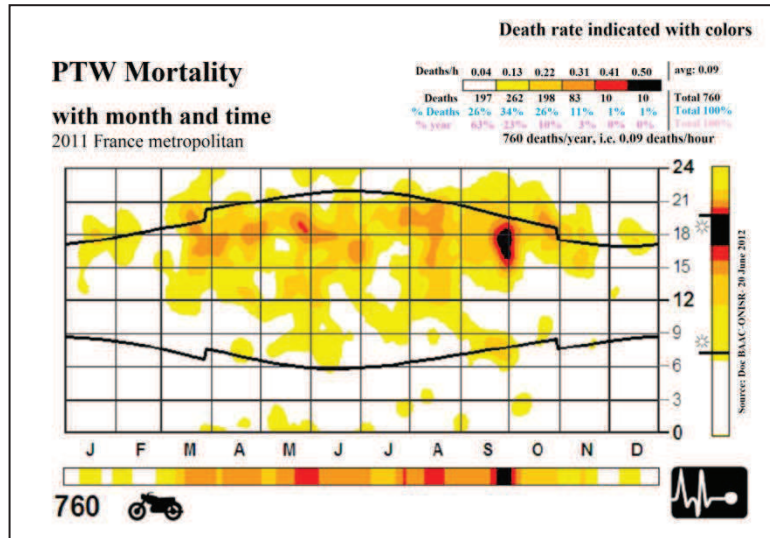


Figure 4: PTW mortality rate: relation with the climate and accident rate

[GUYO08] presented a report in 2008 indicating that the existing data for the PTW are based merely on estimations, but have nothing to do with the real world. In other words there is a lack of information about this category of vehicle.

### 1.1.3. Difficulties in detecting PTWs

PTWs are not easy to detect as they are smaller than any other category of vehicle on the road. This smaller size helps them to travel anywhere in the traffic especially in the inter-lanes. This inter-lane practice results in PTWs being hidden from the sensor by another vehicle of relatively bigger size. Moreover, due to its small size, this category of vehicle can weave in and out of lanes at high speed, thus making its detection very difficult.

The detection of PTWs in traffic would aid the road administrators to find the indicators relating to the use and circulation of this category of users. To our knowledge, there is no operational system that can collect accurate traffic data for PTWs although several solutions exist for other categories of vehicle (Light Vehicle (LV) and Heavy Vehicle (HV)). These indicators would help attain the following objectives:

- Obtaining the statistics (number of PTWs in traffic).
- Establishing the different routes frequented by the PTWs.
- Adapting safety measures for PTWs.
- Calculating the accident risk exposure of PTWs.

In addition to detection, the trajectory tracking of the PTW would enrich our knowledge in:

- Identifying and understanding the interaction of PTWs with other users on the road.
- Evaluation of experimental impacts or safety measures taken by road administrators.

There are many techniques used to detect or count the vehicles moving on the road, for example radars, magnetic loops, manual counting etc. These “classical” traffic sensors are unable to give the exact figures for the PTWs as they often travel in inter-lanes. Hence sensors such as magnetic loops installed on the road are able to detect the PTWs if and only if they pass over them. Moreover, the practice of inter-lane driving hides the two wheelers from sensors such as radars or vision cameras.

So, there is a lack of information for the traffic, mobility and the trajectory of the PTW. Moreover, there is not yet any solid industrial solution (except prototypes in the process of validation) to solve this problem, as is explained later in the chapter. So this research domain remains challenging and hence not often investigated [ONSIR11].

To date, there is no overall solution to this problem that uses a single sensor capable of detecting and counting PTWs in traffic. It is thus difficult to understand the interaction of PTWs with the other vehicles on the road and no state-of-the-art technical solutions can be adapted to measure this category of vehicle in traffic (unlike LVs and HVs) and so this is an issue of concern.

## 1.2. Projects related to PTW safety

The problem of PTW detection is not limited to France but concerns nearly all the countries around the world. This can be seen through the fact that countries like the US, Australia, China and many other European countries have built projects to find a solution to this serious problem.

Here are a few projects that concern PTW security (terminated or in phase).

Road safety / accidentology	RIDER, Surmotori, 2RM, 2besafe
Road safety / interaction – behaviour	Simacom, SafeRider, Damoto, CSC-2RM, 2beSafe, Watch-Over; NCHRP 08-81
Road safety/ Motorcyclist safety	Proteus, Biocasq, Damoto, PISa, counting motorcycles [VAND10], RIDERSAFE

**Table 2: Different PTW safety projects [w3]**

Table 2 shows different projects that concern PTWs especially in Europe. Most of these projects focus on the safety of PTWs, their behaviour in traffic and their onboard systems in case of accident but none of these projects uses a single sensor for the detection and counting of PTWs on highways. Here are the details of a few recent projects in Table 3.

Project Name	Objective	Domain
2besafe	Enhance PTW safety including crash causes and human errors	Road Safety, Rider safety
SafeRider	Study the potential of Advanced driver assistance information (ADAS)/ In-vehicle information systems (VIS) which are integrated in the PTW for the rider's safety and comfort.	Road Safety, Rider safety
CSC-2RM	Study the spontaneous driving behaviour of PTW riders in urban and suburban areas	Road Safety, rider behaviour
Damoto	Develop robust and effective algorithms to trigger riders' protective devices.	Road safety, Rider safety

**Table 3 : Recent Projects concerning PTWs**

Table 3 shows all the recent projects that focus on the safety of PTWs, their on-road behaviour with respect to other categories of vehicles and the protective measures to be taken to improve the rider's safety on the road. But none of the projects focus on counting this category of vehicle in traffic,

especially on the highways where the traffic is random and dense, hence the launch of the ANR METRAMOTO project.

### 1.3. METRAMOTO

For the reasons cited above, the French ANR METRAMOTO (MEasure de TRAffic des deux roues MOTOrisés) project was launched in November 2010 with the goals of finding the technological solutions for better integration of these vulnerable road users. These goals are as follows: [BURA13]

- To develop technical solutions to detect PTWs in traffic or to track and explore their trajectories.
- To explore the statistical indicators for measuring traffic and the trajectory parameters.

These goals will help to understand:

- Traffic behaviour and PTW mobility.
- The risks and interaction of PTWs with other road users.

To study traffic, there are two big classes of sensors: intrusive technologies also known as in-road sensors and non-intrusive technologies also called over-road sensors.

- Intrusive technology: The sensors using this technology have to be embedded in the road, integrated by the road-side or attached to the surface of the road. There are several types of intrusive sensors, some of which are listed below:
  - Electromagnetic loops: They are one of the most commonly used sensors that are used to study traffic. An electric current is induced in the system and is transmitted as a signal when a vehicle moves on the loops installed on the road.
  - Passive magnetic or magnetometer sensors: They are installed by either permanently mounting them in narrow holes dug in the road or they are fixed to the road surface in some manner. The wires are buried under the road and connect to the base station processing unit which reads the electromagnetic data sent by the loop.
  - Pneumatic tubes: They are stretched across the road and are fixed at both sides. These sensors are very fragile in nature and hence are only installed temporarily as they can easily be damaged by heavy or fast moving vehicles.
  - Piezoelectric sensors: This category of sensor converts kinetic energy to electric energy. A voltage is generated when a mechanical impact or vibration occurs. This impact causes the electrical charges of opposite polarity that appear in the inner and outer surface of the material to induce a voltage.
- Non intrusive technology: This technology measures the data from a distance i.e. we do not need to interrupt the traffic to integrate the system on the road. In other words, these sensors are mounted either above the roadway or alongside the roadway. They include video data collection, infrared detectors, microwave radar detectors, ultrasonic detectors, passive acoustic detectors, laser detectors and aerial photography. Some of these technologies are explained below:

- Video image detection: The video is captured by a camera installed by the roadside or overhead. This video is basically an accumulation of several pictures. There are several processing methodologies that allow the extraction of traffic parameters and also the analysis of the video data.
- Infrared sensors: these sensors can be mounted overhead to view the approaching traffic or to view the vehicles from the road side. These sensors are light-sensitive and hence convert the reflected or emitted energy into electrical signals.
- Microwave radar detectors: Low microwave radiation is projected into a detection zone. When a vehicle passes in this zone, part of these radiations are reflected back to the receiver.
- Laser detectors: These sensors can be installed overhead or along the roadside and are often used to classify different vehicles passing underneath. They project the laser rays onto an object which reflects them back, fully or partially. Hence the distance of the object from the laser scanner can be calculated.
- Acoustic array sensors: these sensors measure the vehicles passing at a certain speed by detecting their acoustic energy. A signal processing algorithm can be used to recognize the vehicular traffic in the detection zone through an increase in noise. When the vehicle leaves the detection zone, the sound energy level drops and the vehicle's presence is validated. [GIBS10].

Out of these all technologies, four were chosen for the METRAMOTO project,

- Intrusive
  - Magnetometer sensor
  - Hybrid sensor (Piezoelectric sensor + electromagnetic loops)
- Non intrusive
  - Image Processing
  - Laser Scanner

### 1.3.1. Comparison of technologies

All these four technologies explored in METRAMOTO are commonly used today for vehicle classification, but none are used specifically to detect and count PTWs. However, each of these technologies has advantages and disadvantages. Table 4 shows a comparison:

	<b>Intrusive</b>		<b>Non Intrusive</b>	
	Magnetometer	Piezoelectric	Image Processing	Laser Scanner
<b>Strengths</b>	<ul style="list-style-type: none"> <li>-Cheap technology to install</li> <li>- Insensitive to harsh weather conditions (snow, fog, etc)</li> </ul>	<ul style="list-style-type: none"> <li>-Least expensive system in terms of capital cost and maintenance cost.</li> <li>-Can be used for higher speed ranges</li> <li>- Can monitor up to four lanes</li> </ul>	<ul style="list-style-type: none"> <li>-Captures all traffic information that can then be verified by a human operator.</li> <li>- Enables the study of colour.</li> <li>- Textures can be studied.</li> <li>-Information available for longer period of time</li> <li>-Multiple detection and tracking possible</li> <li>Easy to add or modify the detection zone</li> </ul>	<ul style="list-style-type: none"> <li>- Accuracy</li> <li>- Easy to install</li> <li>- Long range</li> <li>-Multiple detection zone possible</li> <li>- Day or night Operation</li> <li>- Cheap to use</li> <li>- Portability</li> </ul>
<b>Weaknesses</b>	<ul style="list-style-type: none"> <li>-Traffic must be stopped to install the loop</li> <li>-Unable to detect vehicles below a certain threshold</li> <li>-Not suitable for vehicles with relatively low metal content (PTW)</li> <li>-Not suitable for magnetic bridge decks</li> </ul>	<ul style="list-style-type: none"> <li>-Traffic must be interrupted to install the system</li> <li>-Low life span (3 years)</li> <li>-Cannot detect immobile vehicles</li> </ul>	<ul style="list-style-type: none"> <li>- Shadows</li> <li>- Installation and maintenance, i.e. periodic lens cleaning, require lane closure when camera is mounted over roadway.</li> <li>-Performance affected by weather such as fog, rain, and snow; vehicle shadow projection into adjacent lanes; occlusion; day-to-night transition; vehicle/road contrast; and water, salt grime and cobwebs on camera lens.</li> <li>-Affected by strong winds or vibration of the mounting structure.</li> </ul>	<ul style="list-style-type: none"> <li>-Electromagnetic interference with other electronics</li> <li>- Reflected values not high enough with dark objects</li> <li>- Refraction by windshields</li> <li>- Sensitive to harsh weather factors (fog, snow)</li> <li>- Blind sensor. Needs a camera to verify the data</li> <li>- Maintenance, cleaning of lens</li> <li>-affected by strong winds or vibration of the mounting structure</li> </ul>

Table 4: Comparison of Intrusive and Non intrusive technology

### 1.3.2. Choice of the technology

For this research work a laser scanner was chosen because it gives very accurate measurements within the order of a few millimetres. As the laser scanner is small it is very portable and easy to install, unlike video cameras. The laser scanner has a long range (20 to 100 metres) and can scan easily at wide angles making it possible to scan multiple lanes at the same time. This technology is not light-dependent i.e. it can scan as easily in day time as at night. With the laser scanner, there are no problems of shadows (cast shadows and self shadow) as in image processing techniques.

As there is a great variety of laser scanner available on the market, we can have this technology at an affordable price. As the sensor is meant to be placed above the road, with this non intrusive technology, an interruption of traffic is not necessary to install the system.

Moreover the laser scanner data is ideally based on a ‘lane-fit model’ which represents a road data; this model is updated at each instance of time  $t$  with a laser scan data containing the road conditions at time  $t$ .

To understand the research work, we have to understand the object of interest. i.e. Powered Two Wheelers (PTWs). To begin with, a brief introduction to PTWs is given, the type of PTWs and the research work done to date for the detection of PTWs. Then an explanation of different types of laser scanners and different scanners on the market today is given. Finally, the state-of-the-art for the detection of objects using laser scanners is explained.

## 1.4. Research work done for the detection of PTWs

The main goal is to detect and count PTWs in traffic. The first step is to define the object of interest, which is the PTW in our case which comes in different shape and size and is easily seen on the road. After that, a literature search is carried out and the scientific and industrial methods found to date to detect this category of vehicle are presented.

### 1.4.1. Definition of a PTW

A Powered Two Wheeler (PTW) may be described as a mode of transport with two wheels and a motor. Administratively, the term PTW may be used to refer mopeds, scooters, and motorcycles; and commonly includes similar three-wheelers as well [ONSIR11], [SUBI09], [GUYO08], [GOUD11].

According to the registration, there are different subclasses of PTW:

- Mopeds

Mopeds and scooters are PTWs with a ‘stepthrough’ design, usually with an automatic transmission. The use of mopeds is generally restricted to low speed zones in urban areas as they have a maximum engine capacity of 50cc and a top speed of 45km/h.

- Motorcycles

Motorcycles in general are subdivided into two sub classes depending on their engine power.



- Light motorcycles

This type does not exceed 125cm<sup>3</sup> and has a power of 11 kW (15 Hp). This category contains bikes smaller in size and scooters

- Heavy motorcycles

This class of motorcycles exceeds 125 cm<sup>3</sup> and can have a maximum power of 73kW (100Hp).

They can be further subdivided into subcategories according to their use such as utility bikes, roadsters, sport bikes, trails, customs, road bikes and Grand Tourism (GT). However, there are a few exceptions that we also consider as PTWs or the derivatives of PTWs:

- The side-car: As the name says, this category contains a side car next to the PTW.
- The trike: This is a tricycle (3 wheels) with a huge cylinder and has a the back wheel larger than the front wheel.
- The spyder: This is a three-wheeler which resembles a quad, but is not classed as a quad. It has a powerful engine and stable driving that makes it popular in the market.
- The quad: The All Terrain Vehicle (ATV) or quad, is a four-wheeler that is used often for sport activities especially for racing in the muddy regions.

With the variety of PTWs that come in variable dimensions, the order of difficulty for the detection of this category of vehicle increases. However, a few solutions for the detection of PTWs were found.

### 1.4.2. Existing solutions

Since most PTWs have a small number plate and the riders in many countries always wear helmets, the identification of a PTW or its rider becomes difficult. A few riders even remove their number plate and ride at a very high speed to avoid being caught and identified by the authorities. Hence for this category of vehicle not much research work has been done. However, a very few research papers proposing a solution to this problem were found. The research work found is divided in four parts based on the type of sensor employed: laser scanner alone, video alone, laser scanner fusion with a video camera and multiple sensors.

#### 1.4.2.1. Laser scanner

[RIPO12] presented a method with a similar objective to our research work. The author used a laser scanner to classify and count different categories of vehicles (PTWs included). The data read by the laser scanner is processed by first correcting the geometric features measured by the sensor and then the static objects are eliminated. The non measured values are filled by taking into consideration the size of the cluster of these values. If it is a single value, then it is filled with the neighbourhood values. If the whole set of values is missing, then the author suggests leaving it like this. The extraction is done by a depth data normalization process. The information gathered by the laser scanner is isolated in a matrix. The extracted vehicle is contained in this matrix and is classified using a decision tree.



This method was used on real traffic with laser scanner placed on a traffic light pole. So all the vehicles were moving at a very slow speed thereby increasing the chances of detection. The laser scanner was installed for 6 hours and the result is presented with a total of 972 vehicles: 51 PTWs, 675 LVs, 178 Vans, 44 trucks and 24 buses.

The research work proposed by [RIPO12] is a general counter and does not target only PTWs. The method needs a minimum of 20 consecutive scans to validate the presence of a vehicle. The author did not explain the method (pre-processing, processing and classification) in detail and hence it cannot be reproduced easily. The problem of occlusion is discussed but no solution is proposed to overcome this problem. No information is given about the autonomy and the calibration of the system.

What differentiates this work from ours is that in our case, the laser scanner is mounted on a highway where the traffic density and the traffic speed is very high (around 100 km/h). On a highway most of the time, PTWs do not respect the speed limitations and often move in a random way. On the other hand, [RIPO12] proposed to install the laser scanner on a road around a traffic light thereby limiting the PTWs' trajectory and speed thanks to the traffic lights.

#### *1.4.2.2. Video*

[KANH10] proposed a background subtraction method and a simultaneous tracking through a Kanade-Lucas-Tomasi feature tracker (KLT). These two results are then combined and used into a foreground mask, thus extracting the data from the video. The method detects PTWs with an error of around 6% which is due to semi or full occlusions caused by heavy traffic situation.

[KU08] connected the components present in the image sequence and then calculated the length/width and pixel ratio of the vehicles present in the scene to detect PTWs. The results were presented with different climatic and luminosity conditions. The authors showed the detection of PTWs in heavy traffic with an overall rate of 85%.

[PAUN10] proposed a method for the detection of license plates of vehicles on the Indian roads. The traffic in India is well known to be quite random and the license plates do not follow a particular format of presentation. The authors used an RGB camera for the data acquisition. First of all the variance of the input image is determined; if it is more than a certain threshold, then edge detection and region extraction are done. Then processing is done by Gaussian analysis which is followed by connected components analysis. Once the connected region is extracted, a number plate extraction filter is used. This method was tested on static traffic and on several vehicles, but does not give exact figures about the PTWs' number plates. The problem is not the same when the traffic is dynamic as the complexity increases.

[PHAT09] used multiple cameras (vertical and horizontal) to extract multiple geometrical features for the neural networks. Then multi-filtering is carried-out to approximately locate the PTW (present in the scene) and confirm its number plate. This method was tested on real city traffic and gave an overall correct detection rate of 93.2% for PTWs, 93.33 % for the PTWs with license plates and 87.23 % for the PTWs without license plates.

#### *1.4.2.3. Video and a laser scanner*

[NIKN11] proposed an embedded real time system for detecting and tracking all types of objects on the road by a combination of laser scanner and camera. A laser scanner is used to calculate the distance between the object and the sensor, thus generating a 3D laser-map which is used as a priority

to generate objects. A particle filter is used on this laser-map to track the vehicle. Once the vehicle is tracked, a combination of a latent support vector machine (LSVM) and histograms of oriented gradients (HOG) is done for the classification. The system is mounted on a moving vehicle. The authors gave an overall detection rate of 96.7% but did not give a separate detection rate for PTWs.

#### *1.4.2.4. Multiple sensors*

[COIF10] installed multiple laser scanners on the side of a vehicle that was parked on the highway side. The side profiles of the vehicles were studied. Factors such as length and the number of laser points representing vehicles were used as criteria to classify vehicles.

As noted earlier, PTWs move most of the time in between the lanes, hence occlusion is observed and in this paper, the authors have discussed the problem. The PTWs were detected in traffic but at a very low detection rate of 77% due to the occlusion.

A prototype of a PTW classifier is presented by [GIBS10] that uses a multi-instrument sensor designed to detect cyclists at intersections. The sensors are mounted on the road side and include an infrared visible light stereo camera, an infrared thermal camera, and an acoustic sensor. The system is installed at the intersections. The infrared thermal camera first tries to detect a bicycle. If it is not a bicycle, then a stereo vision camera is used to verify whether it is a PTW or a light vehicle. If it is a motorcycle, then an acoustic sensor is used to classify the type of motorcycle (Light Motorcycle, Heavy Motorcycle, Scooter, Moped). This method was tested on a database of 45 vehicles which is very low to obtain a correct efficiency of the system. Moreover mounting a system at an intersection on the road side may create occlusion and this problem is not even discussed in the publication. In a recent publication, [LING13] used the previous work proposed by [LING12] and applied it on a larger database, hence achieving a detection rate of 90% with 3% of false alarms.

[SCHL11] installed a sensor on the PTW. A roll angle (angle between the road and the slanted vehicle) is calculated by using gradient orientation histograms. This could be helpful in estimating the riders' behaviour in traffic.

[MIDD12] did a global comparison of different technologies for the detection of PTWs. The author presented the following technologies:

- Loop/Piezoelectric
- Magnetometers
- Multi-technology system
- The Infrared Traffic Logger (TIRTL)
- Traffic vision video system

These technologies were not all treated on the same database and the results presented were incomplete with no scientific explanation of any technology. What makes this publication important for us is the fact that the author did not discuss about the laser scanner amongst all these technologies presented in his work thus giving another proof about the originality of our work.

[YU10] presented a report on the evaluation of different non intrusive technologies for the classification of different categories of vehicles (including PTW) at the freeways. The author

compared three different sensors such as Autoscope which is a length-based classification sensor with video imaging technology, a TIRTL which is a 15 class axle-based classification sensor with active infrared technology and a HD SmartSensor which is a length-based classification sensor with microwave radar technology. The results were presented lane by lane for each technology. However the number of PTW in the database is not significantly high to show interesting results.

[MING10] did a similar approach as [YU10] using different sensors to evaluate a variety of traffic and environmental conditions on the freeway. Urban traffic conditions were taken into consideration such as heavy congestion with varying weather and lighting conditions. Five different sensors were used such as Wavetronix SmartSensor HD (Radar), AxleLight (lidar), GTT Canoga Microloops (Magnetometer), TIRTL (Infrared) and Miovision (Camera). No official figures were given for the PTWs in the report but they state that the PTWs were detected.

## 1.5. Research work done to date for laser scanners

The first use of the laser scanner for the detection of obstacles was around 25 years ago [HOFF86], [OLIV87]. Since then, several articles have been published, each of them presenting their own ideas and new approaches to get the best possible results. At the beginning of the millennium this laser scanner presented a problem of calculation time, but in recent years the technology of laser scanner has developed and this problem of calculation time has been overcome.

Today, different laser scanners are used in many domains such as aeronautics, road safety, robotics, medicine, sports etc. For this section, we shall be focusing on the road safety domain as it is in the field of our research work (detection of PTWs).

This subchapter is divided into several parts: To start with, a brief introduction to the laser scanner is given. Its principles and techniques are described, along with the different technologies used by laser scanners, and a few existing laser scanners in the European market are listed. Then in the second part different technical and scientific applications are presented. The technical applications signify the applications that have been employed on the road to classify vehicles while the scientific applications are those used in research laboratory (not necessarily employed in real time) dealing with road safety.

### 1.5.1. Principles and techniques

A laser scanner uses infrared light source to read objects and can be used on a wide variety of target (plants, fields, aerosols, clouds, non-metallic objects or even targets as small as a single molecule). This technology has been extensively used in atmospheric research or in meteorology such as NASA's projects, or on an airplane or a satellite to map an environment. Before going into detail, it is important to know the definition of a laser scanner.

#### 1.5.1.1. Principles of the laser scanner

A laser scanner uses an infrared light with wavelengths ranging from 0.25 to 10 micrometers. The reflections can be read from non-metallic objects and surfaces, all the way through aerosol mists, and clouds. Due to a high precision, this technology has been used in meteorology research, traffic analysis and satellite mapping applications [COLV11].

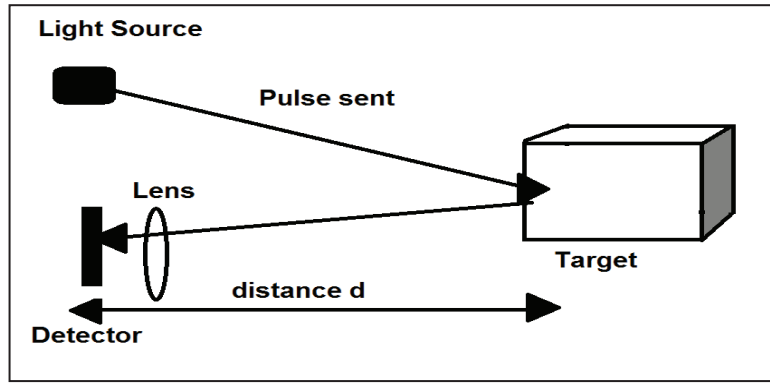


Figure 5: Time of Flight principle.  $d$  is the distance [COLV11]

Table 5 shows an example of different technologies that use an active (optical) laser scanner.

Application	Technology explored
Triangulation	Nautical industry, dentistry
Interferometers	Shape measurement system (symmetry check), Terrestrial laser scanner (monitor snow covered peaks)
Time of flight (Tof)	Traffic (barriers, parking), security system
Structured lightening	Facial detection, automotive industry
Stereo analysis	Medical field, Space

Table 5: Different technologies using various laser scanner applications

Table 5 resumes all the techniques that laser scanners use and the corresponding technologies explored. Using different principles, laser scanners can be distinguished as follows:

- Rotating beam projection device: This category of laser scanners projects rays to the environment with a certain angular frequency and a certain range. They can have a single laser beam or multiple laser beams. If the rays find any limit (obstacle), they are reflected back to the laser scanner, thus giving the coordinates of the obstacle. Two examples of this type of laser scanner are SICK LMS1xx (Single beam) and SICK LMS5xx (Multiple beams).
- Light curtain and multiple light beam device: There are two rod type sensors placed parallel to each other projecting multiple beams to each other. If an obstacle passes in between these rays, the silhouette of the obstacle is formed and noted. An example of such a laser scanner is SICK IP69K.
- Fusion of multiple single-layered laser scanners: They have the same principle as that of a single light beam device, but in this case, multiple laser scanners are combined with each other to produce multiple planes and multiple visions. An example of such a device is SICK TIC102 which is a combination of two LMS111.

One of the objectives of this research work is to find a solution that is simple, robust and the cheapest possible. Combining multiple sensors might prove interesting, but a laser scanner like TIC102 is designed to obtain information for one lane at a time. This means that for a four-lane highway, four TIC102 sensors are needed which lead to a very expensive solution. Whereas the light curtain device is suitable for a single-lane highway as in case of multiple lanes, if more than one vehicle passes through the curtain at the same time, then occlusion can be observed. As PTWs often weave in and out of the lanes, so they will not be visible to the sensor. Hence this type of sensor will not be useful to our case.

Today, the laser scanner is applied in many systems used in the field of geology, road surveys, for 3D measurements (mining, robotics), sports, construction, the army etc. These devices are very compact and are operational either indoor or outdoor. Many manufacturers have developed systems allowing new applications easily available. Here are a few working principles of the laser scanner.

### 1.5.1.3. Different working principles

In today's world, laser scanners are based on several working principles. Each principle is used in different technologies as follows:

Laser scanners have numerous advantages such a high angular resolution because of their short wavelengths, a higher signal to noise ratio that helps measure long distances with precision at an affordable price, light weight and mobility. Laser scanners acquire data in different ways, as shown in the chart below in Figure 6.

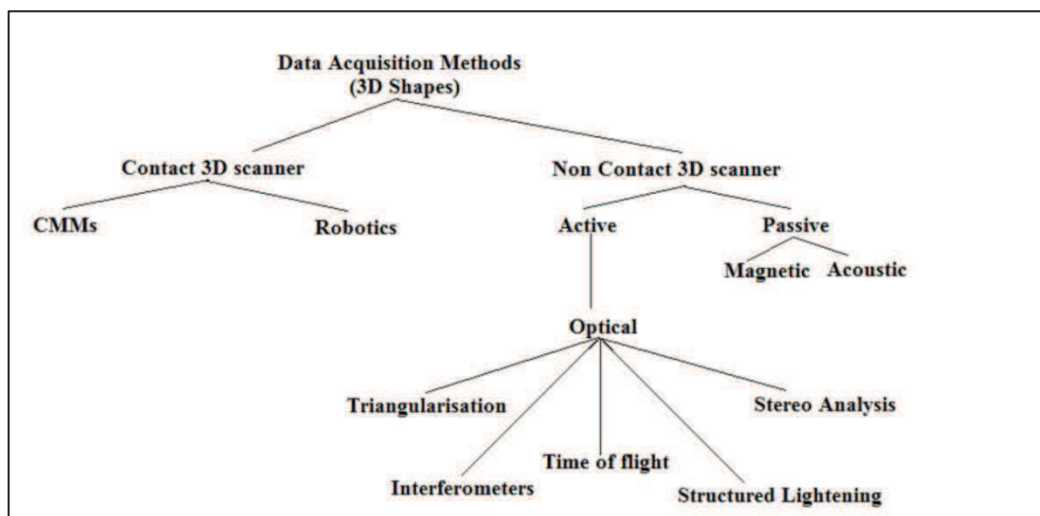


Figure 6: Different acquisition applications [BERG04][FUMA11]

The basic goal of this part is to choose the right type of laser scanner that can be mounted easily above the road and will not be easily affected by climatic conditions such as change in temperature, rain, fog, etc. Some of the different techniques for calculating distance, depending on the applications [BERG04][OHTA04][FUMA11] are: Phase Difference, Doppler, Interferometry, Triangulation and Pulse Timing or Time of flight (Tof).

- Phase Difference uses a carrier wave that is modulated at different wavelengths. As the name suggests, the phase between the transmitted signal and the received signal is determined and the distance can be calculated in terms of an integer number of wavelengths and a fraction of a wavelength which is determined by the comparison of phase. This technique helps to calculate distance with a high precision, but is very sensitive to a sudden change in environment such as luminosity and of course in the real-time traffic scene, PTWs travel with random and fast speed, the environment is prone to random noises linked to the environment. Moreover this type of laser scanner returns non defined values (error values) if the laser beams does not find any object in its range.

One of the prominent manufacturers using this technology is Lecia [w6] and for traffic measurement, such laser scanners are very expensive. They are not very suitable for our research work, however, firstly because we are working on the reconstruction of traffic which is very random and prone to noise. [NEJA06][PFEI07], secondly because we need a system

which is not expensive to use and thirdly we needed a scanner very commonly used for the traffic classification.

- The Doppler technique compares the received frequency with the transmitted signal as a function of time. This change of frequency helps to calculate the range between the receiver and the observer. The technique is used in some of the earlier satellite positioning systems. However, it measures relative positions and does not give the absolute measurement. Hence, it is not very adaptable for our research work.
- The Interferometry method measures small distances with a high accuracy in micrometres. The measurement area, however, is relatively small and it is necessary to strongly stabilise the laser frequency, so this type of laser scanner is best used for indoor purposes only.
- The Triangulation method is used by the sensors having a laser, a detector and a lens placed before the detector. The laser beam is emitted onto the surface of an object and is then reflected back to the detector through the lens. Depending on the position of the reflected beam on the detector, the angle is calculated and therefore the height of the object from the sensor can be known. This method can measure distances with a high accuracy, resolution and speed. However, it can be affected if the target surface is irregular or susceptible to interference and also the laser beam can be dangerous. In a traffic scene, the vehicles present (PTWs, LVs, HVs, etc) may have irregular shapes with shiny surfaces and thus may generate false values. Triangulation therefore may not be adaptable to our research work [FRAN05][NEJA06][PFEI07].
- The Pulse timing method is based on the principle of measuring the time that the signal takes to do a round trip from a laser scanner to a reflective surface. When the system emits a laser pulse towards a fixed target, it triggers a chronometer at the same time. The pulse reflected by the target, reaches the laser scanner, and hence stops the chronometer. As the speed of light is constant and the time of the journey to and fro is known, the distance  $d$  is finally given by the simple relationship:

$$d = \frac{c\Delta T}{2} \quad (1.1)$$

where  $c$  is the speed of light and  $\Delta T$  is the time taken by the rays to do the round trip. The value is divided by 2 to get the distance between the sensor and object.

A laser scanner using the Tof technology was chosen due to its numerous advantages. The computation time is the shortest since this system only requires a single measurement to determine the distance. The value measured is very precise. The technology is used in Radars, Loran, Satellite Altimetry, Airborne Radar Altimetry, Lunar Laser Ranging, Lidars, etc. and is the most suitable for our case.

Before discussing the methods proposed in different research studies on the sensor, a brief summary of the different brands of laser scanner existing in the European market and used for traffic measurement is given below in Table 6. Scan rate is the number of scan points obtained per second. Scan angle is the maximum angle of scan. Max range is the maximum range till which the scanner can scan.



Brand	Model	Angular resolution	Scan rate (pts/sec)	Scan angle (°)	Min Range (m)	Max Range (m)
Lecia	Scan station C5	0.5° to 1.5°	25000-50000	360 Hori. 270 Vert.	0.006	300
	HDS 7000	NA	>10000	360		180
	HDS 8800	NA	8800	360	0.1	2000
Hokuyo	UTM 30 LX	0.25°	1000	270	0.01	30
SICK	LMS 1xx	0.5° to 1°	2500-5000	270	0.5	20
	LMS 2xx	0.25° to 1°	500-2000	180	0.5	80
	LMS 5xx	0.25° to 1°	2000	190	0.7	65

**Table 6: Comparison of laser scanners. \*Scans in a straight line**

### 1.5.2. Applications

When it comes to the detection of moving objects using a laser scanner, the main problem is that the detection and classification depend on the type of object and the environment in which the laser scanner is placed. The main difficulty is dealing simultaneously in the scene with both static and dynamic objects having variable speeds. This is a general problem in our case as well. For example, in the city of Paris, traffic jams are a regular problem but these jams do not affect the circulation of PTWs as they move in between the immobile vehicles.

A lot of work has been done in detecting objects with a laser scanner. Our research work focuses on both the technical and the scientific aspects of the road safety applications of these laser scanners. This section is subdivided into two parts: technical applications and scientific applications.

The technical applications section details different systems using laser scanners that are functional, working in real-time and are deployed on roads, while the scientific applications section explains the research (conference / journal) publications or laboratory prototypes for vehicle detection, pedestrian detection and 3D road reconstruction.

#### 1.5.2.1. Applied applications

Here are a few applications that are employed today on the road for the detection of vehicles with the aim of improving road safety:

- **Electronic toll plazas:** Laser scanners are mostly installed above each lane of the toll plaza and activate an automated vehicle identification system. This type of toll plaza can be seen on most of the motorways in France.
- **Dimension detectors:** For safety reasons, laser scanners are used to detect the dimensions of vehicles passing through tunnels. Some examples can be seen at the entrances to the Fréjus tunnel in the south of France, to the A13 tunnel near Paris and usually at the entrances to car parks.
- **Speed monitoring and inter-vehicular distance calculators:** This system consists of a laser scanner at the side of the road that scans the passing vehicles' profiles. This helps the system to estimate the speed and to find inter-vehicular distances [w5].
- **Counters:** Laser scanners are also used as counters on the road, for counting vehicles and pedestrians [Tana10][Furs00][NIPO12][w5].

- Heavy vehicle eco-tax calculator: This is an association of multi-sensors which is used in France for detecting and taxing heavy vehicles.

Here are a few industries and industrial products that use laser scanners to count different vehicles and are quite well known in the European market.

- ECTN proposes two SICK single-laser scanners (LMS111) for each lane. One is perpendicular to the road, the other at 45° to the normal. The 45° position widens the laser beam projection, thus increasing the scanning region. This combination of two laser scanners is named Traffic Information Collector (TIC102). The technology is said to classify up to 28 different classes of vehicles.
- OSI optoelectronics propose automatic traffic detection sensors used mainly in tolling and traffic management. The system placed alongside the roadway scans the side profile of the vehicles, as they pass through the laser field. The system detects, classifies and provides an axle count for each vehicle.
- TagMaser manufactures a Load Volume Scanner (LVS) to measure load volume without the need for weight to volume conversion. This helps to count heavy vehicles.
- Sensorio is a Belgium-based company, specialised in Doppler-effect laser technologies. They offer solutions for detecting height, width, speed and occupancy of vehicles at toll plazas.
- ADEC Technologies is a Swiss-based company offering several traffic detectors for better traffic management [ADEC12].
- At the end of 2012 in Vancouver, Canada, Egis and Sanef opened the world's largest toll plaza without any barrier, called the free flow [LEMONITEUR13]. This plaza uses a combination of several sensors and is said to have just 3% of detection error.
  - When a vehicle passes under the system, it is recorded by infrared cameras and laser scanner analyzes the vehicle's geometry (length, width and height).
  - Then the magnetic loops confirm the class of the vehicle (LV, HV etc). The vehicles are taxed according to their category by an automated vehicle card reader.
  - At the end, the rear number plate is recorded by the cameras to confirm the presence.
- AutoSense offers several traffic solutions such as AutoSense 600, AutoSense 700, AutoSense 815 which are overhead detection and classification systems using a sensor with a class 1 (safe to human eye) laser scanner and are often found on toll plazas. A single sensor uses a two-beam infrared scanning laser with a beam separation of 10 degrees.
- The Sherlock sensor: This laser radar is an overhead traffic profiler that detects, classifies, counts and gives statistical information about the vehicles passing underneath. The laser scanner scans up to 500 times per second and the system uses a six-beam sensor that covers the entire lane width.
- The 842-Overhead Vehicle Presence (842-OVP) sensor is an infrared passive sensor installed at a certain height of 4 to 6 metres above the highway.



- ClassGard is an Automatic Vehicle Classification (AVC) system proposed by a San-Diego based company named TDS. The system uses a combination of laser scanner, Doppler radar, axle detector and cameras.
- EFKON AG has proposed an Electronic Toll Collection (ETC) for the enforcement of non-intrusive payment solutions. This Austria-based company proposes several traffic solutions that are used by many Asian and European countries.

#### *1.5.2.2. Research applications: Vehicle detection*

On a highway, several categories of objects can be seen such as Light Vehicles (LV), Heavy Vehicles (HV), Powered Two Wheelers (PTWs), and non-vehicular objects such as pedestrians but at the same time we come across different lanes, footpaths, poles, trees etc. To make roads safer, much research work is done on the detection of vehicles, of pedestrians as well as of lanes (lane borders, white lines, etc) and on the 3D route reconstruction, etc.

One of the first articles found for our research, was published in the 1980's [HOFF86]. Since then, there has been an immense change in technology; the demand and the approaches are no longer the same anymore.

Laser scanners can be used in several ways. They can either be mounted on a moving vehicle (thereby becoming dynamic sensors) or can be static (at the side of the road or on a pole). Dynamic laser scanners are most commonly used in the research for the detection of obstacles in front of the vehicle. Usually, multiple laser scanners are combined with a camera and the system is mounted on a vehicle [MICK10][BARG08][IZRI04][STRE04][TYPI08][WU96]. Static laser scanners are used when the environment must be studied from a fixed point [MEND04b][SPAR01][SALO11][DIEW11].

The scanned information about the environment is represented in the form of a laser data map, from which the data must be extracted. There are four approaches to this data extraction: The cluster based approach, the signal analysis method, the motion based approach and the map based method.

- Cluster based approach

The cluster based approach involves the use of clusters of points representing the environment. [BARG08] used a vehicle mounted with several laser scanners working independently on highways and in urban centres. The authors studied the geometrical configuration of objects and also occlusion, in order to distinguish the vehicles present in the scene. [IZRI04] used an omni-directional vision sensor together with a laser scanner mounted on a vehicle. The authors aligned the laser scanner points with a closest to each other (Algorithm of Duda-Hart) and created several clusters. These clusters were then filtered by eliminating the segments of small length but the method is time-consuming and cannot distinguish multiple objects. The idea of introducing boundary boxes [DIET01][FUER02][STRE01] proved to be quite useful to gather the pixels belonging to the same class (clustering) of object. These boundary boxes were calculated by the using the inter distance between the clusters present in the laser scanner image. [ABDE01] gave the idea of calculating the width and height of the vehicle while it is passing under the double rayed beam scanner but this method fails in variant climatic conditions. [XIAN01] proposes to process the laser scanner data by thresholding and clustering and then merging the current laser scanner image with the previous one. To avoid collisions, [MEND04b] integrated an algorithm into a cybercar by using a voting scheme involving several properties of objects to distinguish objects; and a Kalman filter was used to increase the tracking performance.

- Signal analysis method

The signal analysis method uses only signal processing techniques to study different signal output obtained after applying different filters. In a collision avoidance system, [DIEW11] used automotive radar sensors to identify near-collision situation. The author presented a signal processing method (Shannon's theorem, filters such as Chebychev Filters, FFT) to extract information about the driving environment.

- Motion based approach

This approach involves detecting and studying moving objects whose positions vary in time. [HIRA03] presented the line-scan method which is quite robust for light sensitivity but is not efficient when it comes to occlusion. [MONT07] proposed a linear Kalman filter method to segment objects which are then associated with other segments in order to extract objects from the scene. [LEFA02] used the quadratic motion models to define the environment, and then estimated the probable motion between two successive images with a gradient-based multi-resolution robust estimation method. [KAST11] presented a novel way to detect moving objects using a laser scanner to provide the direction and speed of the objects with 3D-measurements of the current surrounding environment, called 3D-Warping. The overall system can be divided into four main parts. The first one handles the raw data, where noise and systematically inaccurate measurements are eliminated. In the second part segmentation clusters the relevant segments in order to satisfy the global and local conditions that correspond to specific features. Then, the feature extraction is carried out. In the third part, 3D-Warping is applied through an intersection analysis to combine the same segments between the two consecutive time-steps  $t$  and  $t - 1$ . Finally, in the fourth part a temporal stabilization is carried out.

- Map based method

This method involves a study of 3D maps using information directly from them. [ROBE00] performed map-matching on the terrain map and then found the group of obstacles by calculating the slope of the terrain. [AYCA11] described an approach for intersection safety. The laser scanner data was extracted by using a local grid map and then the vehicle present in the map was localized by using each individual laser beam. [ZHAO11] used a multi-laser sensing method to process tracking with a trajectory association algorithm. This method used the relationship between a graph-based trajectory labelling algorithm and an EM-based trajectory parameter optimization algorithm. [GOYA08] combined the laser scanner data and a camera image in order to study the data histogram and then used a geometric tri-dimensional model to define the vehicles. [PAGO11] recreated a motor vehicle collision scene from a 3D traffic data using the laser scanner to analyse the dynamics of such events. [WU96] combined a camera with a laser scanner to obtain the information given by both sensors using Dempster-shafar rule of combination.

### ***1.5.2.3. Scientific applications: Pedestrians***

Pedestrians have certain features in common that are similar yet distinctive such as legs, hands, faces etc. For a laser scanner, pedestrians on the road are obstacles sometimes static sometimes dynamic. In this literature, the detection of pedestrians is divided into two main approaches: signature based and motion based.

- Signature based approach

This approach involves a study of the distinctive features that describe pedestrians. [CHEC08] detected pedestrians through a four-plane laser scanner mounted on a car. The authors defined a signature for the pedestrians which helped them to distinguish a pedestrian in the environment. The segmentation was done with a Parzen window. [XAVI05] used the legs as a distinctive feature detected with a single laser scanner. Legs were detected by geometrical relations and the pedestrian profiles were detected with a recursive line-fitting method. The system was mounted on a robot and the tests were conducted in an indoor environment. [FAYA08] used a multisensory system and proposed to exploit geometric features in order to quantify the confidence in the detection process. This confidence was updated by a transferable belief model framework. [MEND04a] suggested aligning the bounding box in the estimated direction of a travelling object. Due to occlusion people's legs or walls were seen in the form of broken segments which were merged by using an inter-distance threshold.

- Motion based approach

Pedestrians may be defined as objects with random movement. This approach involves those methods that either use motion as criteria or use spatial-temporal information. [GATE08a] proposed a recursive method to estimate the true outlines of every tracked target using a set of segments defining the moving obstacle. A Parzen kernel isolates the pedestrians and then a decentralized fusion was carried out. [FURS00] thought of using a high resolution multilayer laser scanner with a 180° horizontal field of view. Based upon the new data, an ego motion is estimated to detect the pedestrians. [GEIG11] built 3D maps from high-resolution sequences in real-time. A sparse feature matcher in conjunction with an efficient and robust visual odometry algorithm is used by combining efficient stereo matching and a multi-view linking scheme to generate consistent 3D point clouds from a laser scanner.

#### *1.5.2.4. Scientific applications: 3D Route Construction*

The construction of route in three dimensions is one of the important road safety applications of laser scanners.

[GOUL06] reconstructed a route by using a laser scanner and a GPS. The laser scanner which gives the raw data is mounted on the vehicle whose position is known through the GPS. The fusion of these two information sources helps to construct road models.

In a similar research work [BRUN07] used a combination of a laser scanner and a fish-eye camera to reconstruct an outdoor environment. The camera adds the notion of colour to the environment scanned by the laser scanner, thus generating a 3D colour textured model of the environment around the vehicle on which the system is mounted.

[HERN09] proposed an automatic method of filtering and segmenting a 3D cloud obtained by a laser scanner. The filtering helps to remove the artefacts while the segmentation helps to extract the contour between the road corner and the route.

[TARE12] compared two methods to calculate the inter-vehicular distance using a 3D generated map. The first approach used a terrestrial mobile mapping laser scanner, while the second used the views taken by the two digital cameras mounted on a vehicle.

## Conclusion

In this chapter a general problem is stated. The number of fatal accidents for this category of vehicles (PTWs) is high and needs attention. It is not easy to directly employ different measures to increase the safety of PTWs unless these vehicles are first detected. Although there are several projects around the world trying to find a concrete solution to this problem, no valid technical solution has been found to date.

Even the different method and state-of-the-art techniques using a laser scanner for the detection of vehicles do not meet requirements. Although, a few solutions have been proposed by industrial actors, they are very expensive and have not proved to be sufficiently robust for the detection of these small vehicles on a large database. However, one study [RIPO12] has been found that does count all types of vehicles (PTWs, LVs and HVs) but in very slow-moving traffic and without provide detailed statistical validation for the different categories of detected and non-detected vehicles. Hence there is still an urgent need to implement a robust method for detecting and counting PTWs in different traffic conditions.

This justifies the report by CERTU [ONSIR11] stating “No concrete research work is has been carried out for the detection of PTWs on urban highways”. Moreover to our knowledge, there is no research project, that solely concentrates on this problem, which is why the METRAMOTO project was launched in 2010.

The main objective of METRAMOTO is to detect and count PTWs on a highway. The proposed solution for this project is intended for use by road administrators. The solution should therefore be cheap, easily deployable on the road, should be as autonomous as possible and should be robust to all the artefacts such as climatic conditions, air turbulences generated by fast moving vehicles, etc. For this research work a laser scanner was chosen out from the four technologies proposed by the ANR METRAMOTO project.

The originality of our work is to detect and count PTWs moving at all the speeds likely to be encountered on an urban highway.

The next chapter will describe the laser scanner that was chosen to meet all the objectives of METRAMOTO. Before installing the scanner, an optimal position for it was chosen by a simulator. Using this scanner, different databases were constructed with real traffic to help us understand the laser scanner data and the different challenges presented by the traffic passing under the system.



## CHAPTER 2: Data Acquisition

---

Introduction .....	31
2.1. Simulator .....	31
2.1.1. Problem statement.....	32
2.1.2. Different configurations.....	33
2.1.3. Description.....	34
2.1.4. Discussion.....	37
2.1.5. Demonstration.....	38
2.1.6. Solution proposed .....	41
2.2. Choice of a laser scanner .....	41
2.3. Road profile .....	44
2.4. Different positions for the laser scanner.....	45
2.5. Data coherence method .....	49
2.5.1. Height.....	49
2.5.2. Road verges.....	50
2.6. Databases .....	51
2.6.1. Controlled site.....	51
2.6.2. Real sites .....	53
Conclusion.....	57

---



## Introduction

To construct the database, it is important to understand the difficulties that exist for the detection of PTWs. Figure 7 shows an example of classical PTW behaviour on the road. We can see that the PTWs are riding between lanes, a common practice with this category of vehicles.



Figure 7: Example of classical PTW inter-lane traffic

It must be noted that for several reasons PTWs are not easy to detect:

- Small size: This category of vehicle is smaller than any other category of vehicle enabling them to move in between two other vehicles (inter-lane) and at a high speed.
- Inter-lane practice: A study conducted by IFSTTAR showed that PTWs travelled on average 85% of their total trajectories on inter-lanes in Paris [AUPE11].
- Occlusion: As they are small and are often between lanes, they are often occluded by the vehicles around them.

The database was created on a controlled site and a real site. By controlled site, we mean that the traffic was controlled, with controlled speed profiles and all the safety norms were taken into account. The real site consists of a highway on which several vehicles of different categories move with variable speeds. Before discussing the database, it is very important to justify the choice of the laser scanner along with the properties of the scanner chosen. In the second part, the profile of the road on which we want install the system is discussed. There are several ways to install a laser scanner. To make a choice of installation, several factors such as road profile, the type of traffic and the behaviour of the vehicles of interest have to be taken into consideration. Hence, the third part justifies this choice. Once the system is installed, data coherence is done which is detailed in the fourth part. The fifth part then gives details about how the database was constructed on a controlled site and on the real site. Before constructing the database, an optimal position of the laser scanner is chosen by the means of a simulator.

### 2.1. Simulator

The main objective of the simulator is to find the position where the laser scanner should be placed, on a gantry, in order to scan as much information about the traffic as possible. This optimal position corresponds to the position where the probability of encountering occlusion on the real site is minimal. This step will help the road administrators to choose the laser scanner position before going to the real site, hence saving time.



To better explain the simulator, this part is sub-divided into several subsections. The first subsection states the problem. The second subsection details the situations (number of lanes and possible positions of the laser scanner) that are taken into account. The third subsection presents the generation of laser scanner data through the simulator. The fourth subsection focuses on the type of traffic that is observed for the simulator. The last subsection explains the results and gives different propositions to get the best possible occlusion-less data.

### 2.1.1. Problem statement

Before defining the problem, it is important to understand the site which has been modelled for the simulator. It is considered that this site can either be a rural road with 1 or 2 lanes or a motorway up to 3 lanes in each direction. Theoretically, each lane is 3.5m wide with a 1-meter wide hard shoulder placed at the side of highways or expressways.

It is important to know that the position of the sensor depends on the nature of object to be detected. PTWs move quite often in the inter-lanes, so, the best possibility to detect this category of vehicle is to mount the laser scanner on a gantry and position it to get the maximum occlusion-free PTW data.

The first and the foremost step is to define occlusion. An occlusion may be defined as the missing data that cannot be observed when the laser scanner rays touch an object which is dense enough to prevent the rays from passing through it, hence shadowing the objects behind it. In simple terms, occlusion is observed when an object blocks the laser scanner rays thus making other objects behind it invisible. This can be seen in Figure 8.

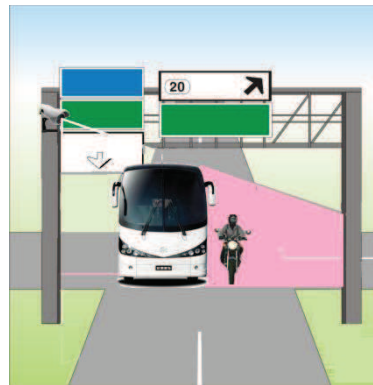


**Figure 8: Occlusion of a PTW by an HV**

Figure 8 shows an example of typical occlusion. The system is placed at the left side of the gantry, the HV occludes the PTW. The occluded region is represented in pink.

The occlusion depends on several factors:

- Height of the laser scanner above the road
- Displacement of the vehicle with respect to the position of the laser scanner
- Height of the vehicle that creates the occlusion
- Density of traffic is an important factor. This factor is directly proportional to the probability of observing occlusion. In other words, when the traffic is dense, large vehicles tend to overlap the small vehicles, hence creating the effect of occlusion.

This occlusion can be calculated theoretically by taking into account all the factors cited above. This is shown in Figure 9.

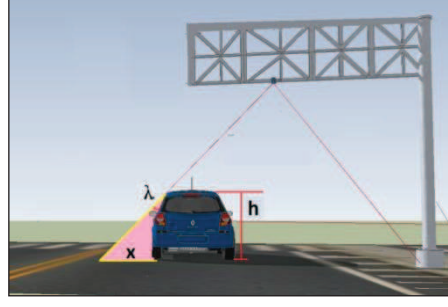


Figure 9: Calculation of shadow

Figure 9 shows the process of occlusion where  $h$  is the height of the vehicle,  $\lambda$  is the angle of projection of the laser that touches the border of the vehicle and  $x$  is the length of the region where the laser beam does not fall and thus cast shadow. This occluded area is directly proportional to the height of the vehicle and the tangent of the angle  $\lambda$ . This relation is given by the following equation:

$$x = h \cdot \tan(\lambda) \quad (2.1)$$

Another factor that affects the non-observed area is the position of the laser scanner. The position has to be chosen with respect to the number of lanes that we intend to scan, the nature of the object of interest and the power of the laser scanner. The nature of the object of interest is especially important. In our case, the goal is to detect and count PTWs which are most often found in the inter-lanes.

Taking all these factors into consideration, a simulator is proposed that studies different positions of laser scanner that is mounted on different road profiles (2-lane or 3-lane carriageway) with an aim to find an optimal position that generates minimum occlusion.

### 2.1.2. Different configurations

In this simulator, two different situations have been presented; the first situation consists of 2 lanes and the second of 3 lanes.

A standard theoretical value of 3.5 metres for each lane is taken and it is presumed that the laser scanner is placed at a variable user-defined height between 5 and 6 meters. These heights correspond to the height of gantries, bridges or poles where the laser scanner is installed in real life.

Figure 10 shows the simulated 2-lane and 3-lane carriageways. A 2-lane case is represented with a total width of 8 metres where 3.5 metres is the width of each lane and 1 meter as the width of the hard shoulder. A 3-lane case is represented with a total width of 13.5 metres with each lane of 3.5 meters each and 2 hard shoulders of 1 metre each.

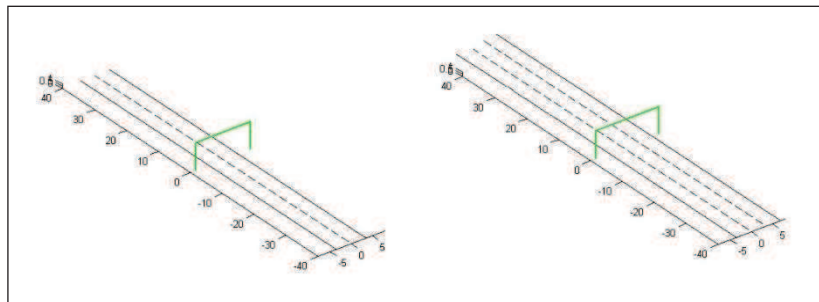


Figure 10: Simulated carriageway (Left) 2-lane and (Right) 3-lane

A reconstruction of different possible laser scanner positions is done in Figure 10. In a 3-lane problem, the lanes are numbered 1 to 3 starting from the extreme left lane, Lane 1 with the fastest traffic.

- Situation 1
  - Above the centre point between the two lanes (Inter-lane).
  - Above the far left edge.
  - Above the far right edge.
- Situation 2
  - Above the far left edge.
  - Above the far right edge.
  - Above the inter-lane of Lane 1 and Lane 2.
  - Above the inter-lane of Lane 2 and Lane 3
  - Above the centre point of the three lanes (middle of Lane2).

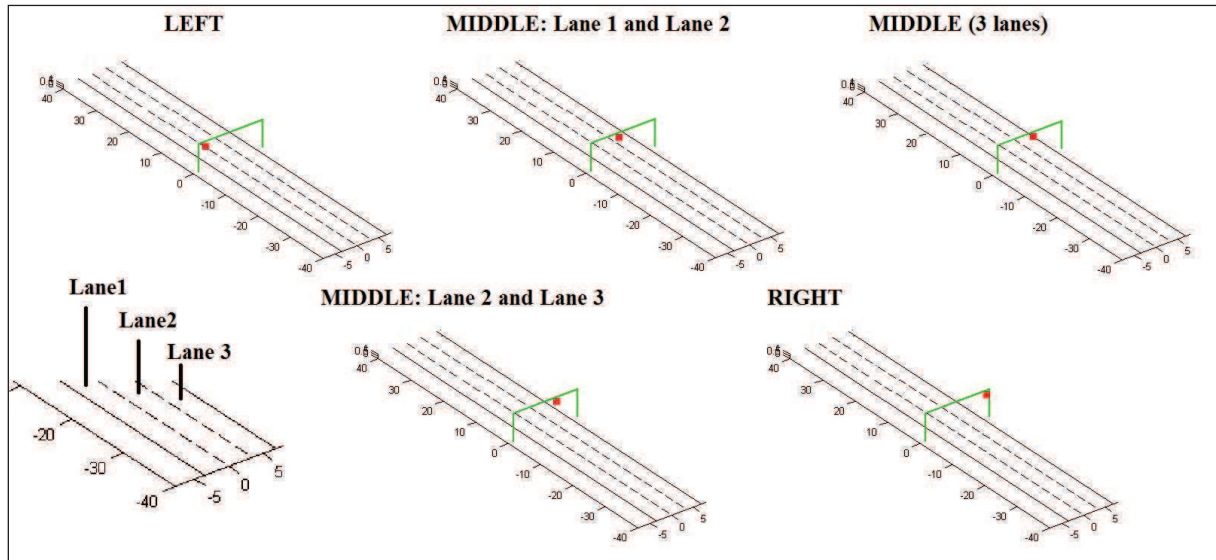


Figure 11: Example of different possible ways to mount a single laser scanner on a gantry when we have 3 lanes

Figure 11 shows an example of all the possible ways of mounting a laser scanner above three lanes. For the simulator, the lane next to the hard shoulder is considered as Lane 1 and the furthest away as the Lane 3.

### 2.1.3. Description

Once the situations and the ways of mounting the laser scanner are defined, we must define the projection angle of the laser scanner installed on the road.

As soon as the laser scanner is positioned, its height is registered. As the goal of simulator is not to study the effect of high speed of vehicle on the laser data, an angular resolution of  $1^\circ$  and the scanning angle of  $[-45^\circ \text{ to } 225^\circ]$  are taken. The distance  $\rho$  is calculated by estimating the interaction of the laser scanner beams with the road.

The following notation is defined:

Vehicle: For each vehicle, a length ( $V_L$ ), Width ( $V_W$ ), height ( $V_H$ ), Speed ( $V_S$ ) and position ( $V_P$ ) is defined.

Road: Let the two extremities of the road be  $ext_L$  (extreme left) and  $ext_R$  (extreme right), respectively. For two lanes in this simulator the middle of the two lanes (inter-lane) is indexed as 0 and the width of each lane is 3.5 metres.

Laser scanner: Let,  $h$  be the height of the laser scanner above the road and  $LR_p$  be the position of the laser scanner placed on the gantry. The scans are registered as segments. Each segment contains the coordinates of the object scanned and the corresponding height. A point 'A' is defined as:

$$Point = \begin{pmatrix} x_A \\ h_A \end{pmatrix} \quad (2.2)$$

where  $x_A$  is the  $x_{coodiante}$  at point  $A$  and  $h_A$  is the corresponding height.

The general format of this segment  $AB$  is:  $Segment = \begin{pmatrix} x_A & x_B \\ h_A & h_B \end{pmatrix} \quad (2.3)$

This segment estimation is carried out as follows:

- If there is no vehicle: Only the extremes of the road i.e.  $ext_L$  and  $ext_R$  are taken into consideration. In this case, as there is no object, no height will be registered. The segment will be as follows:

$$\begin{pmatrix} ext_L & ext_R \\ 0 & 0 \end{pmatrix} \quad (2.4)$$

- If there is a vehicle: The two extremes of the road, the left extreme and the right extreme of the vehicle are also taken into consideration. So, the segment will be as follows:

$$\begin{pmatrix} ext_L & V_{ext_L} & V_{ext_L} & V_{ext_R} & V_{ext_R} & ext_R \\ 0 & 0 & V_{H_{ext_L}} & V_{H_{ext_R}} & 0 & 0 \end{pmatrix} \quad (2.5)$$

where  $V_{ext_L}$  and  $V_{ext_R}$  are the vehicle's extreme left and extreme right coordinates and  $V_{H_{ext_L}}$  and  $V_{H_{ext_R}}$  are the vehicle's height at the extreme left and the extreme right. It is to be noted that  $V_{ext_L}$  and  $V_{ext_R}$  have two heights, 0 (for base values) and  $V_{H_{ext_L}}$  and  $V_{H_{ext_R}}$  (for the points representing the top of the vehicle), respectively. This can be seen in Figure 12.

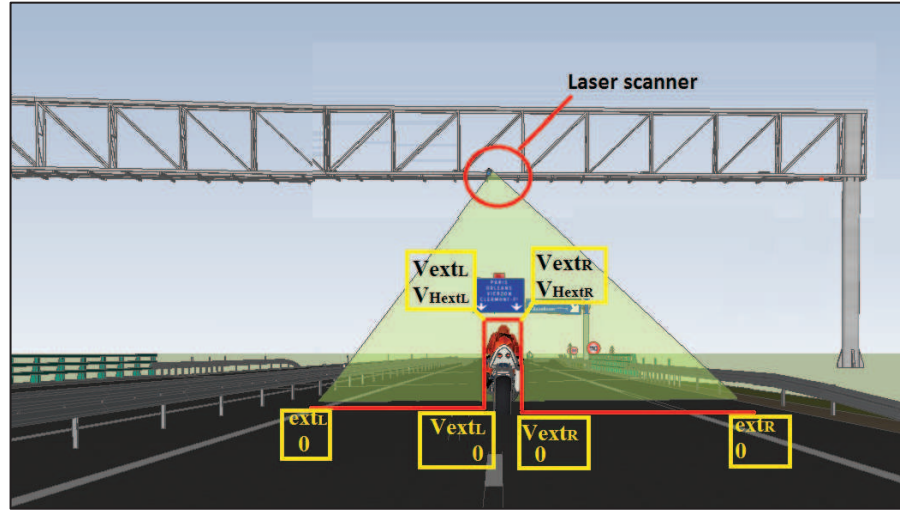


Figure 12: Simulated example of the segment

Figure 12 shows a simulated scene where a laser scanner placed on a gantry at a height  $h$ . The two extremes of the road are  $ext_L$  and  $ext_R$ . The coordinates of the vehicle in the simulator are given in yellow and are presented in equation (2.5). This box is placed at the coordinates  $V_{ext_L}$  and  $V_{ext_R}$  and the two corresponding extreme heights of the box are  $V_{H_{ext_L}}$  and  $V_{H_{ext_R}}$ .

For each beam angle  $[-45^\circ \dots 225^\circ]$  we find the intersection of each segment by a linear system.

The value of  $Rho$  can be estimated by:

$$Rho = \sqrt{(Ip_{Xcoordinates})^2 + (h - Ip_{Height})^2} \quad (2.6)$$

where  $Ip_{Xcoordinates}$  are the coordinates of  $X$  for a scan and  $Ip_{Height}$  is the corresponding height for each  $X_{coordinate}$ .

For the simulator, three types of vehicles were defined: a PTW, an LV and an HV. Each of these vehicles is represented by a box having the dimensions of the vehicle (taken from the constructor, Suzuki (PTW) and Renault (LV and HV)). These makes were used because they were already used in the CETE NC test vehicle fleet. Thus the data estimated by our simulator can be easily verified in real life. The size of each vehicle in metres is given in table 7.

Type of vehicle	PTW	LV	HV
Length (m)	2.0	3.8	13.6
Width (m)	0.7	1.8	2.2
Height (m)	1.8	1.5	2.6

Table 7: Simulator vehicle dimensions

Using boxes having the above described dimensions, a simulated traffic was created consisting of two HVs, two LVs and one PTW and representing the most commonly found situations on the road.

For Situation 1, where there are 2 lanes, two cases are discussed:

- Case1: A PTW followed by an LV in Lane1, an HV in Lane2 moving side by side to the PTW.
- Case2: A PTW in between 2 HVs (Inter-lane case).

Situation 2 corresponds to the three-lane problem and only one situation is discussed:

- Case3: A PTW followed by an LV in Lane1, an HV in Lane2 and an LV in Lane 3.

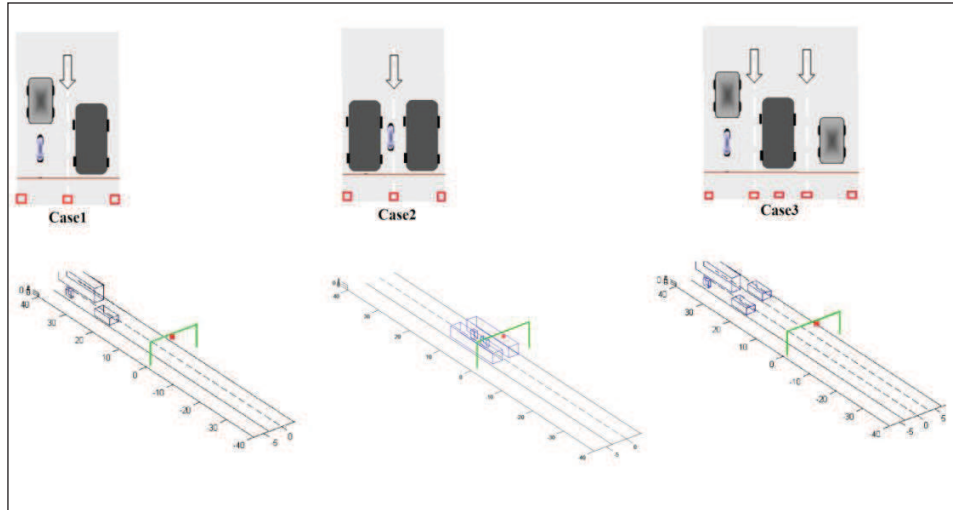


Figure 13: An example of the cases simulated. (Above) Laser scanner position represented in red box. (Below) corresponding simulator scenes.

For each of these cases, the laser scanner was placed in different positions as explained earlier. An example of the three cases described above is shown in Figure 13. The red boxes correspond to the positions of the laser scanner.

#### 2.1.4. Discussion



Figure 14: Simulator

Figure 14 shows the graphic interface of the simulator. On the left, is given a choice of either 5m or 6m for the height of the laser scanner.

In a 2-lane problem, for each height, the laser scanner can be placed in 3 different positions on the gantry, above the inter-lane, above the far right edge of the carriageway and above the far left edge.

In a 3-lane problem, the lanes are numbered 1 to 3 starting from the extreme left lane, Lane 1 with the fastest traffic. For each height, the laser scanner can be placed in 5 different positions on the gantry,



above the inter-lane of Lane 1 and Lane 2, above the inter-lane of Lane 2 and Lane 3, above the centre point of the three lanes (middle of Lane2), above the far right edge of the carriageway and above the far left edge.

Before demonstrating the simulator it is necessary to understand the shadows cast by the vehicles that may occlude the PTW. It is to be noted that only the shadow cast by a higher or wider vehicle may occlude the smaller vehicle. For an HV with a height of 2.4 m the shadow cast can be estimated by using equation 2.1.

$$x = 2400 \times \tan(\lambda)$$

Let us consider that a PTW with a height of 1.8m, width of 0.7m, is moving with an inter-lane distance of 1m with this HV of 2.4m. It means that if the value of  $x$  (cast shadow) is superior that 1.7m (1m inter-distance + 0.7m PTW's width), the PTW will be completely occluded. So, for  $x < 1700$ , the value of  $\lambda$  must be less than  $35^\circ$ . This means that if a beam falls at an angle of  $35^\circ$  from the normal on a 2.4m high vehicle it will cast a shadow capable of occluding a PTW.

This occlusion can be calculated using equation 2.1, thus obtaining  $x = 1680\text{mm} < 1700\text{mm}$ . Therefore partial occlusion can be observed.

### 2.1.5. Demonstration

For the simulator, several cases were created. These cases were created for either two or three lane traffic.

#### 2.1.5.1. Two lane traffic

Here two cases have been implemented:

Case1: A PTW is followed by an LV, and in the adjacent lane, an HV travels parallel to the PTW. In this traffic condition, the laser scanner is mounted at different positions. When laser scanner is mounted above the extreme right of the gantry and the HV blocks the laser beams, thereby creating semi or complete occlusion.

Case2: An HV is travelling on each lane with a PTW moving in between them (on the inter-lane). This is a classical case which can be seen on Parisian roads. It is to be noted that the PTW passes under the scanner at the same time as the 2 HVs. An inter-vehicle distance of 0.8m between the PTW and the HV is taken. Different scenes can be discussed as follows (Figure 15). The images below are shown between scan points (index of laser beams) and accumulation of scans (concatenation of scans during time  $t$ ).

- If the laser scanner is mounted on a gantry above the edge of the left lane, the length of the shadow cast by the HV is higher than the sum of the PTW's width and the inter-distance of the PTW and the HV. Hence it gives an impression as both the HVs are combined as the inter distance between the HVs is inferior than the shadow cast. This can be seen in Figure 15 that is given by the simulator.

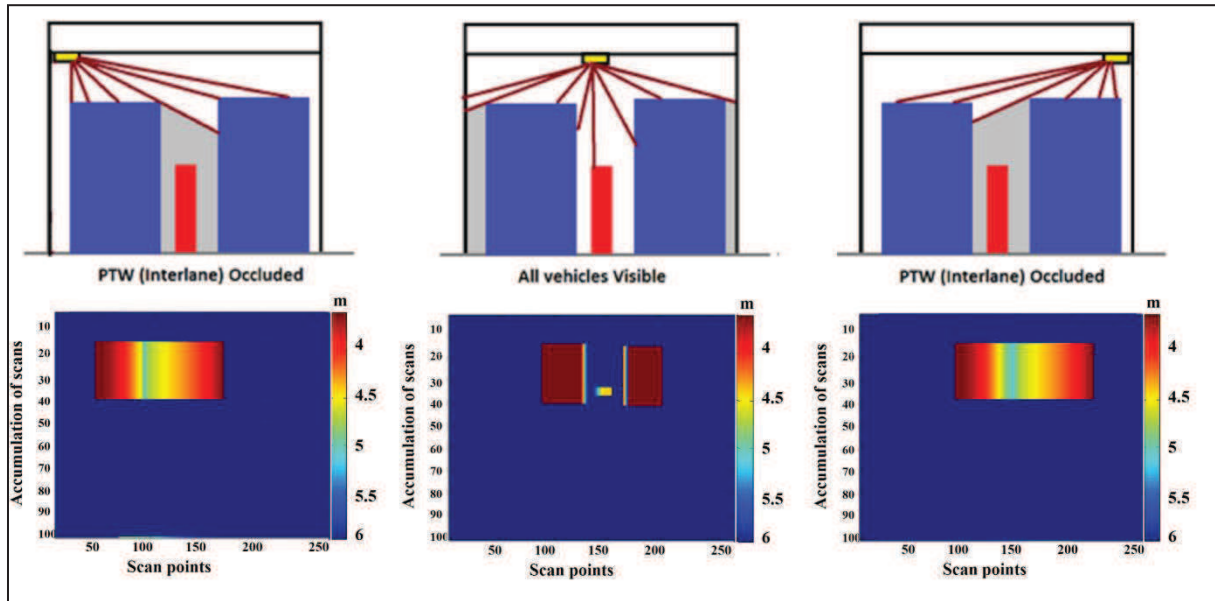


Figure 15: Two lanes simulation with inter-lane traffic

- If the laser scanner is mounted on a gantry above the centre point between two lanes, the shadows are not cast on other vehicles, hence no occlusion is observed. It is to be noted, however, that if any vehicle travels on the hard shoulder, parallel to an HV, it will be invisible to the system.
- The visibility of vehicles moving in the inter-lane could be improved by placing the unit at a height of 6 metres, but it would not be enough to separate the vehicles, thereby generating indistinguishable combined vehicle forms.

In both of these cases (1 and 2) discussed above, in order to detect all the vehicles travelling in two lanes, the best possible solution is to install the laser scanner above on a gantry at the centre point of two lanes. The difficulty level increases with a 3-lane traffic.

### 2.1.5.2. Three lane traffic

In a 3-lane traffic case, only one situation has been implemented. (Figure 16)

As explained above, there are many possible positions for the laser scanner, but the complexity increases with three lanes. The traffic chosen for the 3-lane carriageway is: a PTW with an LV moving behind in the first lane, an HV in the second lane and an LV in the third lane.

From the information shown by the images in Figure 16:

- If the laser scanner is mounted at the extreme left of the gantry, the PTW travelling on the extreme right lane will get occluded by the HV travelling in the second (middle) lane.
- If the laser scanner is mounted above the centre point of two lanes (Lane 1 and 2), part of the PTW can be seen but combined with HV (effect of occlusion). This position will cover all the vehicles travelling on and between the Lane 1 and Lane 2.



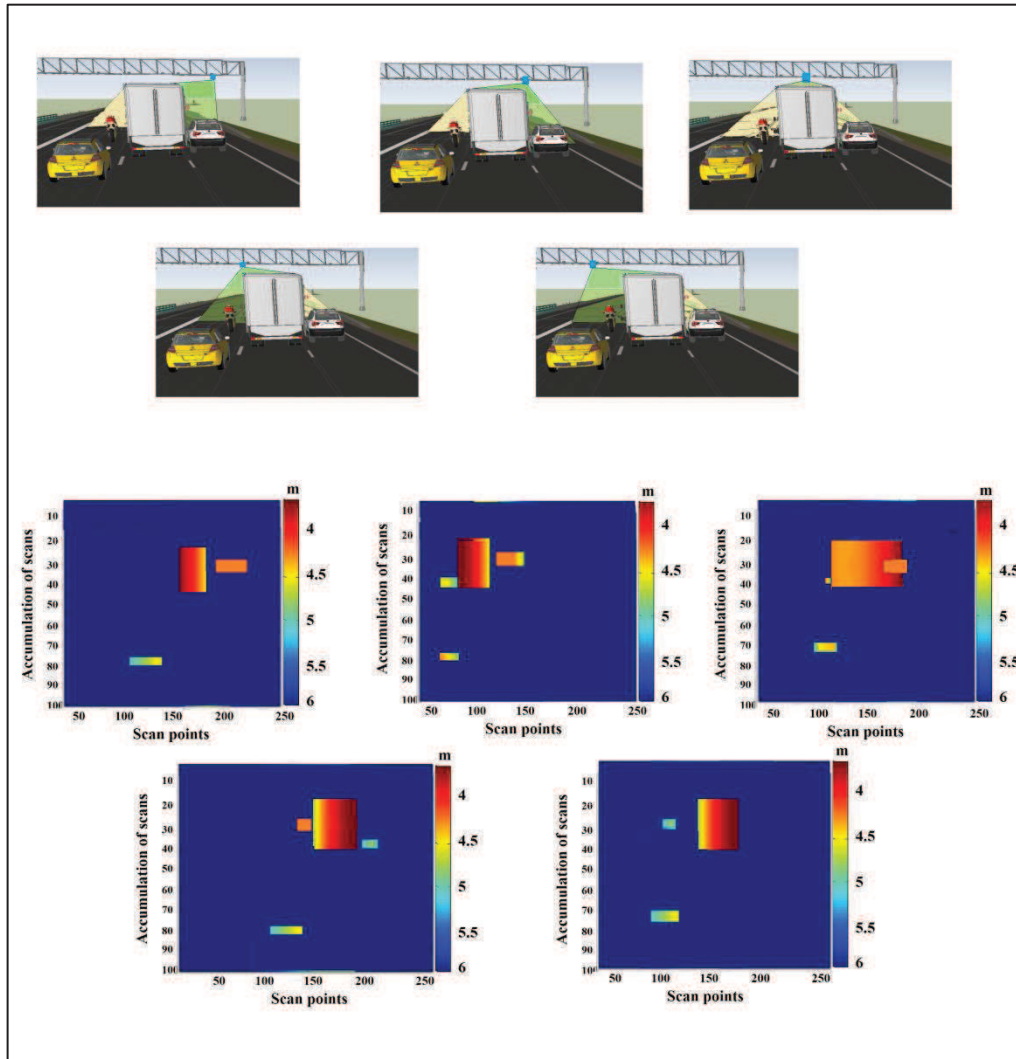


Figure 16: Case 3 simulated data

- When the laser scanner placed above the middle of three lanes, i.e. above the centre point of Lane 2, an effect of combined vehicles is observed i.e. several vehicles form a single vehicle due to the laser scanner beams blocked by the HV.

### 2.1.6. Solution proposed

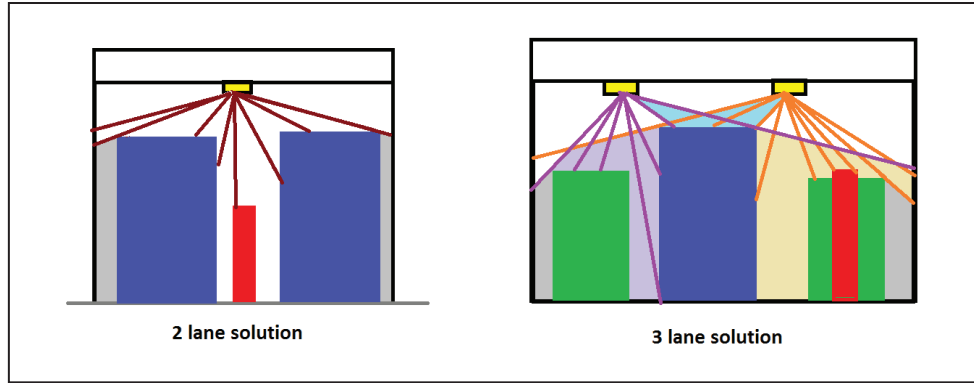


Figure 17: Optimal solution for two and three lanes

Figure 17 shows the best suitable laser scanner positions for 2-lane and 3-lane carriageways. When there are 2 lanes, placing the laser scanner above the centre point between them seems to be an optimal solution to have a minimum chance of occlusion. Taking a scanner with a higher angular resolution can be a solution but in all cases no sensor can see through objects, thus this problem of occlusion cannot be overcome with a single laser scanner.

With the 3 lanes, using two laser scanners is an optimal solution. One scanner must be placed above the middle of Lane 1 and Lane 2 while the second above the centre between the Lane 2 and 3.

For a 3 lane carriageway, the proposed solution remains expensive as two laser scanners instead of one are needed, but there is always a compromise needed either with cost or the quality of result desired. However, for this research work, we are restricted to one scanner laser.

## 2.2. Choice of a laser scanner

For this research work, a system able to detect, classify and count vehicles is needed. This system is to be mounted above the highway either on a bridge, a gantry or a pole having a height of 5 metres to 6 metres that could cover at least 2 lanes. As we are short in terms of budget in this research work, we opted for a single laser scanner to obtain all the two-lane traffic data.

For a vehicle to be really detected by a scanner, at least 2 consecutive scans are needed, meaning that a minimum time of contact is required for the scanner to read these 2 scans. This time corresponds to  $t$  ms which may vary with the type of laser scanner used.

The reason of setting two consecutive scans as a threshold is that one single scan may correspond to a noise. But having two consecutive scans, with a minimum threshold height (0.4m), validates the presence of a vehicle. This threshold of 0.4m corresponds to the height of the LV's bumper.

In our case the length of the PTW is presumed to be 2 m.

Let  $F_c$  be the frequency of the laser scanner and  $T_c$  be the time taken by the scanner to complete a scan (to and fro). Hence,

$$T_c = \frac{1}{F_c} \quad (2.7)$$

$L_{ptw}$  is the length of the PTW and  $V_{ptw}$  the speed of the PTW. Time for the PTW to pass entirely under the laser scanner (considering that the first beam of the scanner falls at the start of the PTW)

$$t = \frac{L_{ptw}}{V_{ptw}} \quad (2.8)$$

Hence the number of scans is:

$$nb_{scans} = \frac{t}{T_c} \quad (2.9)$$

Figure 18 shows a graph of the relationship between the number of scans and the speed of the PTW when passes below a laser scanner scanning at different frequencies.

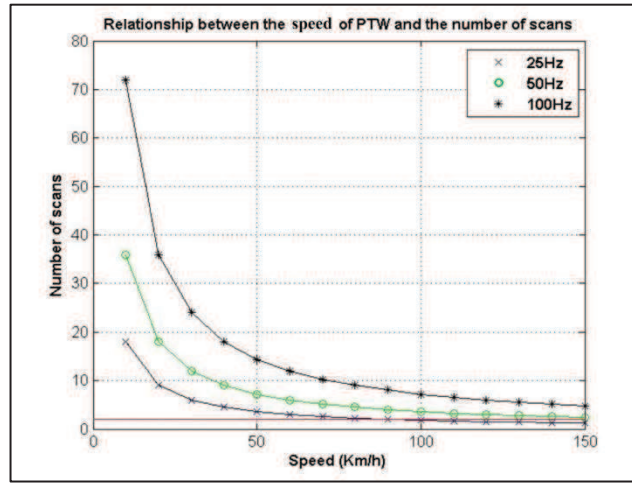


**Figure 18: Relationship between speed (0km/h to 150 km/h) of PTW and number of scans. Red line corresponds to the limit of the data acquisition (2 scans) for a PTW with a length of 2m.**

Figure 18 shows that at 25 Hz, the laser scanner has less time to obtain sufficient number of scans when the PTW is travelling at more than 80 km/h the PTW will not be visible to the laser scanner. At 50 Hz, however, the PTW remains visible up to 144 km/h. When the scanning frequency is at 100 Hz, the PTW is visible even at 180 km/h.

If a vehicle of 2m long is moving at a speed of 40m/s (144km/h) under the laser curtain, it will take 1/20s to pass under the laser scanner. A laser scanner at 50Hz will take 20ms to complete one scan. Hence, the laser scanner can scan up to a maximum of 2 scans in this time. This information might be sufficient to extract a vehicle from the scene but not to classify correctly. This remains one of the limitations that has to be taken into account while choosing a laser scanner. One of the solutions is to upgrade the type of laser scanner (100Hz) or use multiple laser scanners.

The laser scanners with a scanning frequency of 100 Hz or more are usually quite expensive and one of the most important considerations when choosing a system will probably be the price of the sensor. The system is meant to be simple and affordable to any sector (public, private or any other). Hence although the Velodyne, Lecia, Hukoyu or Adec laser measurement devices may provide greater coverage or accuracy, they are priced well above the products of SICK. A list of sensors is shown in ANNEX 1.

Hence, the SICK Laser Measurement System (LMS) 111 [SICK08] was pre-selected for this research work. It is one of the simplest and cheapest laser scanners that exist on the market with a price tag of 6000€. The laser scanner can be placed above the centre points between two lanes, hereafter called the

inter-lane and at a certain height (usually 5 to 6 metres) on a gantry or the underside of a bridge with unknown environments and climate conditions. The reason for installing laser scanner above an inter-lane is that most of the time this is where PTWs travel. Hence, with a range of 20m, this scanner can easily scan both lanes correctly.

The LMS111 laser scanner is a non-contact measurement system (NCSDs) that scans its surrounding in two-dimensions (distance and angle). The specification of the LMS 111 (Figure 19) is as follows:

- Scanning angle : from  $-45^\circ$  till  $225^\circ$  (i.e.  $270^\circ$ )
- Angular resolution :  $0.25^\circ$  or  $0.5^\circ$
- Scanning frequency : 25 Hz or 50 Hz
- Distance measuring range : up to 20 m



Figure 19: LMS SICK 111(Left). Installation of the laser scanner on the experimental site (Right)

To correctly detect an object, the laser beam must be fully incident on it. For information to be correctly retrieved, the reflected ray should have a minimum amount of energy. If the beam falls partially incident to the plane, the reflected ray may have less energy than the minimum energy necessary for the information to be retrieved. Figure 19 shows the LMS SICK 111 and its installation on our experimental site.

The information given by the laser scanner varies as a function of the following parameters:

- Height of the laser scanner: the higher the position of the laser scanner, the less reliable the information gathered becomes. While placing the sensor on a road, this parameter must be taken into account, as the road is shared by many categories of vehicles with variable heights, such as motorbikes (usual PTW height  $\sim 1.80$ ), and Heavy Vehicles (usual HV height 4m). There is, therefore, a compromise between the height of the laser scanner and the intensity of information to be retrieved.
- Beam diameter: As the distance of the laser scanner from the objects increases, the beam diameter of the scanner increases. The height-dependent beam diameter  $R$  is given by:

$$R = d \times 0.015 + 8 \quad (2.10)$$

The value 8 is the beam diameter at the optical cover in millimetres and  $0.015 \text{ rad}$  is the expansion angle of the laser rays per millimetre. The height-dependent beam diameter is given in table 8.

Distance (mm)	2000	3000	4000	5000	6000	7000
R (mm)	38	53	68	83	98	113

Table 8: LMS 111 Laser beam expansion

- Distance between each laser point: The distance between individual measured points increases when the distance of the object from the laser scanner increases. The distance between the measured points is also dependent on the configured angular resolution. The distance-

dependent spacing between the measured points is defined by the tangent of the angular resolution multiplied by the distance (Figure 20).

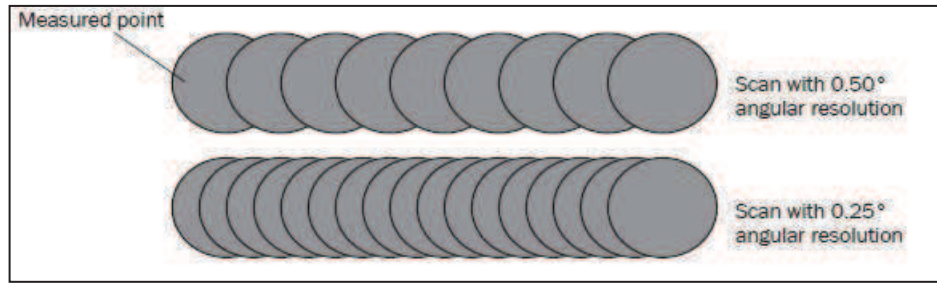


Figure 20: Distance between measured points [SICK08]

This single-planer laser scanner gives data in  $\rho$  and  $\theta$ , where,  $\rho$  is the distance in millimetres between the laser scanner and the object and  $\theta$  is the angle in degrees of the laser scanner. So, in a scan, for each 541 value of  $\theta$  there is a corresponding value of  $\rho$ .

### 2.3. Road profile

One of the major problems for the detection of PTWs is the behaviour of the rider during difficult traffic conditions such as traffic congestion or jams. So, it is important to study the site or the type of road on which we want to install the sensor in order to find an optimal configuration for easy retrieval of information irrespective of traffic conditions.

As explained in the section simulator, the site has a certain profile, from a rural road with 1 or 2 lanes to a motorway up to 3 lanes in each direction. These lanes have different speed limits according to the safety norms. Classically each lane is 3.5m wide but this value may vary from 3.2m to 3.6m depending on the terrain. A 1-meter wide hard shoulder is often placed at the side of highways or expressways (Figure 21). In France, expressways generally have two lanes with a maximum allowed speed of 90km/h to 110km/h while motorways have two to four lanes with a maximum authorised speed of 130 km/h. An example of a simulated scene is shown in the Figure 21.

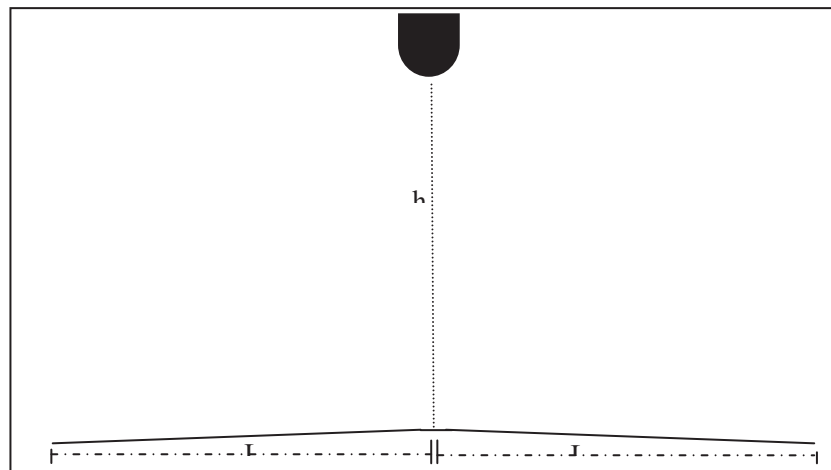


Figure 21: A simulated scene. Laser scanner installed at height  $h$  and above the centre point between two lanes. Each lane measures  $L$  metres.

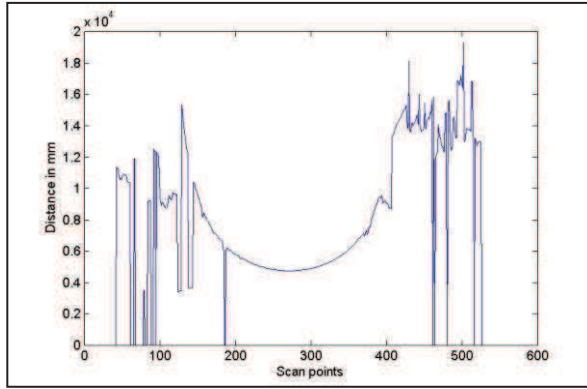


Figure 22: Empty scan

Figure 21 shows a laser scanner (in black) installed at a certain height  $h$  and above the centre point between two lanes. Each lane has a width of  $L$  metres, which depends on the profile of the road. The road is not exactly flat, but has a certain camber to allow proper drainage.

Figure 22 shows an example of an empty scan corresponding to the laser scanner reading when no vehicle is passing under the sensor.

The road is represented by the signal (laser scanner return values) in the form of an arc. This

arc is our Region of Interest (ROI) where the probability of finding vehicles (PTWs) is maximum, i.e. road.

## 2.4. Different positions for the laser scanner

There are several configurations for a laser scanner. As indicated earlier, each configuration depends upon the type of object to be detected, the problems that might be encountered (occlusion, artefacts) and also the zone to be covered.

**Roadside mast-mounted:** The first possibility is a roadside mast-mounted configuration (Figure 23). A sensor processes a field of view covering an oblique area that can be upstream or downstream of the unit. This configuration will cover the vehicle directly in front of the system, but other vehicles can be occluded. This might occur when a high-sided vehicle in the nearest lane occludes a smaller in one of the other lanes.

**Gantry:** The second option is a laser scanner mounted under a bridge or on a gantry, thus giving a field of view directly below or slightly oblique to the system. We can also call it the face configuration.

**Cross-fire:** The third possibility is a cross-fire configuration, when the system is installed on the roadside at ground level and the beam is fired across the road. Such a configuration may encounter side-by-side masking and hence is suitable only for only single lane roads.

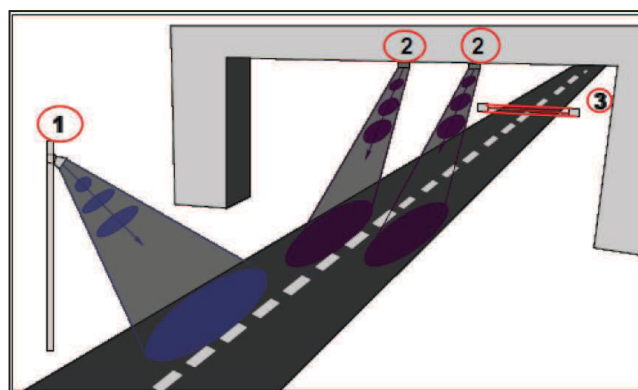
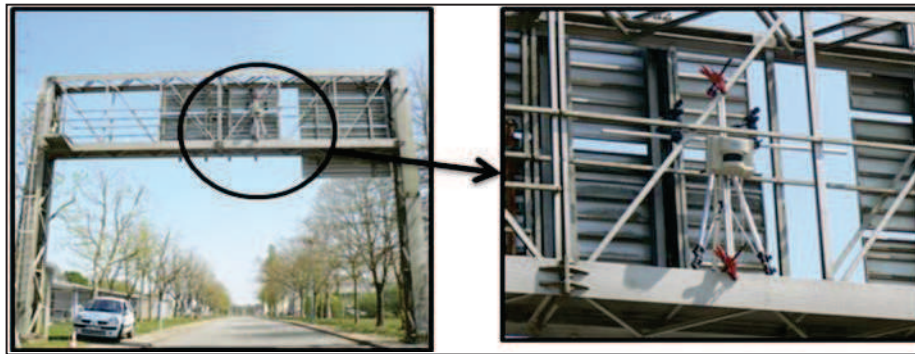


Figure 23: Possible configuration: 1. Roadside mast-mounted 2. Gantry or under the bridge 3. Cross-fire

In the start of the project, a test was conducted at the site of IFSTTAR Nantes. The aim was to check which configuration is best suited to obtaining the data with maximum of precision.



The site where the first experiments were conducted is shown in Figure 24 (site IFSTTAR Nantes). Only the first two configurations shown in Figure 23 (roadside mast-mounted and gantry) were studied. The aim was to analyse the very first data of the laser scanner as can be seen in Figure 24.



**Figure 24: (Left) System installed on the site of IFSTTAR Nantes. (Right) A close up of the system (Gantry configuration)**

In Figure 25, two images of the site with different configurations can be seen. As discussed before, when the laser scanner is roadside mast-mounted, the PTW tends to be occluded behind the larger vehicles. Hence in dense traffic, especially in big cities where PTWs remain most of the time in inter-lanes, this configuration would fail to count the PTWs correctly.

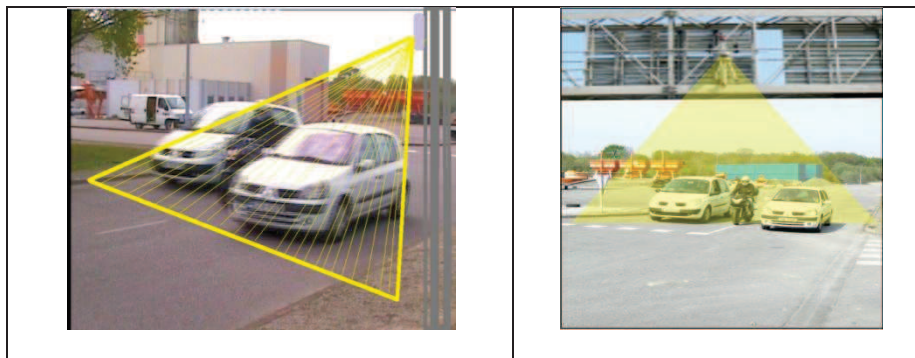


**Figure 25: Configured images. (Left) Roadside mast-mounted: Laser scanner installed at the roadside. (Right) Gantry: Laser scanner placed above the traffic.**

Table 9 compares and summarizes the two configurations

Roadside mast-mounted		Gantry	
Advantages	Drawbacks	Advantages	Drawbacks
Easy to install	Inter-lane vehicles tend to be occluded by larger vehicles	Vehicles can be seen from above even in inter-lanes	Must be installed with precision (unit installation angle)
	Artefacts		Artefacts

**Table 9: Comparison between roadside mast-mounted and gantry configuration**

Table 9 compares both configurations. When the laser scanner is installed vertically above the lane, it gives a complete vision of the vehicles that pass below. The field of vision is directly proportional to the height of the laser scanner above the ground, but as the height increases, the accuracy of the values read by the laser scanner decreases. So, a compromise is necessary when choosing a suitable installation configuration of the laser scanner.

As PTWs move in between lanes, they are subjected to occlusion in dense traffic, so a gantry-mounted configuration is the best suited to our case (Figure 25; configuration 2). The laser scanner can either be

installed directly above the road structure (on gantries or on the underside of bridges) or at a slight angle. To choose the appropriate position, during the very first tests, the laser scanner was placed at different angles to the unit ( $0^\circ$ ,  $60^\circ$  and  $77^\circ$ ) as shown in Figure 26. These angles were chosen by IFSTTAR Nantes while experimentations.

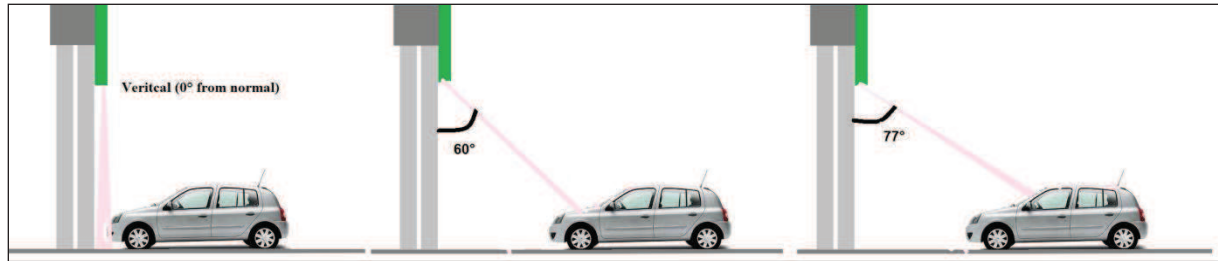


Figure 26: Three different projection angles. From left to right:  $0^\circ$ ,  $60^\circ$  and  $77^\circ$ .

The main variables to consider are as follows:

- The position of the laser scanner: This is a very important factor. As shown in the simulator part, for a 2 lane carriageway, it is easier to detect vehicles if we place the laser scanner above the centre point between the 2 lanes of interest (inter-lane).
- Height: With an increase in height, the field of vision increases, but measurement precision decreases. [JEAN13] explained in his research work the relationship between the distance of the laser scanner from the object and the precision. At various distance 10,000 measures were taken and then the mean distance and the variance was calculated. The author showed that for 5 metres to 6 metres distance there can be a measurement error of as much as 20 to 30 mm. In our case, the system is installed on a bridge or a gantry above the highway where the height is predefined but unknown, so we need to adapt our system accordingly. Bridges and gantries usually have a height around 5 metres to 6 metres but are not always orthogonal to the road.
- Angle of projection: The field of view is depends on the distance of the scanner from the object and the beam projection angle; the more the projection tends towards the normal ( $0^\circ$ ), the greater the influence of the speed of the vehicle, and thus, the shorter the time of contact.

If the lens is angled at  $77^\circ$  from the normal, it will give a view of the environment including for example trees, poles and surrounding buildings (Figure 27: Right). At an angle of  $60^\circ$ , the field of view will decrease and thus include fewer artefacts. This can be seen in Figure 27 (at the left).

At both of these angles, if an HV passes under the beam first and is followed by a PTW, the PTW will not be completely visible. When the laser scanner is placed perpendicular to the road, however ( $0^\circ$  from the normal), only the events occurring immediately under the scanner are visible and so fewer artefacts will interfere in the data. The explanation is given below.

An example of the two configurations  $60^\circ$  and  $77^\circ$  from the normal is shown in Figure 27. The corresponding images show the views that will be read by the laser scanner (LMS 211); they contain uninteresting information. Below are the corresponding scan data with angles on the X axis ( $-90^\circ$  to  $+90^\circ$ ) and distance in metres on the Y axis (80m).



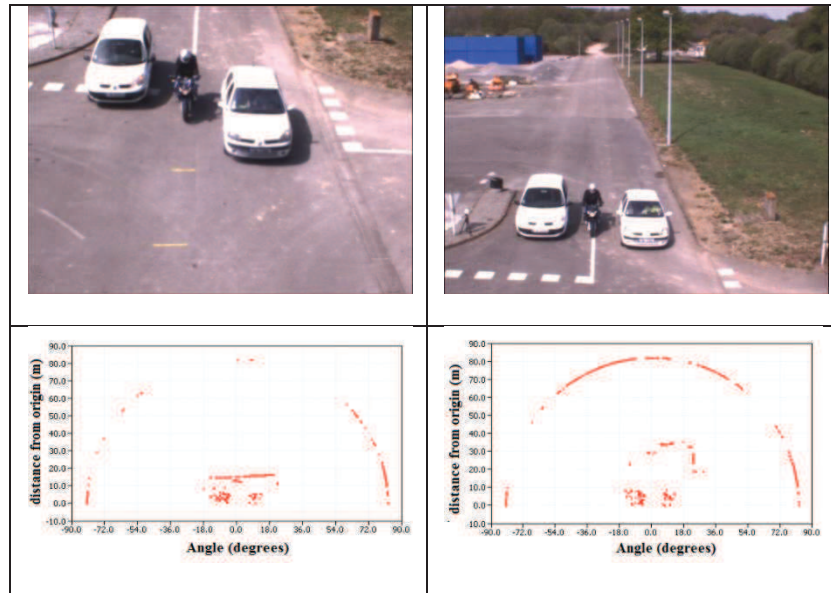


Figure 27: Configuration 60° (Left). Configuration 77° (Right).

In the first image at the left, the system is angled at 60° from the normal. Three vehicles can be observed, but at the same time some environmental artefacts can be seen and are included in the laser data above. The straight line in the middle is the road, the three points just below correspond to the vehicles. A large number of cloud points can be seen around -10° and +10°, corresponding to the trees around the gantry. A faint arc shows the range of scanner, which is around 80m.

When the system is angled at 77° from the normal (right), along with the vehicles we can see several artefacts such as the light poles on the left, the metal debris and a metal cabin in the top right corner. These can also be seen in the corresponding laser data above. Cloud points can be seen around -10° and +10°, corresponding to the artefacts, with the metal cabin at a distance of 35m and an angle of +2°.

In these two cases the probability of interference of the environment (artefacts) is very high. Even after a dynamic or static background subtraction, the risk of encountering noise is very high. For example, with wind, the trees will move and so will their leaves. This may disturb the reading of the laser scanner by creating an important noise. Moreover, these two configurations may face a classical problem in the laser scanner data which is a noise mostly described as “mixed” pixels [DIET01] (Figure 28). These pixels may be generated when the beams refract (bend to a certain angle) from the vehicle instead of reflecting (returning towards the laser scanner) and hence generate noise.

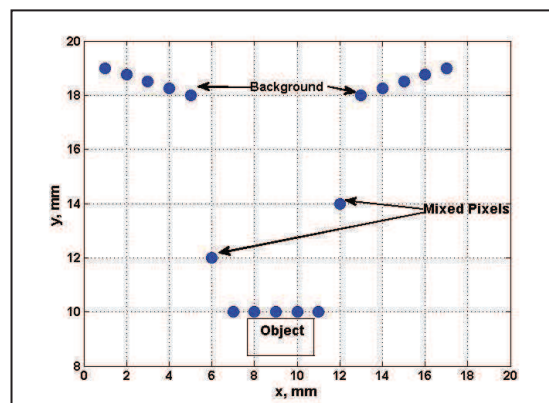


Figure 28: Mixed pixels [DIET01]

There is another case which is not described in Figure 27. When the laser scanner is completely perpendicular or is angled at  $0^\circ$  from the normal on a gantry, the beams focus towards the road and hence minimizes the risk of encountering artefacts. But, at the same time, as this curtain is just a few millimetres wide, the time of contact of the beams with the vehicle is decreased.

Table 10 compares of the three different angles:

Comparison		
$0^\circ$	$60^\circ$	$77^\circ$
<ul style="list-style-type: none"> <li>- Less artefact interference.</li> <li>- Information retrieved directly proportional to height the of the laser scanner.</li> <li>- Information retrieved directly proportional to the angle of incidence.</li> <li>- Information retrieved directly proportional to the speed.</li> </ul>	<ul style="list-style-type: none"> <li>- Huge interference of artefacts</li> <li>- Mixed pixels</li> <li>- Omnipresence of environmental factors</li> </ul>	<ul style="list-style-type: none"> <li>- Huge interference of artefacts</li> <li>- Mixed pixels</li> <li>- Omnipresence of environmental factors</li> </ul>

Table 10: Comparison between three vertical configurations

## 2.5. Data coherence method

This is a very important step for the unit to work correctly. As it can be installed either on a bridge or on a gantry, of unknown height, unknown type and unknown number of lanes below it, the system should be able to recognize the parameters (height, road verges) and initialize the data automatically by finding the Region of Interest (ROI).

As a prerequisite, an empty scan is needed which is a scan of the environment with no vehicle present. This prerequisite is necessary because the installation site is not known beforehand nor is the type of traffic to be measured. The data coherence is carried out as follows:

### 2.5.1. Height

In a scan, the road corresponds to an arc of a certain length that depends on the width of the road. Figure 29 shows an example of an empty scan where the road is represented by inverted values in the form of an arc.

The height of the laser scanner above the road is the minimum value in this arc. The height corresponds to the value read by the system when a ray is projected perpendicularly. In a scan of 541 points, this height will be found by searching for the middle value of the scan i.e. 270. During the

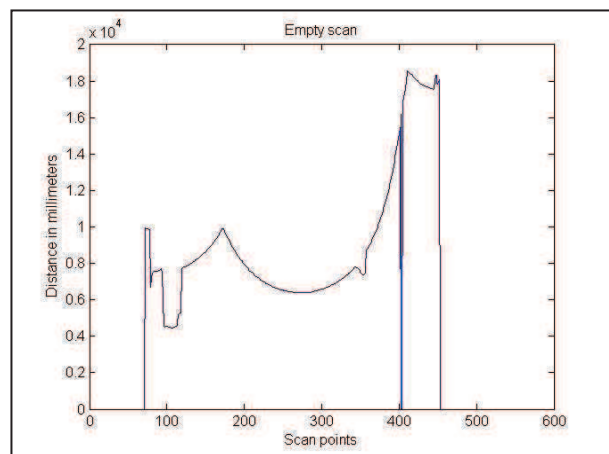


Figure 29: Empty scan

installation, the scanner may be put at  $88^\circ$  or  $92^\circ$  instead of  $90^\circ$ , so, taking this margin into account, an interval of values (*int*) is defined where the probability of finding this minimum value is highest. The basic equation of laser scanner is given by [PFEI08]

$$P_R = \frac{P_E D_R^2}{(4\pi\beta_E^2 r^4)} \sigma \eta_{Atm} \eta_{sys} \quad (2.11)$$

where  $P_R$  is the received power,  $P_E$  is the emitted power,  $\sigma$  is the backscattering cross section and is a product of the directional reflection strength ( $\rho$ ) and area of the object.  $\beta_E$  is the beam divergence  $r$  the range,  $D_R$  the receiving aperture diameter, and the  $\eta$ -terms describes atmospheric and system transmission. A scan  $I$  contains 541 values of  $P_R$  (for LMS111). Hence, the height  $h$  is given by:

$$h = \min \{I(270 \pm \text{int})\} \quad (2.12)$$

where  $I$  is the scan, *int* is taken as 10 i.e. a tolerance of 5 degrees is allowed. So the height ( $h$ ) corresponds to the minimum value between the 260<sup>th</sup> scan point and 280<sup>th</sup> scan point. The index of the scan measurement is defined as  $O$  (the point of origin) where the value of  $h$  is found.

### 2.5.2. Road verges

As given in the equation (2.10), the height-dependent beam diameter is given by

$$R = d \times 0.015 + 8$$

Figure 30 shows the distance ( $d$ ) dependent beam diameter ( $R$ ).

Imagine that two consecutive beams have been projected on the road by the laser scanner. Figure 31 shows the case. The distance between two measured points is equal to half the diameter of the beam projected [BENJ08].

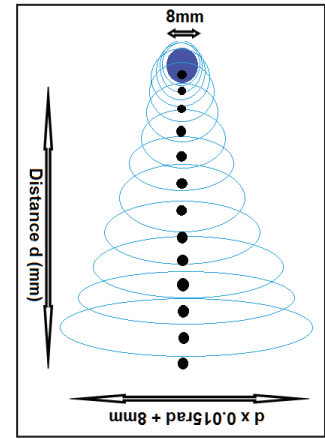


Figure 30: Beam projection

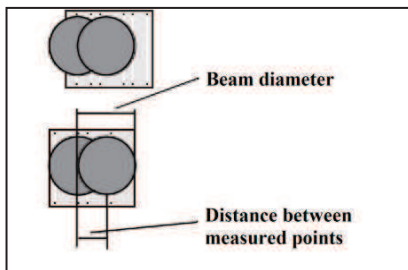


Figure 31: Beam diameter and distance between two measured points [BENJ08]

From Figure 31, the distance between two measured points ( $m$ ) can be given by

$$m = \frac{R}{2} = \frac{d \times 0.015 + 8}{2} \quad (2.13)$$

So, for one scan point, the inter distance is  $m$ . Hence, for  $L$  metres (one lane), the number of measured points is given by:

$$n = (\sum_i m_i) \text{ till } n < L \quad (2.14)$$

where  $m_i$  is the distance between  $i^{th}$  and  $i+1^{th}$  beams. Knowing the index of the scan measurement ( $O$ ), the number of points defining the verge of the road can be defined.

$$\begin{aligned} Br &= O + Nbr \times n \pm \Delta_r \\ &= O + Nbr \times (\sum_i m_i) \pm \Delta_r \\ &= O + Nbr \times (\sum_i \frac{R_i}{2}) \pm \Delta_r \end{aligned}$$

$$= 0 + Nbr \times \sum_i \left( \frac{d_i \times 0.015 + 8}{2} \right) \pm \Delta_r \quad (2.15)$$

and

$$Bl = 0 - Nbl \times \sum_i \left( \frac{d_i \times 0.015 + 8}{2} \right) \pm \Delta_l \quad (2.16)$$

where  $Br$  and  $Bl$  are the right and left verges respectively.  $Nbr$  is the number of lanes to the right of the scanner and  $Nbl$  is the number to the left.  $\Delta_r$  and  $\Delta_l$  are the respective errors that can occur at either side while installing the system i.e. the system is not exactly above the centre point of the two lane carriageway.  $d_i$  is the distance between two consecutive measurements until the length 'L' is attained.

The road verges are given by

$$B = \{Bl, Br\} = \left\{ 0 - Nbl \times \sum_i \left( \frac{d_i \times 0.015 + 8}{2} \right) \pm \Delta_l, 0 + Nbr \times \sum_i \left( \frac{d_i \times 0.015 + 8}{2} \right) \pm \Delta_r \right\} \quad (2.17)$$

This will give the scan point index that will be used to extract ROI (which will be the road) and for processing the signal.

To sum up, here are the conditions for the system to work correctly:

- At least one empty scan to find the parameters (Height, road verges).
- The unit must be installed above the inter-lane.
- The exact number of lanes should be known a priori to the user. For example, in the case of a three lane carriageway, number of lanes at the left and at the right.

Theoretically, the width of a lane is 3.5m, but *in situ* this value may not be accurate and can vary from one road profile to another. A value of  $L$  is thus kept as a user-defined variable.

## 2.6. Databases

Once the system is able to find its parameters, the database is created with the laser scanner traffic data. The first database was constructed at the controlled site with regulated traffic consisting of pre-defined scenarios, speed and inter-vehicle distance.

After testing and validating the laser scanner on the controlled site, the second database sets were constructed at real sites where none of the conditions (traffic, speed, scenarios) were regulated or known in advance.

### 2.6.1. Controlled site

Our database was created by getting a certain number of vehicles to pass under the laser scanner on an experimental site with the regulated conditions. Figure 32 shows the experimental controlled site of CETE Normandie Centre.

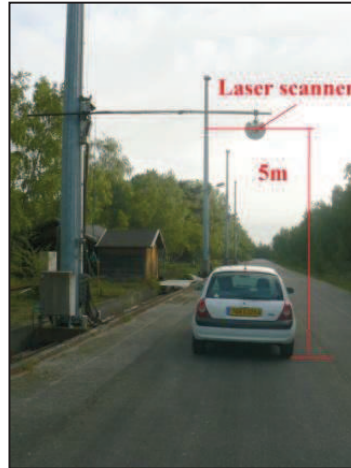


Figure 32: Our controlled experimental site

In Figure 32, the laser scanner was placed  $0^\circ$  from the normal, at a height of 5m to 6m from the ground and at a distance of 3m from the left side of the lane. A camera was placed next to the laser scanner to verify the ground truth. The road at this experimental site was as wide as a double lane, with a width of 7.5m and a length of 400m.

Two categories of vehicles were involved (a PTW and LVs). For this controlled site, only one PTW was used and the database was limited to a few classes of LVs: three super minis, one compact multipurpose vehicle, one panel van and one van. All these LVs were white. The database was inspired from real traffic scenarios. (Figure 33)

The PTW passed with either a rider alone or with a rider and a passenger. Taking safety measures into account all these scenarios were conducted with speeds varying from 20km/h to 120km/h giving a total of 100 laser scanner sequences. Each sequence was registered for a duration of 5 seconds to 10 seconds maximum. Figure 33 gives a description of all the cases defined by the team in charge of auditing all the information linked with the database construction, test and validation of the methods developed.

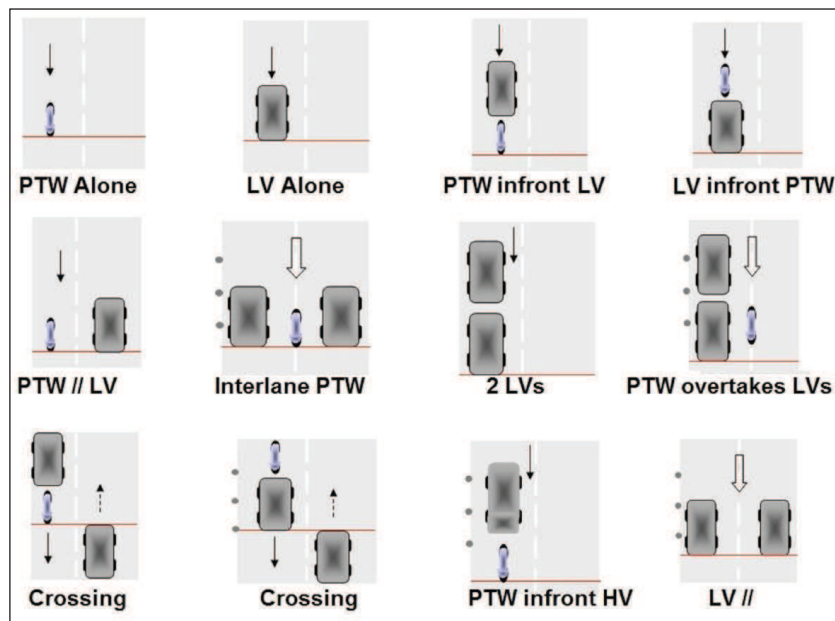


Figure 33: A visual example of the cases discussed above and used create the database.

All the situations shown in Figure 33 were reconstructed using the same vehicles on the same site. Hence the information was rich in vehicles with varying speeds, but limited for different possible shapes and colours. Table 11 shows the number of different vehicles that passed under the laser scanner when it was installed at different heights.

	h=5m	h=6m	Total
PTW	52	25	77
LV	61	30	91
HV	0	0	0
Total	113	55	168

Table 11: Different categories of vehicles passing under the laser scanner at different heights

### 2.6.2. Real sites

Two different sites were chosen for the experimentations *in situ*. The first experiments were conducted on an expressway (SUDIII or RN338) to enable us to understand the differences between a regulated site and a real site. The second site was on the A13 motorway near Paris. This site was chosen within the framework of the ANR METRAMOTO project as the Parisian traffic usually consists of a higher percentage of PTWs and is notorious for the behaviour of the motorists, thus increasing the level of difficulty.

#### 2.6.2.1. Expressway SUDIII

This database was constructed on an urban highway (SUDIII) which is also known as the RN338. This highway links the region of Rouen to the A13 motorway. Figure 34 shows the SUDIII site where the system was installed.

This site has a speed limit that varies from 90km/h to 110km/h, with 2 and 3 lanes. The point where the laser scanner is placed is limited at 90km/h with 3 lanes. Figure 34 shows both types of carriageway, 2 lanes in one direction (on the left) and 3 lanes in the other direction (on the right). This expressway carries 60.000 to 75.000 vehicles per day (2011) in both directions with many types of vehicles such as heavy vehicles (trucks, buses), mini trucks, vans, light vehicles (SUVs, cars, quads) and PTWs.

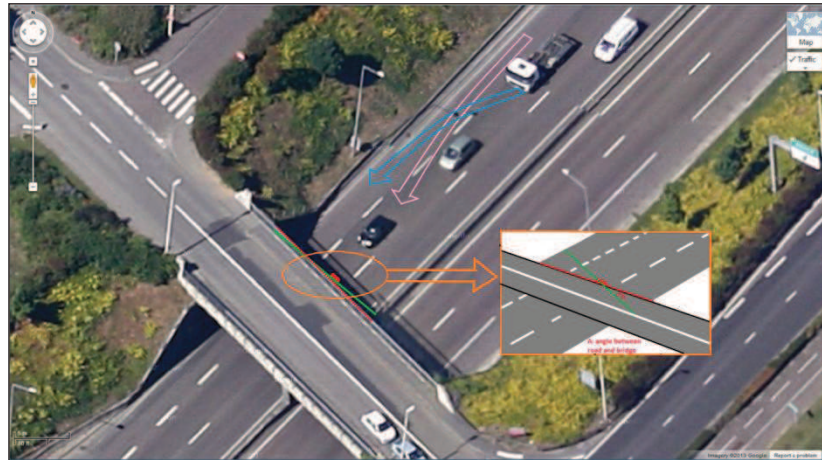


Figure 34: SUDIII: A view of the Highway.

The highway consists of 3 lanes out of which the first 2 lanes are the principle lanes while the third lane serves as an insertion path and also as a deceleration lane. In this 3-lane expressway, the lanes are



numbered 1 to 3 starting from the extreme left lane, Lane 1 with the fastest traffic. The traffic on Lane 2 is influenced by Lane 3 as most vehicles, after entering and before leaving on the highway, will travel in Lane 2. The bridge, under which the laser scanner was mounted, is not at a right angle with the road (Figure 35).



**Figure 35: The installation site. Pink arrow, the insertion path; Blue arrow, the deceleration lane. Zoom: Green line, at a right angle to the road; Red line, the bridge. (Google Maps).**

Figure 35, an overhead view of the site is shown. In the controlled site, it was presumed that the laser scanner would be installed orthogonally to the road (green line). But in reality, the bridge was not exactly at a right angle to the road. The data were corrected as shown in the next chapter.

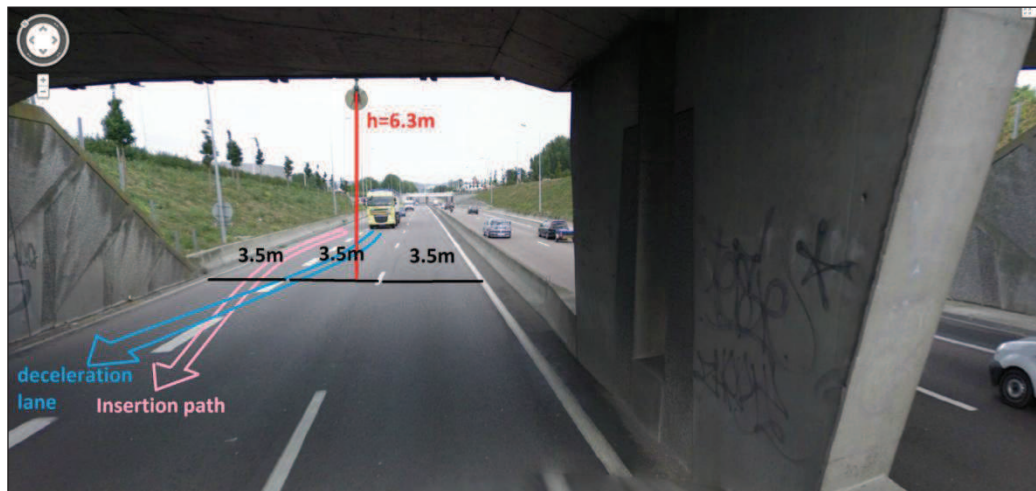


**Figure 36: Reconstructed scene of the site. The laser scanner is installed at 6.3m above the second lane .**

Figure 36 represents a reconstructed scene of the real site. The laser scanner was placed above Lane 2 at a height of 6.3 metres. There are 3-lanes, each approximately 3.5 metres wide.

For this database, the system recorded 3 ½ hours of data with a total of 6874 vehicles in Lanes 1 and 2, as shown in Table 12.

Category of Vehicle	Lane1+ Lane 2
PTW	30
Non PTW (LV and HV)	6844
Total	6874

**Table 12: Database table (Ground Truth)**

In Table 13, the traffic distribution per lane is shown in more detail.

Category of Vehicle		Lane 2	Lane 1	Total per category	Distribution/ category %
PTW		21	9	30	0.4%
Other	LV	3190	1749	4939	71.9%
	HV	1104	801	1905	27.7%
Total		4315	2559	6874	100.0%
Distribution / Lane %		62.8%	37.2%	100.0%	

**Table 13: Different categories of vehicles per lanes (Ground truth)**

Table 13 shows the number of vehicles per category travelling in each lane, under the unit. Lane 2 has the highest number of vehicles with 62.8% of the total traffic. The HVs present in Lane 2 are greater in number than in other lanes. This highlights the fact that on a 2-lane carriageway, the HVs mostly remain in Lane 2, where they usually travel more slowly than other categories of vehicles.

The data read by a laser scanner depends on the shape and colour of the objects present. A light-coloured vehicle, for example, will produce a better return signal than a dark-coloured one. This return signal and object colour relation is discussed in detail by [JEAN13]. Figure 37 shows the number of vehicles of different colours travelling during the first 10 minutes of the recording on this real site for all the three lanes.

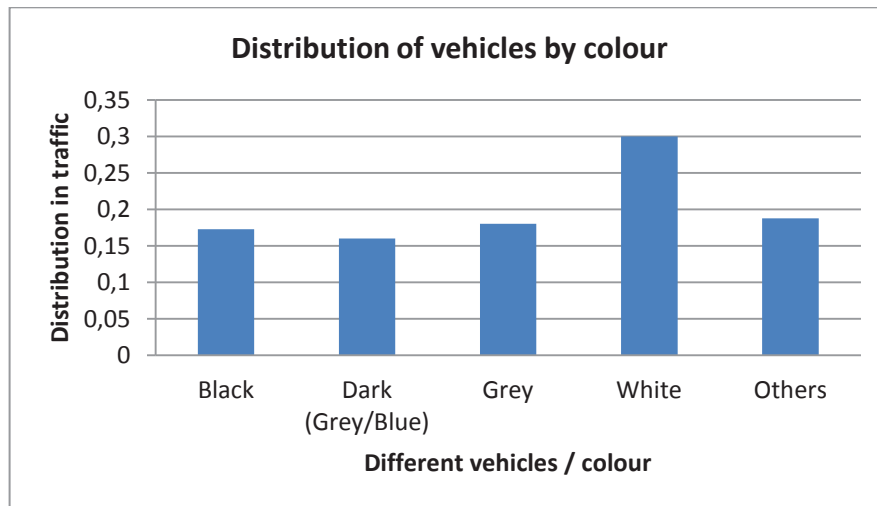


**Figure 37: Distribution of vehicles of different colour present in the scene. *Others* corresponds to orange, green, yellow etc**

#### **2.6.2.2. A13 motorway**

The second part of the experiments was conducted on the A13 motorway. This site differs from the previous sites (controlled and SUDIII) as the traffic observed is much denser and most of the time the inter-lane practice of the PTWs can be observed. This 3-lane site has a speed limit that varies from 110 km/h to 130 km/h. The site can be seen in Figure 38. This motorway carries 100,000 vehicles per day (2011) in both directions with many types of vehicles such as HVs (Trucks, Buses), lorries, vans, LVs (SUVs, cars) and PTWs.





**Figure 38: Experimental Site A13**

For this database, the first 6 minutes of the recording is used (from 7:00 am till 7:06 am) with a total of 584 vehicles on 3 lanes. Here are the tables with details of vehicles with respect to the lanes; Table 14 and Table 15 (Ground Truth).

PTWs/ Lane	Lane 3	Inter-lane (3-2)	Lane 2	Inter-lane (2-1)	Lane1	Total
PTW	0	0	3	43	8	54
Percentage	0%	0%	5.5%	79.6%	14.8%	100%

**Table 14: PTW traffic on the A13 motorway**

Table 14 shows the PTWs per lane. It can be seen that nearly 80% of the time, PTWs were found on the inter-lane between Lane 1 and Lane 2. This shows how common the inter-lane practice is amongst PTWs. A detailed overall traffic distribution per lane is shown in the table below.

Overall traffic/ Lane	Lane 3	Inter-lane (3-2)	Lane 2	Inter-lane (2-1)	Lane1	Total
PTW	0	0	3	43	8	54
Other	177	1	163	2	187	530
Total	177	1	166	45	195	584
Percentage	30.3%	0.1%	28.4%	7.7%	33.4%	100%

**Table 15: Overall distribution per category of vehicle on the A13**

Table 15 details the overall traffic distribution per lane. The traffic on the whole was fairly well divided between each lane, but the greatest percentage of vehicles was found in Lane 1 with 33.4% of the total traffic.

## Conclusion

In this chapter, a simulator is presented with different possible positions for a laser scanner mounted above the different carriageway profiles. This simulation helped to choose the correct position for an overhead laser scanner.

A data coherence method is proposed that helps to find the site parameters such as the unit's height and the road verges.

Using this suitable position the database was constructed on the controlled site at CETE Normandie Centre, following the norms defined by Ms.Christina BURAGA of CETE Méditerranée. Defining a norm means that all the non-intrusive technologies explored in the project ANR METRAMOTO have the same database and hence may be compared. The main objective of this database was to test the feasibility of the technology in the regulated environment.

A second database is constructed on the operational site, expressway SUDIII with an aim to study the difference and the different challenges that may occur while switching from a regulated to an uncontrolled environment.

Finally, a third database was constructed within the framework of project ANR METRAMOTO, on the A13 motorway where the traffic conditions were much more challenging and complex.

All this raw data contains a lot of information. The data coherence method helps to extract the Region Of Interest (ROI), thus only the carriageway is studied and hence fewer artefacts need to be treated. Before the processing, the raw data needs to be pre-processed and then an extraction algorithm applied. These extracted objects have many distinctive properties. These properties are extracted and are used as parameters in order to classify and distinguish between PTWs and other category of vehicles which will be discussed in the next chapter.



## CHAPTER 3: Extraction and classification

---

Introduction .....	61
3.1. Pre-processing .....	62
3.1.1. Signal rectification .....	62
3.1.2. Transformation into a spatio-temporal domain.....	68
3.2. Extraction process.....	71
3.2.1. Last Line Check .....	71
3.2.2. Vehicle counter .....	73
3.3. Classification .....	74
3.3.1. Choice of parameters .....	77
3.3.2. Support Vector Machine (SVM).....	81
3.3.3. K Nearest Neighbour (KNN) .....	81
3.3.4. Learning data set .....	82
3.4. Implementation of the method.....	83
Conclusion .....	86

---



## Introduction

This chapter presents the method developed for the detection, classification and counting of PTWs using the raw data in polar coordinates given by the laser scanner. The data contains important information that has to be extracted. This information also comprises noise that can be either represented in 2D or in 3D.

Our goal is to single out PTWs from the rest of the traffic using a single plane laser scanner which is placed on a lamp post, bridge or gantry at a certain height. Each scan contains information of the scene scanned by the laser scanner. The idea is to accumulate this information (space) during a certain period of time (Temporal) and then generate the data in a spatio-temporal domain. This accumulated data is processed by studying a single piece of information (scan) at a time.

This idea is presented in the form of a chart below (Figure 39).

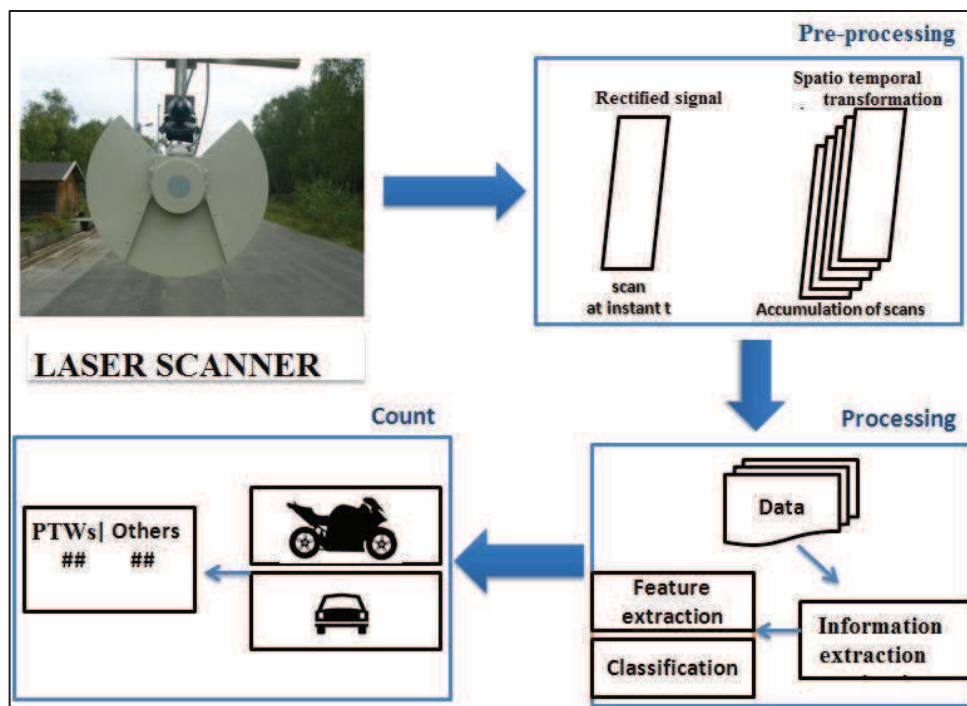


Figure 39: An overview of our system

Figure 39 presents an overview of the system. The laser scanner shown above is placed on a light pole. First, the pre-processing is carried out in order to rectify the laser scanner information. This information is then accumulated and transformed to obtain information in the spatio-temporal domain that is in 3D (2D in space and 1D in time). The processing part consists of extraction and classification. The extraction step is done by applying our Last Line Check (LLC) method, which compares the variation of height and the width of the vehicles that pass under the unit.

The accumulation of scans helps to compare the groups of scans ( $1 \dots t-1$  time instants) with a scan of reference ( $t^{th}$  instant) in order to find the variation of height for the vehicle. This scan of reference is an empty scan of the environment. When a vehicle passes under the scanner, the method checks the variation of the height of the last intensity read by the unit, hence the method has been named the ‘Last Line Check’ (LLC). Once the data is completely extracted, the vehicle is classified and counted.

A brief reminder: before applying any type of processing, it is important to choose a correct set-up for the installation of the laser scanner on the road. In our case, a mast-mounted configuration is chosen. For more information please refer to Chapter 2; Data acquisition, where the data coherence method and the construction of a database are discussed.

### 3.1. Pre-processing

In this step, the laser scanner signal is first pre-processed, as explained in the section below, subdivided into two parts.

- Signal rectification: Elimination of the maximum possible noise and extraction of the Region of Interest (ROI) to obtain a signal that contains exploitable and useful information.
- Transformation into the spatio-temporal domain: Accumulating the information representing space during a certain period of time in order to obtain the spatio-temporal domain.

#### 3.1.1. Signal rectification

There are two main types of noise contained in the laser scanner data. The first type may be generated by several external factors, such as trees, vehicle windscreens, etc. that bend the laser beams towards environment (diffract or refract) instead of reflecting them back to the sensor. This phenomenon creates what is known as ‘mixed pixels’ [GATE08b].

The second type of noise is Gaussian white noise. This is a typical noise that may deform the information given by the laser scanner. Such noise can be generated by certain unavoidable factors such as wind, dust etc. Figure 40 shows the laser scanner installed on our controlled experimental site at CETE NC where the experiments were conducted in a regulated environment.

The Figure 40 shows the laser scanner mounted at a certain height on a rod that had one loose unsupported end, which led to an oscillatory motion in strong winds or when a vehicle passed at high speed and close to the unit. This motion creates noisy laser scanner data, an example of which can be seen below (Figure 40).

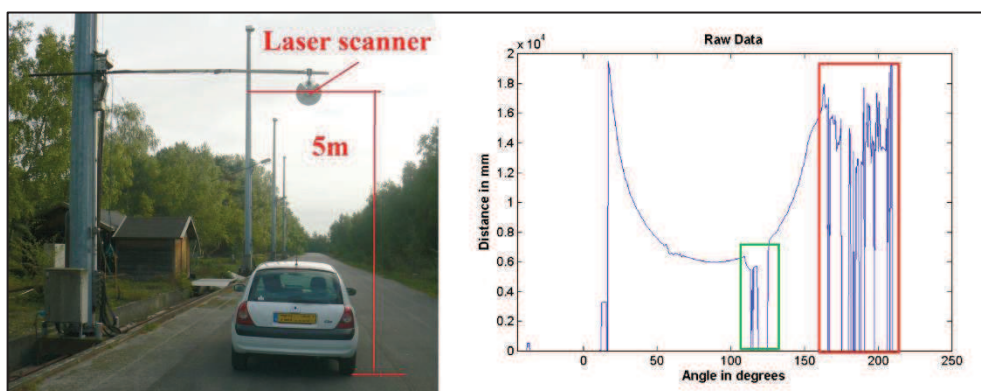


Figure 40: (Left) An example of the scene when a vehicle passes below the laser scanner. (Right).The raw data in polar coordinates with the vehicle shown in green and the environment (trees, pole etc.) in red

Figure 40 represents the laser scanner data, on the right hand side, with the angle in degrees on the abscises ( $X_{axis}$ ) and the distance of the laser scanner from the object in metres on the ordinates ( $Y_{axis}$ ). The graph gives the environment information that shows the distance of the laser scanner from the moving vehicle on the road.

As discussed in Chapter 2, a  $270^\circ$  angle of the LMS111 is scanned from  $-45^\circ$  to  $225^\circ$  with an angular resolution of  $0.5^\circ$ , thus giving 541 points at 50Hz. This laser scanner has a range of 20 m, represented on the  $Y_{axis}$ . This scanning angle was chosen because  $270^\circ$  is a larger angle and thus gives us a larger field of view; the laser scanner motor rotates at a fixed speed (20ms for a scan) and so is independent of the choice of angle. For the angular resolution, more detailed values of the vehicles passing under the laser scanner are obtained if  $0.25^\circ$  is chosen. However, this configuration however takes longer to scan, so if a PTW is moving at a very high speed, the laser scanner would not have enough time to retrieve the minimum amount of information required to detect it correctly. Hence an angular resolution of  $0.5^\circ$  was chosen.

In Figure 40, the signal boxed in green is a vehicle with white noise, and the information boxed in red corresponds to irrelevant data representing environmental artefacts which are not on the road, but in the surrounding. The raw point clouds cannot be used directly because:

- They contain noise (environmental factors, etc.) that should be eliminated first to applying any method to avoid false detection.
- Some of the data in the scan contains uninteresting information (trees, poles, etc.) and should be removed.

The first and the foremost step of pre-processing is the application of a pass band filter to minimize the artefact noise and to eliminate the maximum of the Gaussian noise that exists at ground level and the noise due to the reflection of laser rays towards the environment, this reflection generates values higher than the height of the laser scanner. To obtain useful information, the following steps are proposed:

- Region of Interest (ROI): This is the region representing the road. The extraction part depends upon the type of road (motorway, main roads with single or even dual carriageways) and the height of the support on which the laser scanner is placed. This region can be extracted using the data coherence method discussed in the previous chapter.
- Accumulation of scans post ROI: A single scan may be defined as

$$I^t = [h_1, h_2, \dots, h_n] \quad (3.1)$$

where  $I^t$  contains the total height (difference between the height of the scanner and the distance between the scanner and the object) values scanned at an instant  $t$  and  $h$  is the height of the objects passing under the unit. Each element of the signal (array) contains a value that gives information about the height of the object that passes under the scanner. (Figure 41)

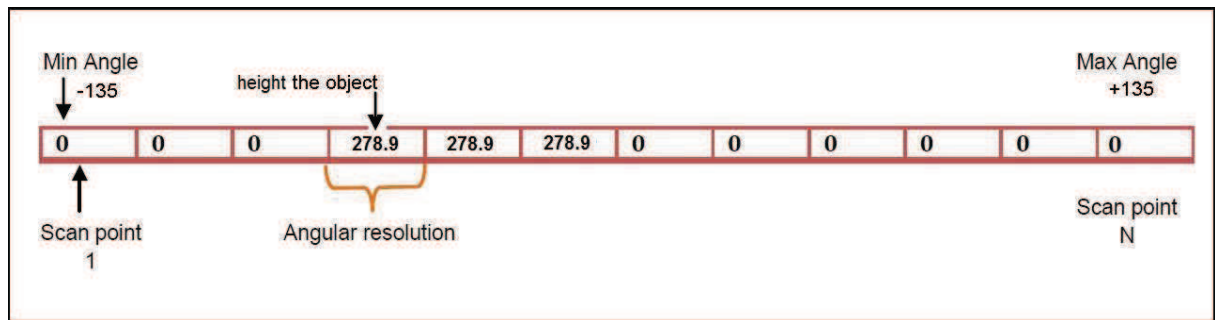


Figure 41: Example of a data array (scan)

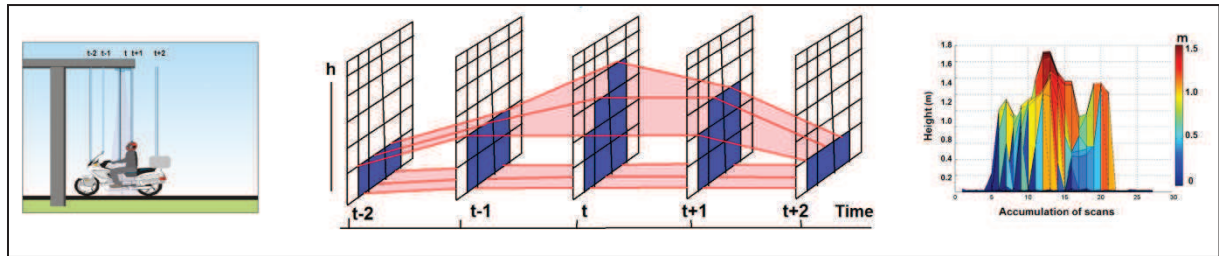


Figure 41 shows an example of a single scan (information) representing the height of the vehicle passing at an instant  $t$ . This height can be obtained by subtracting the distance of the laser scanner from the ground and the distance of the object from the scanner. This information is stored in the form of an array shown in the equation 3.1.

During the total time period ( $T$ ), it is supposed that a total of  $nb$  scans are performed by the scanner. Each scan is independent of the others. If these independent consecutive scans are concatenated or accumulated, the 3D information of the object that passed under the scanner can be obtained.

$$S = \bigcup_{i=1}^T I_i \quad (3.2)$$

$S$  contains an accumulated independent consecutive scans by the laser scanner during time  $T$ . Figure 42 shows an example of  $S$  showing a PTW obtained after an accumulation of scans. The PTW shown at the extreme right is a representation in 2D with the third hidden axis showing the scan points representing the road ( $Z$ -axis).



**Figure 42:** (Left) Image representing a motorbike passing below a unit (Middle) An example of accumulation of data in 2D. (Right) The reconstructed data in 3D; X\_axis: Accumulation of scans, Y\_axis: height of the vehicle and Z\_axis: Scan points representing the road (Hidden)

Post pre-processing,  $nb$  scans are accumulated thus giving a complete profile of the vehicle in 3D as represented in Figure 42. On the far right the silhouette of a Powered Two Wheeler (PTW), obtained after the accumulation of all the scans, can be seen. When we accumulate the scans, the information retrieved is independent of the direction of the vehicle passing under the scanner. In other words, two vehicles going under the scanner in the same direction and two vehicles passing each other in opposite directions cannot be distinguished.

- Application of a ‘fill’ filter: Before applying other steps of rectification, a ‘fill’ filter is applied. Some values are non-observed and thus are returned as perfect zero values. The exact shape of these non-observed values can be seen by the spatio-temporal transformation. They usually exist around windcreens, for example. The problem increases when the vehicles are black as darker colours have a very low remission. A light-coloured vehicle will produce a better return signal than a dark-coloured vehicle. This fact has also been demonstrated in a research work [JEAN13]. This is why the ‘fill’ filter is applied and the principle is as follows:
  - A non-observed value in the data corresponds to a perfect zero value while other values that represent a road or surface have non-zero values. As the prototype is meant to be integrated in a real-time system, each scan is treated independently.
  - All the zero values in each scan are put together by proximity.
  - These group of zeros values are compared to a model  $M$  that represents an empty scan.

- If the neighbourhood values of the group correspond to other values than those present in  $M$ , they are filled with the values corresponding to the neighbourhood (non-zero) values.
- If the neighbourhood values of the cluster correspond to the values present in  $M$ , then an injection process is triggered. This model  $M$  is explained below
  - A model  $M$  is defined, taken from an empty scan (with no vehicles) which is the reference scan. An empty scan containing the road is in a form of a parabola with a Gaussian white noise. This hence can be represented as:

$$M = \frac{2h R_{mul}}{1 + \cos\theta} + N, \quad N \sim N(0, \sigma) \quad (3.3)$$

where,  $h$  corresponds to the height of the laser scanner above the ground. As we know, the slope of a parabola changes constantly as we move across the graph.  $R_{mul}$  is therefore defined such that it corresponds to the reference scan,  $\theta$  is the angle ( $-135^\circ$  to  $135^\circ$ ) and  $N$  is the Gaussian white noise with  $\sigma^2$  as the variance.

- Neighbourhood check: For each extreme point in the cluster, the neighbourhood values of the signal are checked and compared with the values of  $M$ . The comparison helps to decide whether there is a value that can be associated to a vehicle present in the neighbourhood.
- If the point at the extreme position has neighbourhood values different from the value of  $M$ , we consider that an object is present around this void value. This void value is usually a windshield. These missing set of values are filled with the neighbouring values. (Figure 43)

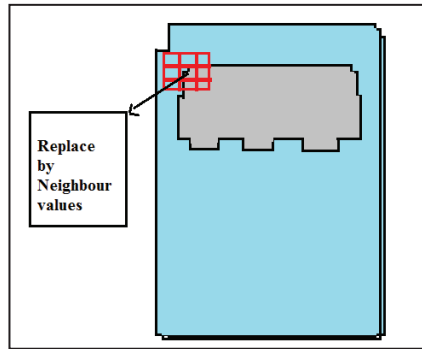


**Figure 43: Principle of checking the neighbourhood. In blue are the values representing a vehicle while in grey are the non-observed values. Extreme points in black.**

- If the extreme points of the non-observed values (Figure 43, in black) have neighbourhood values that are the same as those of  $M$  (with a margin of 2% Gaussian noise), we consider them to indicate a non-observed vehicle and the following process is carried out:
  - The index values of the zero values are known and are compared with the values present in  $M$ .

$$I_i^t = M_i - v \quad (3.4)$$

where  $I'_i$  is the scan at instant  $t$  with  $i$  the index of non-zero values,  $v$  is the value filled in the non-observed zone.

In our research, a value of 1500mm is taken as the value of  $v$ , which corresponds to the height in mm of a typical LV and thus would help our method to classify the vehicle, as will be discussed later. The threshold value below which all the values shall be considered as noise is taken as 400mm.

- Inducing values means adding noise or unknown values to the system. A counter is therefore introduced to help us track how many times the artificial value was injected. Each time  $v$  is injected in a cluster, the value of the counter is incremented.

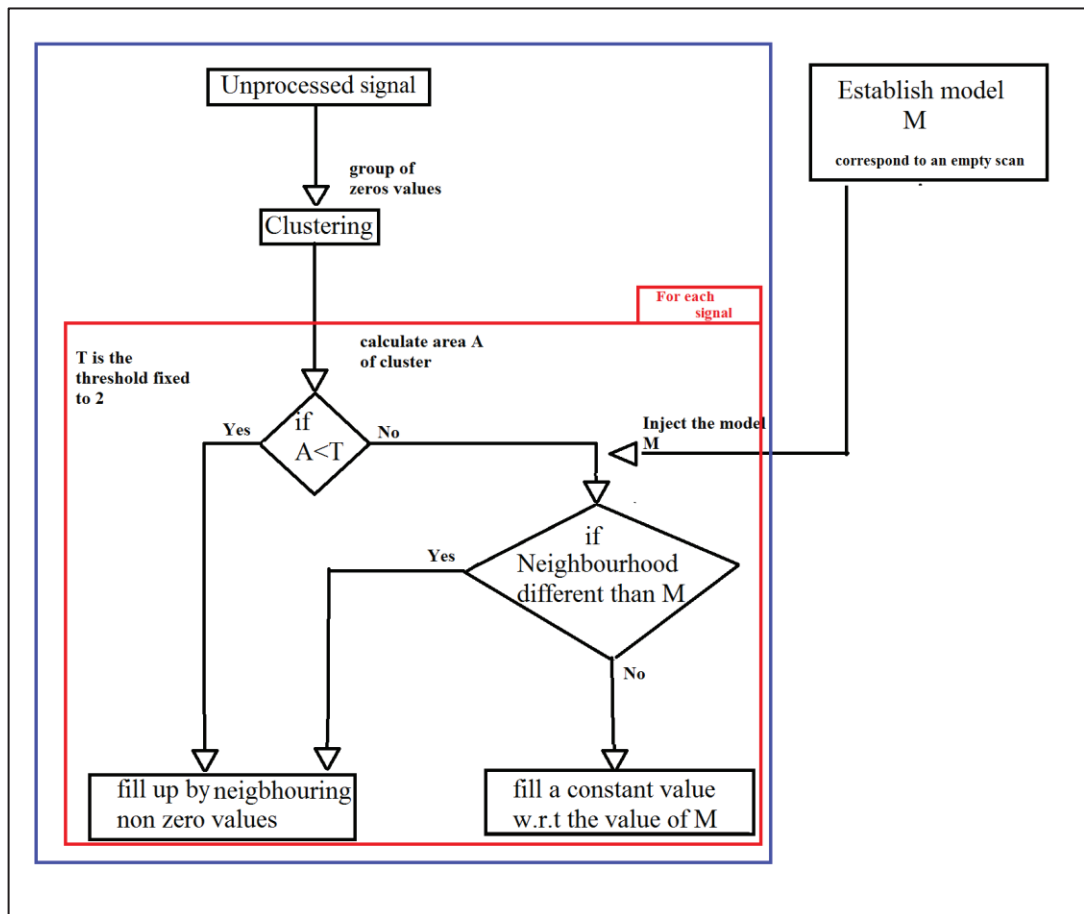


Figure 44: 'fill' filter (w.r.t : with respect to)

To explain the concept better, the flowchart of the 'fill' filter is given in Figure 44.

- Changing the coordinate system representation of the data: The raw data contains information in polar coordinates. In the start of our research work, the data was transformed in to semi-Cartesian coordinates system i.e. converting height into metres and then keeping the angles (semi-polar). The problem with such a coordinate system is that the information read is deformed at the corners of the object. Here is an example in Figure 45.

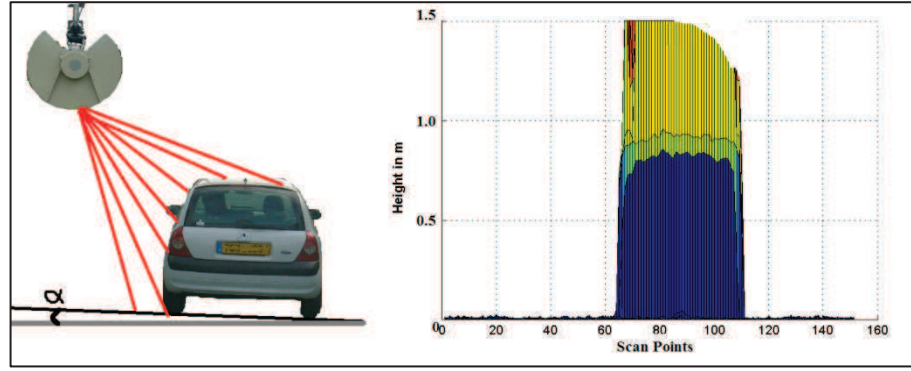


Figure 45: Deformed information at the corner.  $\alpha$  is the transversal inclination angle of the road

Figure 45 gives an example of the deformed information that can be observed in the right image.  $\alpha$  is the transversal inclination angle of the road is shown in equation 3.6. The edge of the reconstructed vehicle is the form of a slope. This can be explained by the simulated image on the left. The second to the fifth rays from the bottom, fall on the profile of the car, hence giving different height values for each corresponding scan point. This variable height when plotted with respect to the scan points, gives the ‘slope’ effect.

With this coordinate system, the blind spots, where the laser beams do not fall, cannot be observed, giving a deformed shape. In the next chapter we will see in detail the results obtained and the problems encountered while using the semi-polar coordinate system that led us to transform the data into the Cartesian coordinate system.

The data thus has the height in metres on the  $Y_{axis}$  and the distance in metres on the  $X_{axis}$ . Figure 46 shows a general notation for the data representation. Here the  $Y_{axis}$  represents the height in metres and the  $X_{axis}$  the distance of the object from the normal angle. In France, we have certain roads which are built with a certain slope. To obtain a precise rectified data, this slope, which is the transversal inclination angle  $\alpha$ , is taken in consideration.

It is to be noted that in this step a single scan at a time is processed.

The transformation from polar to Cartesian coordinates is as follows:

$$\begin{bmatrix} x \\ y \end{bmatrix} = \rho \begin{bmatrix} \cos \beta \\ \sin \beta \end{bmatrix} \quad (3.5)$$

$$\beta = \alpha + \theta \quad (3.6)$$

and

$$\theta = 90 - \theta_h \quad (3.7)$$

where  $\beta$  is the angle calculated from the transversal inclination angle  $\alpha$  and the angle  $\theta_h$  that the laser scanner ray makes with the normal angle (height). This step is necessary in order to compensate the probable inclinations that may occur either while installing the scanner or either the road structure above which the unit is installed is not straight.

This step gives us the rectified values (Y axis and X axis) in metres.

A background subtraction is done at every instant of time  $t$ . Only static subtraction is taken into account, as the system is meant to be installed on unknown sites with random factors (wind, fast moving objects, etc). Dynamic subtraction might generate false alarms.

Figure 46 shows the process explained above. Top left is the raw data representing information in terms of angles in degrees and the distance of the laser scanner in m from the road. A vehicle is surpassingly moving on a road that makes a certain angle. Top middle: the vehicle in the ROI (road). Top right, application of the 'fill' filter to each scan. Bottom-right, transformation spatial temporal: accumulation of scans to get the shape of the values the non-observed values. Then the convertor from polar to Cartesian coordinates is applied taking into consideration a probable angle of inclination. Bottom- middle, the result after rectifying one signal at a time by using a geometrical concept (Cartesian transformation- single scan). Bottom left, we can invert the image by data normalisation through background subtraction and by establishing a threshold to eliminate the absurd values (reflected beams towards environment).

The information obtained is an example of information retrieved by the laser scanner during one scan at an instant of time when a vehicle passes under the unit.

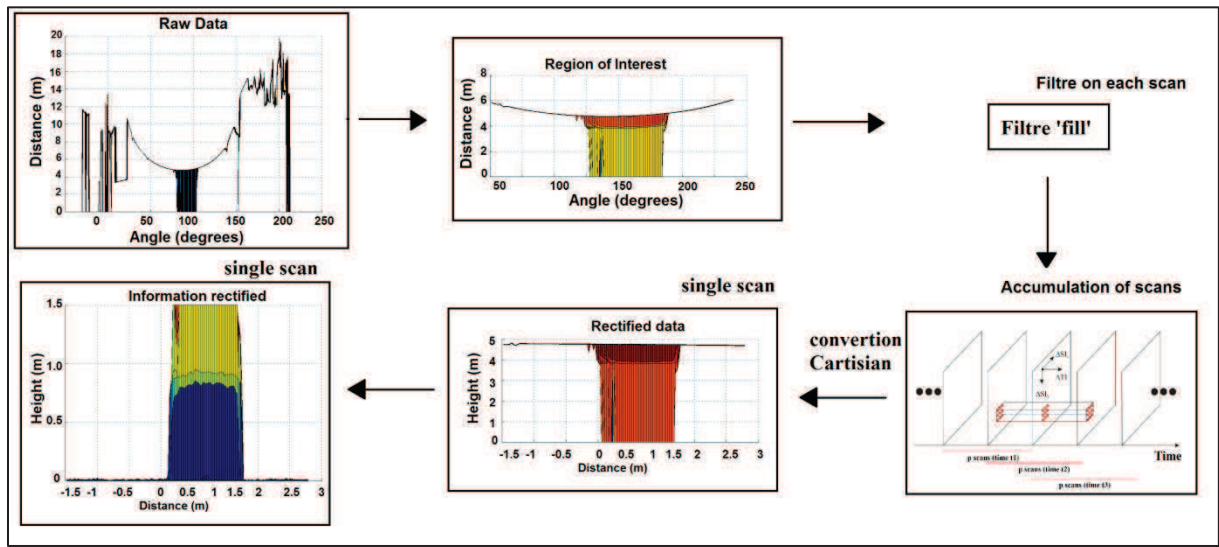


Figure 46: Pre-processing of the raw data.

### 3.1.2. Transformation into a spatio-temporal domain

Figure 46 explains the process of retrieving relevant information from a single scan.

Let us consider,  $\{card(p) < nb \text{ and } p \in \{I_1^t, I_2^t, \dots, I_{nb}^t\}\}$ . The value of  $p$  is calculated by estimating the maximum number of possible scans for a Heavy Vehicle (HV) of classical dimension moving under the scanner with a minimum speed (20km/h). For example, for  $nb=76$  and  $p \in \{I_1^t, I_2^t, \dots, I_{76}^t\}$ ,  $card(p)=76-1=74 < nb$ .  $S$  is the space that contains the independent consecutive scans ( $I^t$ ) and  $nb$  is the total number of scans during the total time  $T$ . The value of  $I^t$  at an instant  $t$  gives the information about space at time  $t$ . Once this information in space is known, the notion of time is added by accumulating scans to get the data in a spatio-temporal domain. This is explained in Figure 47.

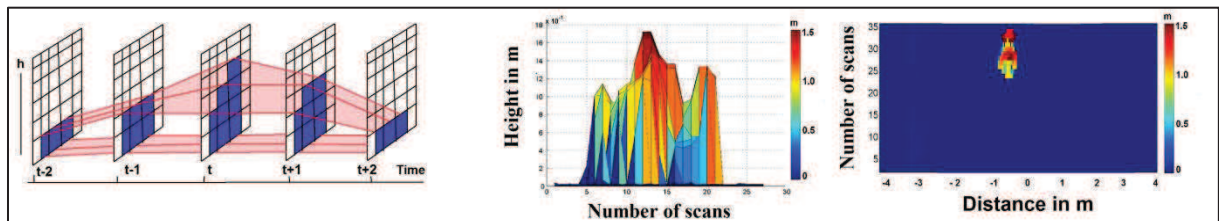


Figure 47: Spatio-temporal domain: accumulation of  $p$  scans, a 2D reconstruction and the view from above.

In Figure 47, on the left, we can see a set of accumulated scans. In the middle a reconstructed 3D laser scanner image is shown. On the right, a 2D scanner image is shown with the distance in metres at  $X_{axis}$ , with  $p$  scans accumulated on the  $Y_{axis}$ . The laser scanner measurements are shown in the form of an image representing the height of the vehicle. At instant of time  $k$ , the value of the image ( $Img$ ) representing this spatio-temporal domain is given by

$$Img^k = U^i [I^i] \quad (3.8)$$

or

$$Img^k = [I^k, I^{k+1}, \dots, I^{k+p}] \quad (3.9)$$

with  $Img^k$  containing all the  $p$  scans at instant of time  $k$ .

### 3.1.2.1. Shadows or the non-observed zones

Before applying the extraction algorithm, the nature of the data obtained after pre-processing has to be studied. The blind spot information is now represented as the shadows. An example of such shadows obtained after accumulation of scans is shown in Figure 48. The image contains inverted values and this explains why the road (in red) has values around 5 metres while vehicle tops are around 1 to 3 metres. This non-processed image is inverted in order to clearly show the shadows.

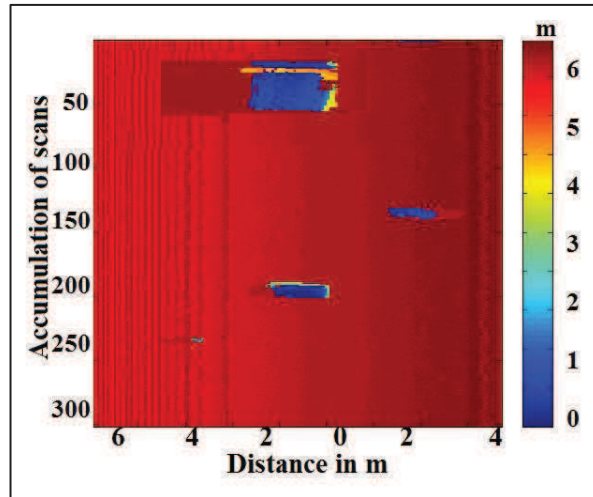


Figure 48: Inverted image, Shadows (non observed zones) in dark red around the vehicles.

The position of the unit installed on the site can be estimated by looking at the projection of the cast shadows in Figure 48. In the scene explained above, three vehicles can be seen, two cars on the left with their shadows falling on the left, and, one car on the right with its shadow falling on the right. This shows that the unit might be placed in between the two cars on the left and one car on right, i.e. around 60<sup>th</sup> scan point.

The darker region (in dark red), corresponds to the blind spot values projected as shadows. They are formed when the laser beams are not able to reach the area occluded behind the vehicle.

As explained in Chapter 2, the shadows can be calculated theoretically (Figure 49) by using the formula (3.10)

$$x = h \tan(\lambda) \quad (3.10)$$



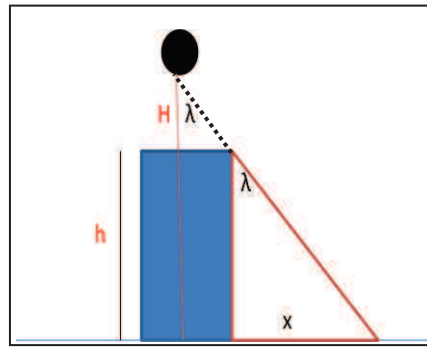


Figure 49: Shadows

There are certain cases, when the ‘shadowy’ zone cannot be easily estimated. The first case on the left in Figure 50, shows the ‘shadowy’ zones perfectly estimated at each side, while on the right, the exact length of the shadow cannot be precisely estimated.

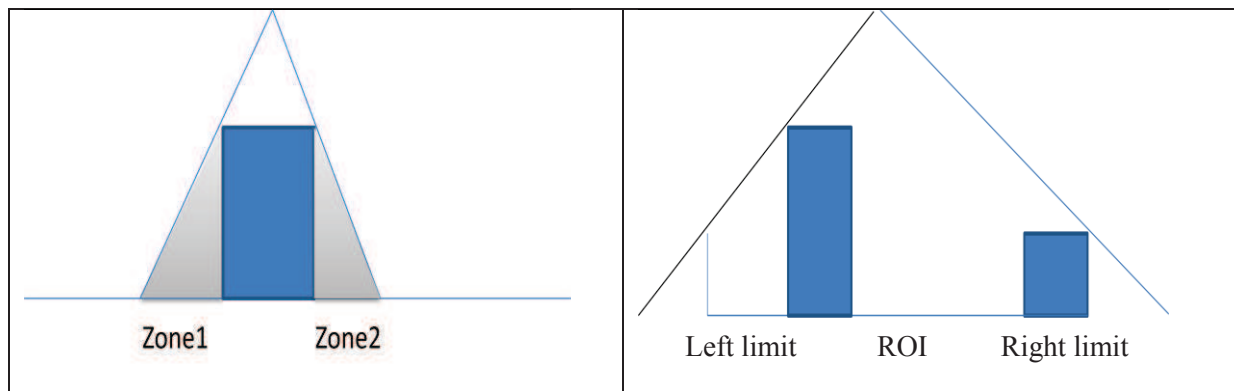


Figure 50: When the object is exactly below the laser scanner (Left). Zone 1 and Zone 2 correspond to the ‘shadowy’ zones. When the objects are at border of the region of interest (Right), complete shadow or partial shadow is cast outside this zone. Hence the exact length of the non-observed zone cannot be estimated.

### 3.1.2.2. Precision

The precision of the values helps to distinguish different categories of vehicles. It helps to compare the values read from the laser scanner with the ground truth and know to what extent our data after pre-processing is reliable. The scanned width of the vehicle is estimated by subtracting the distance of the unit from the two extreme corners of the vehicle passing under the laser scanner image (the first and the end point of the  $X_{axis}$ ).  $\theta$  is the beam projection angle. E is the footprint of the laser beam. The box in black is the vehicle with true values while the box in orange is the estimated value of the vehicle calculated by the laser scanner. The precision is obtained by comparing this scanned width to the ground truth.

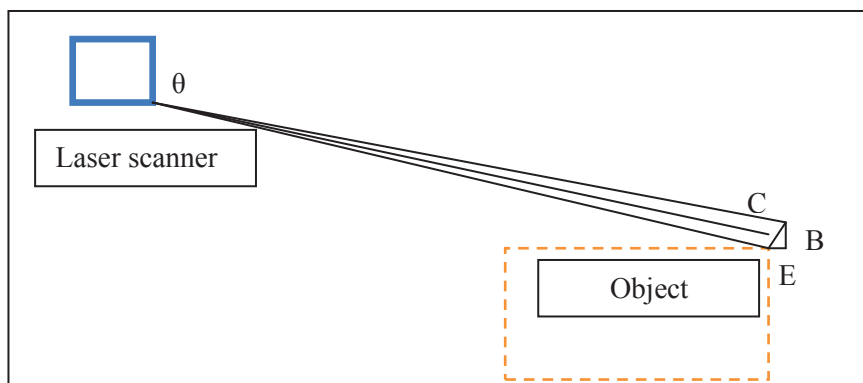


Figure 51: Laser scanner partially falling on the object. E is the error.

As shown in Figure 51, the footprint  $E$  can be estimated by assuming that the rays fall at the extreme corner of the object. On contact with the object, the ray touching the object will bounce back to the laser scanner. This can be partial or complete contact. By partial contact we mean that half or less than half of a conical ray falls on the object, but when it reaches the laser scanner again, it returns the value as if there was a total contact with the object.

Using trigonometric formulas,  $E$  can be calculated as:  $E = C \cos(\theta)$ , where  $\theta$  is the angle of projection of the laser beam and  $C$ , is the hypotenuse of the right angle triangle formed.  $C$  is equal to  $R$ , which has a value of  $8 + d \times 0.015$  (Equation 2.10). The error is therefore given by:

$$E = (8 + d \times 0.015) \cos(\theta) \quad (3.11)$$

From the equation 3.11, it can be seen that  $E$  is directly proportional to the distance between the laser scanner and the object ( $d$ ): the higher the laser scanner, the higher the error. The precision values help to show the robustness of the values measured by the laser scanner, to validate the coordinate system chosen and thus the ground truth values of the vehicles can then be used to construct the learning base of the dataset for classification.

## 3.2. Extraction process

After the laser scanner signal processing, the next step is the extraction of the relevant data from the processed signal. A new approach called Last Line Check (LLC) has been applied to extract the information. Once an object is extracted it is then classified.

### 3.2.1. Last Line Check

This new approach is based on the variation in the height (beam intensity returned to the sensor) as an object passes under the laser scanner. Therefore, the height of the last scan ( $t^{\text{th}}$  scan) is checked at each instant of time  $t$  (Figure 52). As shown in equation (3.1), a scan at an instant  $t$  can be written

$$I^t = [h_1, h_2, \dots, h_n]$$

Where  $I^t$  is the value of the distance measured by the laser beam during a scan. This distance is given by:

$$\text{Distance} = \frac{(c \times \text{Tof})}{2} \quad (3.12)$$

where  $c$  is the speed of light and Tof is the time that the beam takes to arrive at the vehicle travelling below and return.

Figure 52 shows the last scan (or the most recent appearing in the scene) on the left, with a vehicle entering the scene. On the right, a corresponding intensity values representation of the scan is shown.



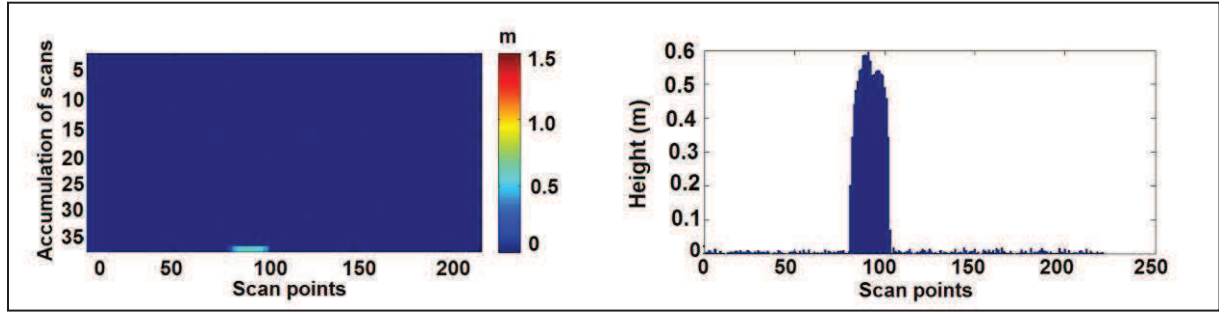


Figure 52: (Left) Vehicle entering the scene. (Right) Intensity (height) representation of the scan.

$I^t$  is the value of the height observed in the laser scan at instant  $t$  and  $n$  is the number of scan points. When a vehicle passes under the system, the variation of height is noticed by the laser scanner. To determine when one or more vehicles enter the scene, we consider the change in intensity (height) and the area of occurrence. In other words, a change is said to have occurred when,

$$Th < \delta I \quad (3.13)$$

where:

$$\delta I = I_t - I_{Reference} \quad (3.14)$$

$Th$  is the minimum threshold above which the intensity is considered to contain information that can be explored. This threshold is calculated by using experimental facts. In our case it is chosen as 0.4m as there is no vehicle with a height below this chosen value.

$\delta I$  is calculated by taking into account the difference between two scans, one representing the height read in a empty scan ( $I_{Reference}$ ) and the other, the scan at instant of time  $t$  ( $I_t$ ).

When a change in height occurs, it is registered and a counter is triggered to count the number of consecutive changes in the same zone. Once the height of the vehicle passing below the unit falls below  $Th$ , the counter is stopped, and the total number of scans containing a vehicle is recorded, along with the region where the change occurred (width of the vehicle).

For example, in equation 3.15, the values in red correspond to the values of height that are above the threshold at two consecutive instants  $A$  and  $B$ . Each of these scan is of size  $n$ . The equation below shows an example of a multiple entry of vehicles at the same time and in different regions.

$$\begin{aligned} & [I_{A1}, I_{A2}, \overbrace{I_{A3}, I_{A4}, I_{A5}}^{\text{red}}, I_{A6} \dots \dots \overbrace{I_{Ap}, I_{Ap+1}}^{\text{red}}, \dots, I_{An}] \\ & [I_{B1}, I_{B2}, \overbrace{I_{B3}, I_{B4}, I_{B5}}^{\text{red}}, I_{B6} \dots \dots \overbrace{I_{Bp}, I_{Bp+1}}^{\text{red}}, \dots, I_{Bn}] \end{aligned} \quad (3.15)$$

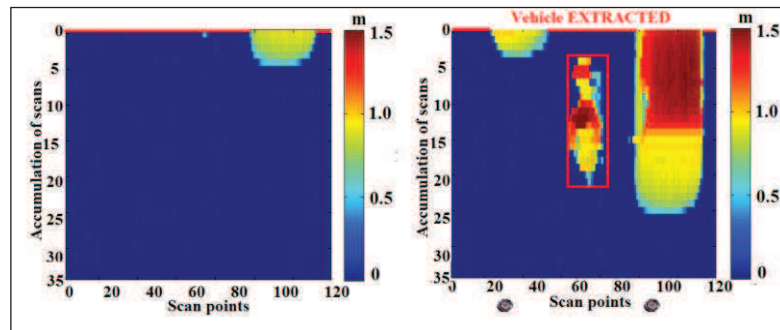


Figure 53: Illustration of the LLC method: (Left): 2 vehicles entering the scene. (Right) One vehicle completely entered and extracted boxed in red.

Once the vehicle has completely entered the scene, we extract it. Figure 53 shows an illustration of the LLC method. On the left: a vehicle enters the scene and the counter is activated. On the right: when the vehicle has completely entered the scene, the counter stops as soon as the intensity becomes normal and the vehicle concerned is extracted. The algorithm is as follows:

Algorithm: Last Line Check ( LLC )
Data: laser scanner data sequences
Result: Vehicle extracted
<p>Compare the change in height of the last scan with the threshold</p> <p>If the change in height is more than <math>Th</math>;</p> <p>Register the scan point position where the height change is noticed (register_vehicle)</p> <p>Count the number of times the change is noticed consecutively (update_vehicle)</p> <p>When the intensity becomes less than <math>Th</math>, extract the vehicle with the maximum zone (width) and number of times (length). (extract_vehicle)</p> <p>Close the completed registration (close_registry)</p>

In the algorithm above, *register\_vehicle* corresponds to the creation of an array with a unique ID that is allotted to each newly noticed vehicle. A flag is opened at the same time when the intensity is higher than the threshold. This flag authorises the *update\_vehicle* to update the length of the vehicle each time an intensity change is found in the same area and to register the maximum size of the corresponding zone (width). *extract\_vehicle* draws the boundary box using the length and width of the vehicle with a given ID. *close\_registry* closes the flag, and thus the registry containing this closed flag will not be accessible to any further change.

The flowchart below explains the overall concept idea of our method.

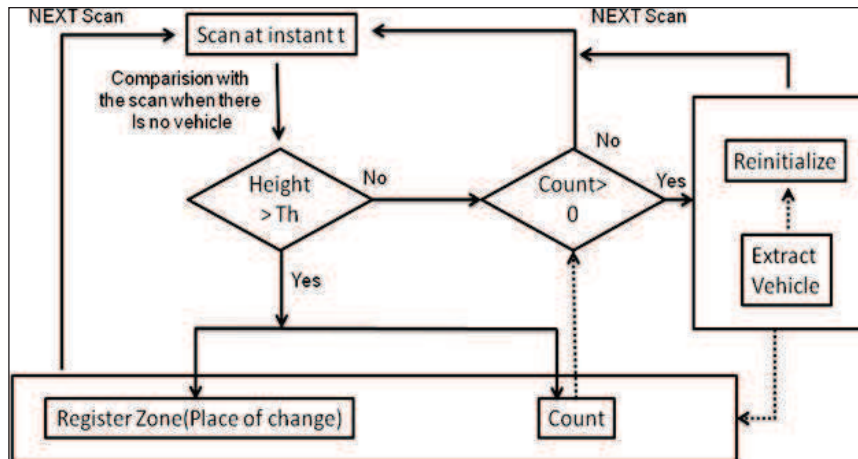


Figure 54: Flowchart describing the LLC method's working principle at an instant  $t$

Figure 54 gives a detail of the LLC method. It is to be noted that this method can be applied to simultaneous multiple entries.

### 3.2.2. Vehicle counter

Vehicle counting methods are not only proposed by industry but also by many research laboratories that are contributing their knowhow. Hence in this section, a few counting methods used by several research laboratories are presented. Then our vehicle counter method is presented.

- Laboratories: existing approaches

[FURS00] proposed a double light curtain to extract the number of objects crossing this curtain. The double curtain is used to estimate a rough differentiation of length between the passing objects. [TANA10] used multiple laser scanner placed horizontally to count either pedestrians or vehicles. The direction of cars is estimated from the position of the target. This method cannot be used where cars and pedestrians co-exist. [VEIC11] proposed to install a laser scanner per lane and the pre-process the laser scanner data for each lane. After this step, the vehicles were identified by using a threshold. They were then counted on each lane and the information from each lane was finally combined.

- Our approach

A vehicle can only be counted once it has completely entered the scene. This vehicle is firstly extracted and then classified. Our extraction method, the LLC method, contains a counter. It keeps in memory information from the very instant a vehicle begins to enter the scene. The information is contained in an array with a unique ID, a flag, the region where the intensity change is noticed and an up-dater that counts the number of times the change is noticed consecutively in the same region. Each state of vehicle at instant  $t$  is modelled using a 4-dimensional state vector (ID, Flag, Up-dater and Region of occurrence) into a state model which is given in the Table 16.

ID	Flag	Up-dater	Region
----	------	----------	--------

**Table 16: State model: Registering a vehicle**

Each time a vehicle is registered, a flag is associated with that vehicle. This flag opens when there is a change in intensity and closes when the intensity goes below the threshold. The closed flag triggers the classification and then triggers the counter. The matrix area where the vehicle's information is filled is reinitialised. The reason for doing this is to avoid the saturation of the memory if the system is installed on a highway with heavy traffic where the number of vehicles present can be high.

### 3.3. Classification

The objective of classification is to identify various objects that belong to different classes present in a scene. The classes are formed by defining certain object characteristics that help to distinguish one object from another.

This section briefly describes various classification methods used in order to categorize different types of data. There are two different broad categories of classification: [FLAM11]

- Supervised classification: This is an essential tool to extract quantitative information when the classes are already known as in the following examples:
  - Naïve Bayes classifier: a simple probabilistic classifier based on applying Bayes theorem with strong independence assumptions.
  - Linear discriminate of Fisher: the objective is to find a hyperplan that could separate the classes of data.
  - K nearest neighbours: this is a very simple approach which looks for the  $k$  number of nearest neighbours (KNN). In this classification, a  $k$  number of neighbourhood values

is attributed and the points having a minimum of distance with respect to these chosen points are clustered.

- Neural networks (ANN): a mathematical model inspired by the structure or functional aspects of biological neural networks. A neural network consists of an interconnected group of nodes (artificial neurons). The key in the neural network is the hidden unit which makes it possible for the network to learn functions where the outputs are not linearly separable. The advantages of neural networks are that they are very good at handling numerical inputs and they can be taught learning functions from examples. They have been successful in learning to recognize handwritten characters, spoken words and human faces. Their advantages make them useful for a wide variety of other tasks, in addition to classification.
- Support Vector Machine (SVM): a binary classifier to separate classes with a hyperplan. This hyperplan can range from a simple linearly-separable problem to complex problems. An SVM using the linearly-separable parameters can be considered as a linear classifier for binary classification problem with labels  $y$  and features  $x$ . We use  $y \in [-1,1]$  instead of  $[0; 1]$  to denote the class labels, rather than parametering the linear classifier with the vector, using parameters  $w$ ;  $b$ , and hence the classifier is written as

$$h_{\{w,b\}}(x) = g(w^T x + b) \quad (3.16)$$

where  $g(z) = 1$  if  $z > -1$  and  $g(z) = -1$  otherwise. This  $\{w, b\}$  notation explicitly treats the intercept term  $b$  separately from the other parameters. The classifier hence directly predicts either 1 or -1, without first going through the intermediate step of estimating the probability of  $y$  being 1.

- Unsupervised classification: here the main idea is to partition the data into the most probable classes. In other words we look for a distribution of individual classes or categories. Fusion of elementary calculations shows that the number of possible partitions is of a very high order. The methods using such types of classification are limited when it comes to the execution time of an iterative algorithm that converges toward a partition that corresponds to a local optimum.

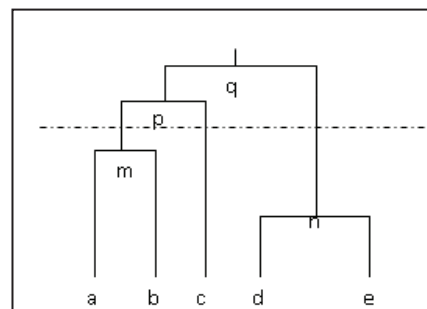


**Figure 55:** Example of a decision tree over five objects a,b,c,d,e. The points m,n,p,q are the nodes of the tree. The discontinuous line indicated the level below which we can define three classes [FLAM11]

The types of classification that follow unsupervised learning are:

- Hierarchical clustering: the regrouping of the individuals in an iterative manner by starting from the base and progressively constructing an inverted tree. At each step or

grouping, a user-defined distance is calculated between the groups and an individual, and the group is reformed. Figure 55 shows an example of a decision tree.

- Classification by dynamic reallocation (Kmeans): the number of classes,  $k$ , is predefined. The classifier is initialized with  $k$  cluster centres by random selection, all individuals are assigned to the class whose centre is closest to the chosen distance. In the second step the algorithm computes the centroids of the newly-formed classes. This process iterates until the convergence to a local minimum is found or the maximum number of iterations set is achieved.

Here is a bibliography of different methods used in traffic classification problems. Mathematically expressed, when an object moving on the road is detected, a probability is established that the object considered may belong to either a vehicle class or a non-vehicle class. This can further be segmented depending upon the dimension, shape etc of the object. Classification methods employing the dimensions of objects, line segments, or bounding boxes as the parameters are the most commonly used.

However, one of the problems when using a laser scanner is that the detected shape of an object varies depending on the position of the object relative to the laser scanner [TYPI08]. Also, the effects of speed, occlusion or even natural conditions (climate) play an important role in affecting the shape of the object (vehicle).

A formal probability equation for this general approach is given by [FAYA08]. [MEND04b] used a Gaussian Mixture Model (GMM) classifier for the laser scanner data.

As mentioned earlier, there are not many studies dealing with the detection of PTWs in traffic. [GIDE08a] proposed to study different geometrical classes to classify vehicles in traffic. [MONT06] used a GMM to model each class of vehicle and then an MAP to classify them. [IZRI04] used the algorithm of Duda-Hurt to get the classification results. [HIRA03] presented the method of inter-clustering to create different object clusters and then classify objects. [ARRA07] and [MONT07] used the adaboost algorithm for the classification problem. [DIET01] and [FURS00] used a pre-defined model to distinguish different vehicles. A prior knowledge about the road users was used to classify the detected objects. The length and width values were compared against the predefined bounding boxes to choose an object class. A similar approach was taken in [MEND04a] except that additional features were considered during classification. Each feature detected contributed a weighted “vote” towards a class and the highest scoring class was assigned to the object. One major problem when using the object dimensions during classification is the effect of occlusion. If an object is partially occluded, the object dimensions will be affected and could lead to a misclassification. This problem is addressed in by [BARG08]. The author considered the occlusion of the object during the voting process. However, this does not consider object dynamics during the verification phase. [MEND04] and [GATE08a] came up with KNN, whereas [HOSS01] proposed an automatic vehicle classification system on highways with the help of double scan by a laser scanner. [DAHL06] suggested using a Kmeans classifier. [WONG04] classified the vehicle by matching point clouds and hence getting the physical characteristics. [MAAT93] proposed using an SVM, taking into consideration the length and the width of the vehicles in the scene. This distinctive parameter helped to distinguish between the PTW and the other categories of vehicles. [FURS00] used a laser scanner to study the outline of different kinds of vehicles. All the classification methods employed above were used specific parameters to identify this category of vehicle in the traffic. So, before going into details about the classifier, the different parameters that we shall be using for classification are presented.

### 3.3.1. Choice of parameters

One of the major difficulties for classification is the correct choice of parameters. For this research work, the exploitable parameters extracted from the vehicles are as follows:

- Width ( $W$ ): The shape of a vehicle is often defined in terms of length and width. It is to be noted that the shape of the vehicle captured by the laser scanner changes with the speed of the vehicle.

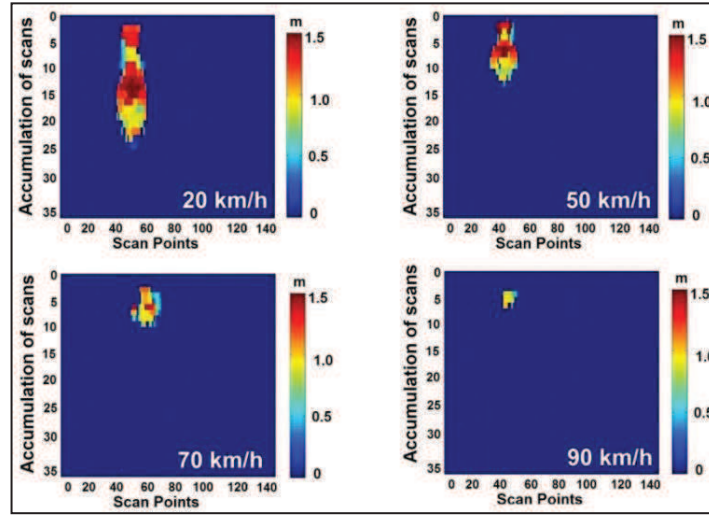


Figure 56: A PTW at different speeds varying from 20km/h up to 90 km/h

Figure 56 shows an example of the laser scanner images of a PTW from 20km/h up to 90km/h. This demonstrates the difficulty of the problem, when with the same PTW at different speeds we have different corresponding data for the shape. The global area of the vehicle decreases with the speed, but we can still see that the width ( $W$ ) of the PTW remains nearly the same. The width is one of the factors that are independent of the speed of the vehicle. This parameter can be defined as the maximum number of the scan points registered during the LLC method extraction process.

- Scanned length: This is one of the most variable parameters that can see during the detection of a vehicle. As seen in Figure 56, the scanned length of the vehicle decreases gradually with increasing speed. This is due to the fact that the faster the vehicle; the shorter the time the laser scanner has to scan it. The scanned length is inversely proportional to the time of contact between the vehicle and the laser beam. This fact is also explained in the chapter Motivation and Overview, where the performance of the laser scanner with respect to the speed is explained.
- Height: This parameter can be measured by using the distance between the laser scanner and the vehicle ( $d$ ) and the angle of beam projection  $\theta$ :

$$h = d \cos \theta \quad (3.17)$$

where  $h$  is the height of the vehicle and  $d$  is the distance between the laser scanner and the vehicle. This parameter may be very effective if we want to distinguish between LV and HV. But the height might not prove to be very effective when it comes to distinguishing between a PTW and an LV for the following reasons:



- The height of a PTW depends on the category of PTW and also the height of the rider. This value is usually around 1700mm and this may also correspond to the height of an LV.
- The correct height of a PTW on the road can only be registered if the laser rays fall on the helmet or the shoulders of the rider. This is not a very probable case as it depends upon the speed of the PTW or the time of contact between the laser scanner and the PTW.
- Height sum: This is the sum of the image pixels representing the height of the vehicle that is extracted and put into the boundary box by the LLC method. The image shown in Figure 57 was formed by accumulating a certain number of laser scans.

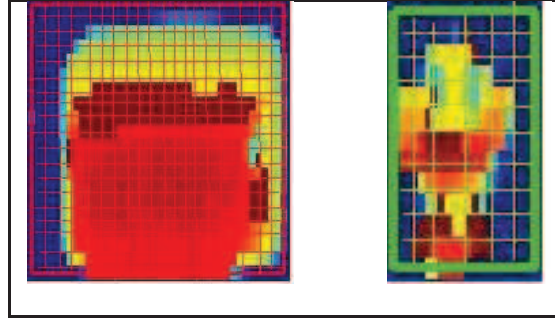


Figure 57: Left: LV at 50 km/h with a Height sum of 8.89e5. Right: PTW with a Height sum of 1.92e5.

Figure 57 shows an example of the sum of the pixels (height) of the vehicle extracted by our algorithm and put in the boundary box. As the LV is larger in area, with an evenly divided height, it has higher value than the height sum of the PTW, which is small and of uneven height. The problem with this parameter is that it is directly proportional to the length of the vehicle. In other words, the faster the vehicle, the less time available for the laser scanner to scan it and hence the lower of this parameter.

- Height sum to scanned length ratio: With the increase in the speed of the vehicle, the scanned length gradually decreases. If we take the ratio of the height sum to the scanned length of the vehicle at variable speeds, we may create a significant descriptor that is independent of the scanned length. This parameter can be defined as:

$$HL = \frac{\sum_i h_i}{l} \quad (3.18)$$

- Number of pixels representing the height ( $Nbx$ ): This is the maximum number of pixels that represent the height of the vehicle. For example, the highest point representing the height of the PTW will be the rider's helmet, whereas for an LV it will be the roof. A filter is implemented to eliminate any value corresponding to the height of the laser scanner (total reflection or beam projection towards environment). Then, we take the maximum value present for the vehicle and hence use the algorithm of region growing, clustering all the values within a margin of 5% of this maximal value.

Let  $h$  be the value of the pixel. The cluster  $C$  is then given by:

$$C = \bigcup_{i=1}^n h_i \quad (3.19)$$

$Nbx$  is thus the sum of the number of points in the cluster.

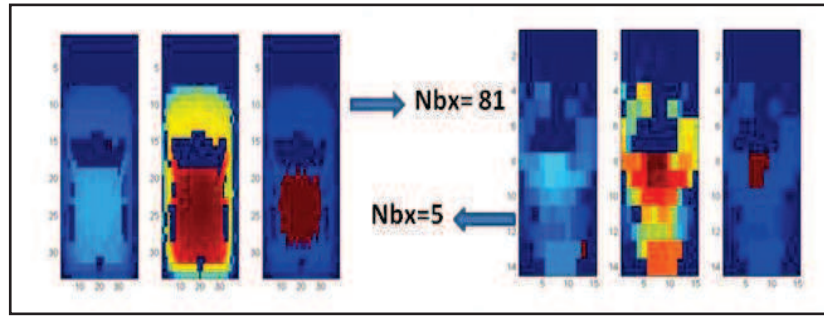


Figure 58: Left: An LV raw image, after filtering and the region growing. Right: a PTW: similar processing.

In Figure 58 the processing is shown through three images for an LV and a PTW. The first image corresponds to the extracted vehicle. Then a filter is applied to eliminate any reflection (if any) is applied. After that, a region growing algorithm is used on the values within 5% of the maximum height value. The number of pixels in red can be counted at the end.

- Height to the  $Nbx$  ratio ( $H\_Nbx$ ):  $Nbx$  may fail when the laser rays do not actually fall on the helmet of the rider but on the rest of the PTW, thus giving a larger set of values that may even correspond to the size of the set of values representing a fast moving car. To normalize the data, the height is divided by the  $Nbx$ . (Figure 59).

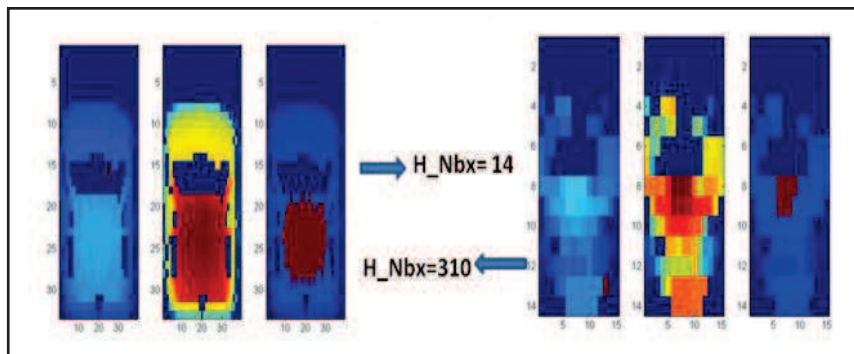


Figure 59: Height normalized by  $Nbx$

Figure 59 shows the values of  $H\_Nbx$  are much more distinctive than  $Nbx$ .

To better represent all the parameters explained above, a sample of 40 vehicles is taken consisting of 20 PTWs and 20 other categories (LVs). All these vehicles passed at variable speeds between 20km/h and 120 km/h. The values obtained for each parameter were then plotted on the graph. This graph helped us to compare and choose the right parameter(s) that can give the best solution to optimally separate two classes: PTW and non PTW (LV, HV).

Figure 60 shows a comparison of plots of different parameters. Beginning from the top left to right and then going down, parameters such as width ( $W$ ), Heightsum over length, Number of points representing maximum height of the object ( $Nbx$ ) and Height over  $Nbx$  can be used to linearly separate PTW and other classes of vehicles. However, *Heightsum* over length and  $Nbx$  fail to linearly separate the two classes when the vehicle is moving very slowly, in a traffic jam for example. In such cases a vehicle may be read as a limousine and therefore, can confuse the classifier. Nevertheless, the  $H\_Nbx$  is a very strong parameter when the traffic is fluid as it shows its robustness to the cases having speed to length interdependences.



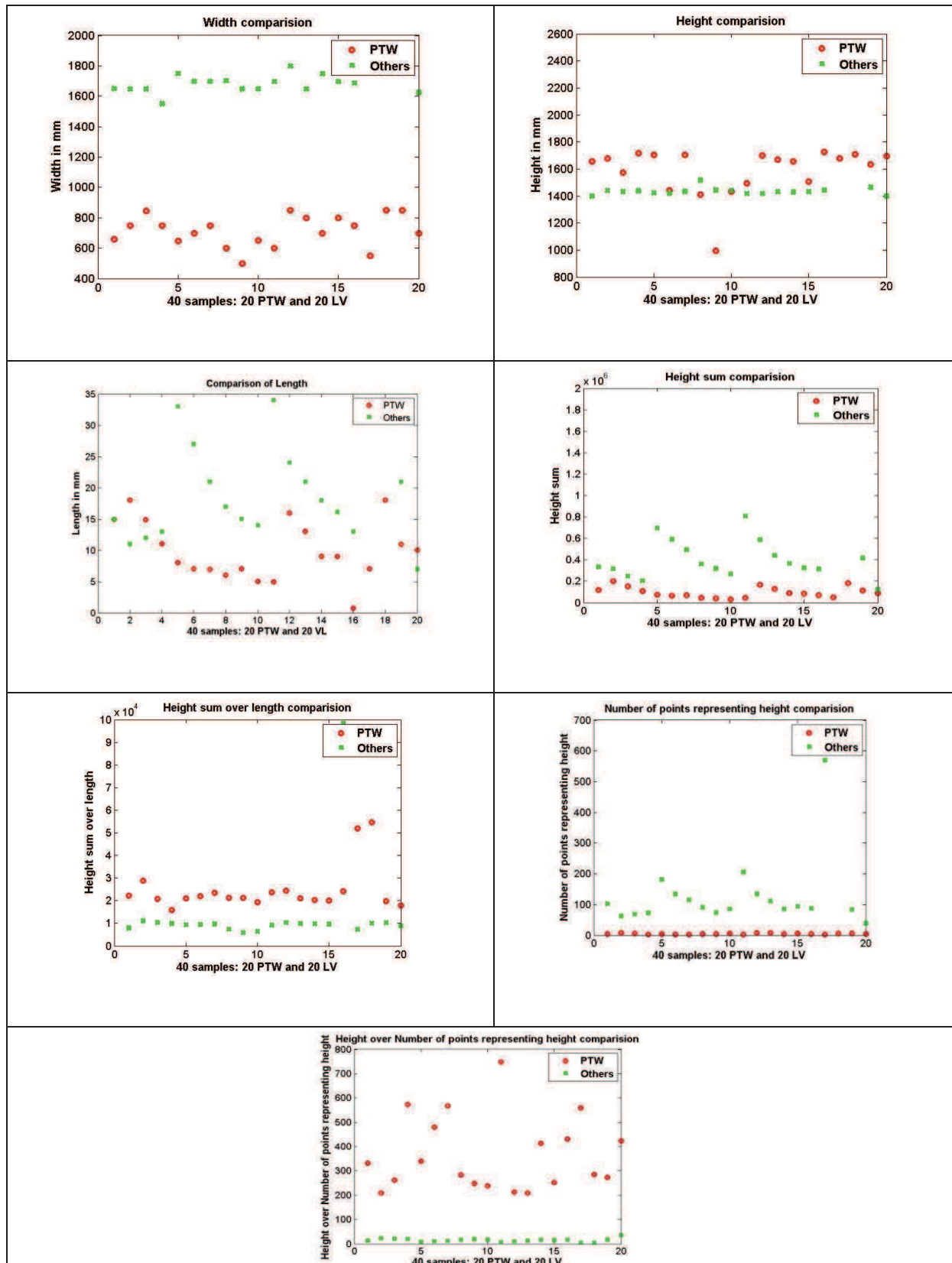


Figure 60: Comparison plots of different parameters

Once the parameters are selected, they can be applied to the classifier. For this research work, two different classifiers, a Support Vector Machine (SVM) and a K nearest neighbourhood (KNN) are chosen.

The goal of this research work is to distinguish PTWs from the other categories to vehicle. A Support Vector Machine (SVM) is a binary classifier, so can help to classify the data in to PTW and non PTW traffic. KNN is a clustering algorithm, so a sample is classified based on how far it is from the centroid of the cluster while the SVM uses the clusters chosen, not by the centroid but rather by a hyperplane that segregates one region from another region. However, both classifiers have been implemented in order to decide, by comparison, which one is the best to solve our problem. To sum up, here is a table that gives the difference between the two methods of classification explained in Table 17.

SVM	KNN
Binary	Multiclass
Rapid	Time consuming if K is large
Decision with the help of support vectors	Decision based on entire training set

**Table 17: Difference between SVM and KNN**

### 3.3.2. Support Vector Machine (SVM)

A SVM is based on supervised learning of  $Q$  training points, where each input  $x_i$  is of  $D$  dimension and is in one of two classes  $y_i = -1$  or  $+1$  i.e. the training data is in the form:

$$\{x_i, y_i\} \text{ Where } i = 1..Q, x_i \in \mathbb{R}^D \quad (3.20)$$

A problem is said to be separable linearly, when a function is of the form:

$$D(x) = \text{sign}(f(x)) \quad (3.21)$$

$$\text{where, } f(x) = \sum_D w^T x + b \quad (3.22)$$

where  $D$  is the dimensionality of the feature vector  $x$ ,  $w$  is an optimal weight vector and  $b$  is a constant.

A hyperplane separates two different classes of data from each other whose decision function being given by the formula:

$$\Delta(w, b) = \{x \in \mathbb{R}^D | w^T x + b\} \quad (3.23)$$

This classifier is one of the most widely used (like Neural Networks) as it is very robust, and we chose it because SVM is a binary classifier well suited to our application of differentiating either PTWs or other vehicles (LV, HV) in a traffic scene.

### 3.3.3. K Nearest Neighbour (KNN)

A KNN may be defined as a non-parametric lazy learning algorithm. By non-parametric, we mean that no assumptions are made on the data distribution, whereas ‘lazy algorithm’ means that no training data points are used, so there is no explicit or only a minimal training phase. Due to the lack of generalization, KNN needs most of the training data during the testing phase. In the worst case, where all the data points may be used to take a decision, more time and more memory will be needed to compute a solution.

KNN data points can be scalar or multidimensional vectors that are presented in a metric space. Since these points are in feature space, they can be presented in distance. The distance most commonly used is the Euclidean distance. Each set of training data consists of vectors and to each of these vectors

there are associated class labels. A simple example of these class labels can be a binary output (PTW or non-PTW in our case). But KNN is equally efficient with the arbitrary number of classes.

KNN consists of a number 'k' which decides how many neighbours i.e. distance metrics should influence the decision. The algorithm behaves differently with respect to the value of  $k$  chosen, so there are two global classes. If the number of classes is even, then it is preferable to give  $k$  an odd number. If  $k=1$ , then the algorithm is very simple to compute as no factor of  $k$  is used in the KNN algorithm.

- Case 1 when  $k = 1$  or Nearest Neighbour Rule

This is the simplest case. Let  $x$  be the point to be labelled and the point closest to  $x$ , say  $y$  is to be found. According to the nearest neighbour rule, the labels of  $y$  are assigned to  $x$ . The method is quite simple and sometimes even counter-intuitive. It may result in a huge error if the number of data points is not very large.

A simple way to explain the principle is to consider that we have a large dimensional plane with a large number of points. Consider a point  $x$  with a lot of neighbours and let  $y$  be the nearest neighbour. If  $x$  and  $y$  are sufficiently close, then there is a high probability that  $x$  and  $y$  belong to the same class.

- Case2 when  $k=K$

This is just an extension of the earlier case. We now try to find the  $k$  nearest neighbour and then implement majority voting. Imagine a new point to be classified for 2 classes  $C1$  and  $C2$  and with  $k=7$ . There are 4 instances of  $C1$  and 3 of  $C2$ . By majority voting, the new point will be labelled as  $C1$ .

Another solution is to add weight to each point and this may be calculated using its distance. For example, under inverse distance weighting, each point has a weight equal to the inverse of its distance to the point to be classified. This means that neighbouring points have a higher vote than the furthest points.

It is to be noted that the accuracy increases when the value of  $k$  is increased but the computation cost also increases. A simple approach to calculate the value of  $k$  is using the rule of thumb

$$k = \sqrt{n} \quad (3.24)$$

where  $n$  is the size of the training set [w8].

### 3.3.4. Learning data set

The learning data set was made by taking into account all the possible conditions that we have in our base. This consists of a mixture of the vehicles taken from the data set of controlled site and the data set of a real site. Here is a recapitulation of the data sets:

At the controlled site, the database was constructed using one PTW, five different types of light vehicles and one van (which is also considered as a Light vehicle). All these vehicles are white in colour and passed at different speed varying from 20km/h to 120km/h in a straight line and respecting all the rules of road security. The height of the laser scanner with respect to the road was either at 5 meters or 6 meters.

For the real conditions, however, the road had a maximum authorised speed of 90km/h, but there was the likelihood of motorists travelling above this limit. There was a greater variety of vehicles (different

colours and makes, sizes, some with side-cars). Motorists do not always respect the road safety rules and the vehicles do not always move in a straight line (overtaking, changing lanes etc).

For the training data set all the cases from the controlled site with different speeds were used, together with the first 2 minutes of the laser sequences from the real site data. The values are shown in Table 18.

	PTW	LV	HV	Total
Controlled Site	28	24	0	52
Real Site	4	70	6	80
Total	32	94	6	132

Table 18: Training set

### 3.4. Implementation of the method

The previous sections explained the theoretical aspect of the method. This section focuses on the experimental results obtained at each step of the method to demonstrate, how the algorithm works. A general flowchart of the system is as follows (Figure 61):

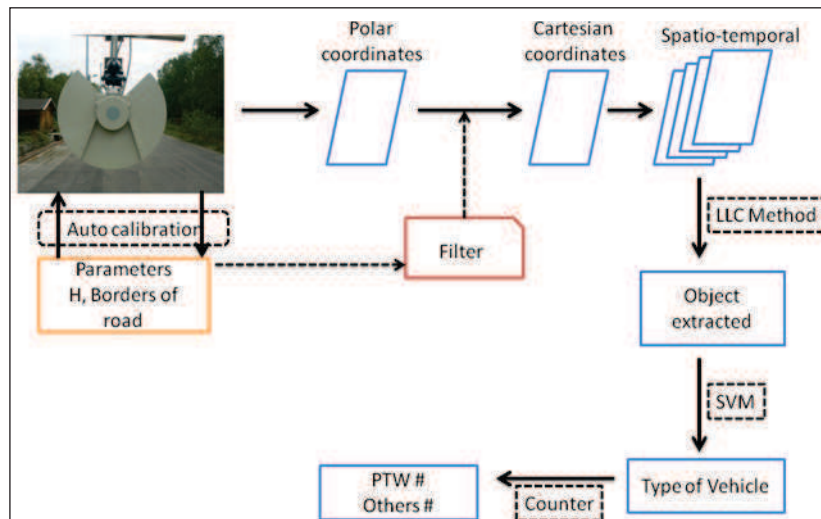


Figure 61: Final overview of the system

To explain the demonstration, a sequence of 200 scans is taken, corresponding to 4 seconds of laser scanner data. During these 4 seconds there are 4 vehicles: 1 PTW, 2 LVs and 1 HV. These vehicles have unknown speeds, the laser scanner is placed at an unknown height and at an unknown position (above the centre point of two lanes or not). The only thing known by default is that the system is installed on a three-lane highway.

As none of the information about the site is known in advance, the first and foremost step is the data coherence step. For that, an empty scan is taken with 541 scan points (Figure 62). First, we will assume that the true value of the height is found in an interval of  $\{270 \pm \text{int}\}$ , where int is 10, hence allowing an error of 5 degrees while installing the unit on the road. So, we look in the interval at points  $\{260, 280\}$  to find the minimum value corresponding to the height of the system.

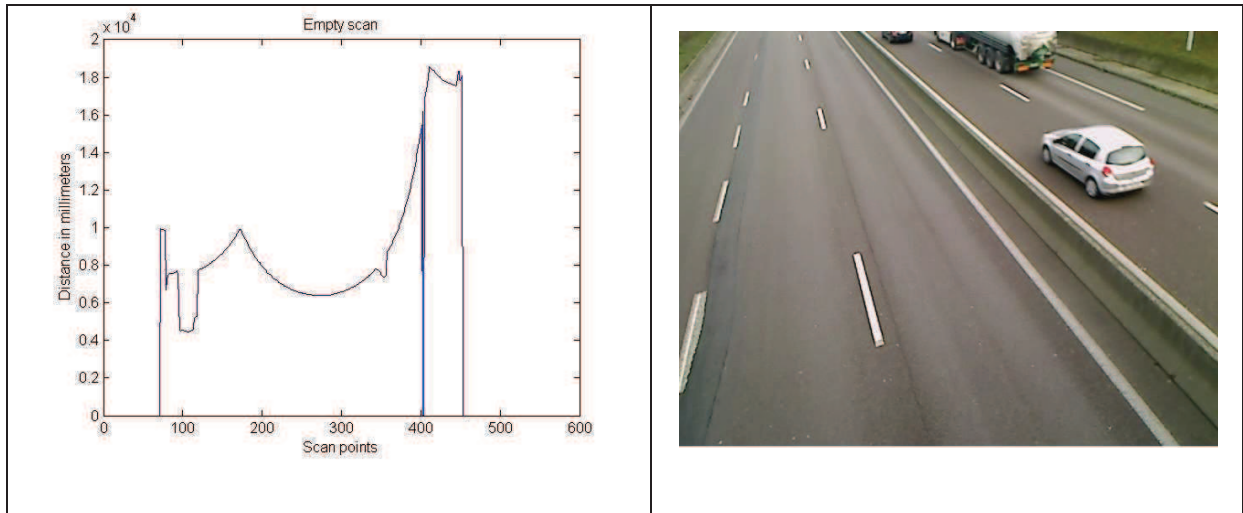


Figure 62: Empty scan on the left and the corresponding image on the right

In Figure 62, the left image corresponds to an empty scan with 541 scan points. By a brief visual examination, we can estimate the minima of the arc around the 270<sup>th</sup> scan point. A bend can be noticed around the 350<sup>th</sup> point, which by correlating with the image (on the right) can be estimated as the road divider. The points after the road divider correspond to the road in the opposite direction.

Therefore an interval of {260,280} is taken and the minimum value in this interval corresponds to the height of the laser scanner. In our case, the minimum value of the height is 6.38 metres and the corresponding index value of the scan is 272.

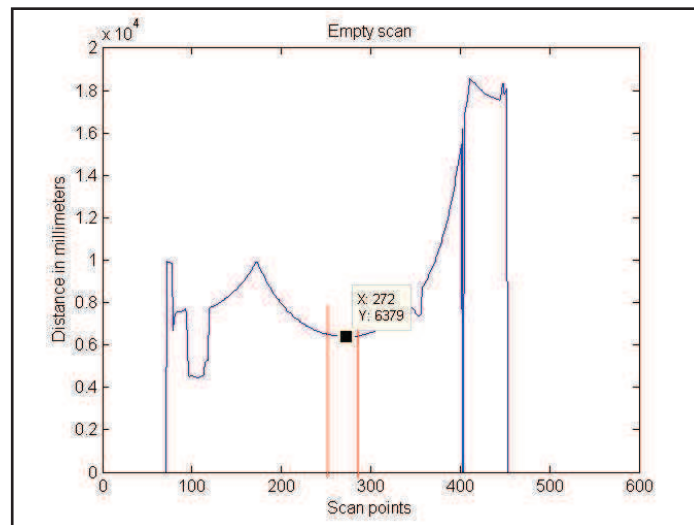


Figure 63: Empty scan with the interval of values where probability to find the correct height is maximum.

In Figure 63 shows the corresponding result. The height of laser scanner is now known, to be 6.38 metres. Once the height is known, the diameter of the laser beam,  $R$ , at the point of origin, which is 272<sup>th</sup> scan point can be calculated by using the equation 2.10:

$$R = d \times 0.015 + 8 = 103.68\text{mm}$$

In this demonstration, we have chosen 2 lanes on the left of the laser scanner and 1 lane on the right of the laser scanner. With all parameters known, the road verges (interval  $B$ ) can be calculated using the equation 2.10.



So,  $Border_2 = \{208, 342\}$  for two lanes (1 on the right and 1 on the left) while  $Border_3 = \{160, 342\}$  for three lanes. By comparing this with the ground truth, the actual points are,  $Border_{GT_2} = \{215, 345\}$  for two lanes and  $Border_{GT_3} = \{170, 345\}$  for three lanes. The delta of error increases the further we are from the laser scanner.

Once the parameters are determined, all the 250 scans are accumulated and the following result is obtained (Figure 64).

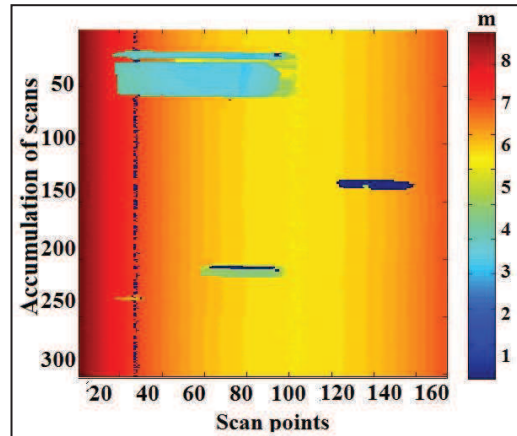


Figure 64: Image formed by the accumulation of scans

In Figure 64, four vehicles are present in the scene. By visual contact, we can estimate that there is one HV, two LVs and one PTW. In this primary accumulation of scans, the information is missing; for example, the black car has a near-zero value. This demonstrates that the laser scanner returns a near zero value when the vehicle has a dark or black colour. For the second car, however, the rays are reflected back, so it can easily be seen in Figure 64. The PTW is moving at the leftmost corner. As it is moving fast and is smaller in size, it is represented by a very small number of scans. The shape of the HV is stretched as it is represented in the semi-Cartesian coordinates.

After the application of 'fill' filter and changing the coordinate system (accumulation of scans i.e. time and distance in m), Figure 65:

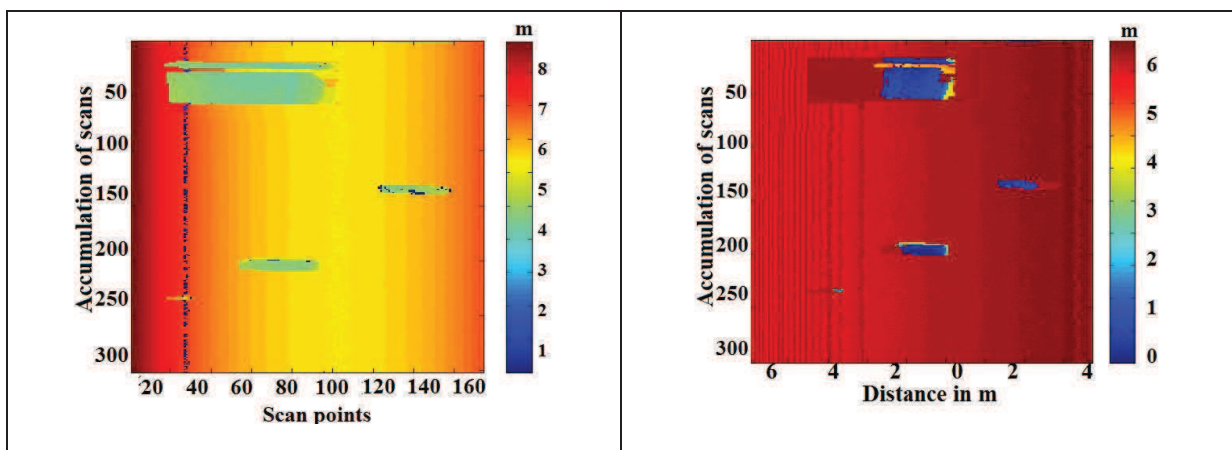


Figure 65: Before and after: (Left) semi-Cartesian coordinates system (Right) After changing the coordinate system.

On the left of Figure 65 the case after the application of the 'fill' filter is shown. All the missing values have been filled up. The windshields of the cars have also been filled up. On the right, when the coordinate system is completely changed, the information is given in terms of accumulation of scans and the distance in metres. The non-observed zone (shadows) can be easily retrieved by the naked eye.

Once the information is obtained after signal processing, the extraction is done by the LLC method. Here is the result after the processing:

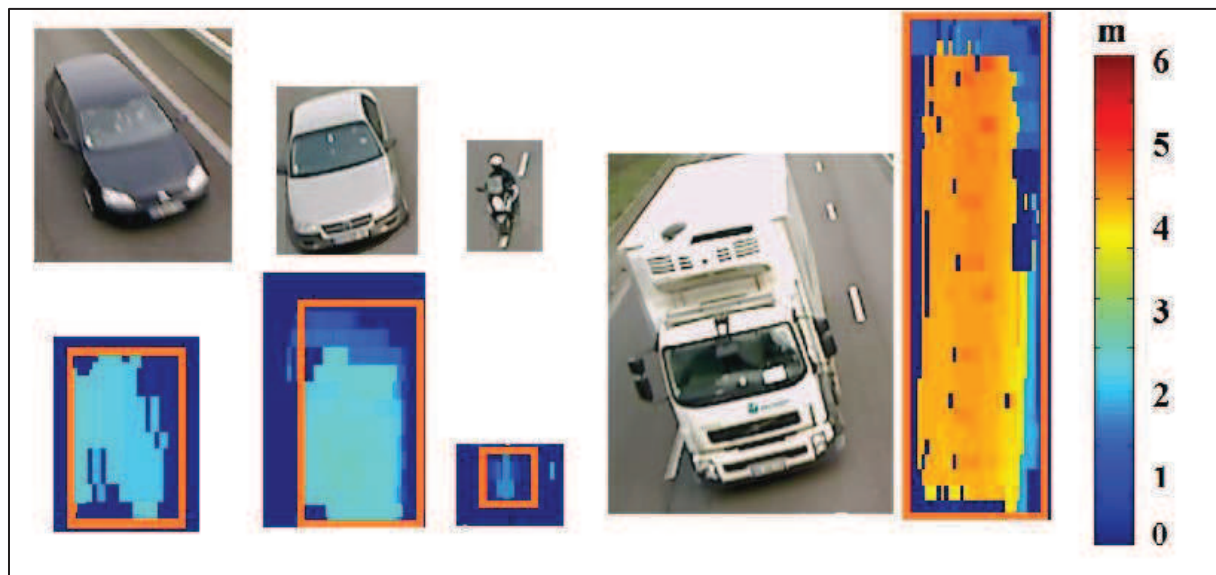


Figure 66: Vehicles extracted through LLC and their corresponding real images

Figure 66 shows the vehicles extracted, with their corresponding real images. All the detected vehicles are boxed in orange; it means that they are just extracted and not yet classified. As the system is at a height of 6.3 metres, we have an error of 194mm in the measurement. If the difference of estimated and ground truth value falls in the interval of  $3\sigma$ , this means that we are 99% certain of the values calculated by our method.

Here is the table of  $W$  measured by our method and the ground truth.

Vehicle	VW Golf	Opel Omega	PTW	Volvo mini truck
Width found (mm)	1608	1680	776	2095
Ground Truth (mm)	1786	1776	790	2140

Table 19: Comparison of the ground truth with the width found

Table 19 shows that all the calculated values are in the margin of  $3\sigma$  when we compare the values with the ground truth values. This shows that we are 99% certain of the precision of the calculated values.

Once the vehicles are extracted, they are classified. Here we have used SVM using two parameters  $W$  and  $H_{Nbx}$ .

## Conclusion

This chapter presents the detection, extraction and classification process from the laser scanner data obtained after the application of data coherence method.

To process the data in order to extract and classify vehicles, this chapter is divided into three main parts:

The raw signal contains noise and missing values. These missing values are due to dark objects present in the scene or to the windshields of the vehicles. Pre-processing is carried out and consists in rectifying the signal and accumulating scans. The following steps are proposed:

- The raw signal is taken and a filter pass band is applied to eliminate all the low values linked with the artefacts i.e. (Gaussian noise mostly) and high values (reflection towards the environment).
- A model  $M$  is defined. This model is the representation of an empty scan which is used as the scan of reference.
- Then the fill filter is applied. This filter fills the missing values depending upon the size of the group of missing values.
- For this filtered signal, the coordinates are changed from polar to Cartesian, thus, giving the transformed signal.
- This signal contains information in space at an instant of time  $t$ . So, the accumulation of space is carried out during the time period  $T$ , giving us the data in the spatio-temporal domain.

The accumulated data contains information about the vehicles on the road. Once the signal is rectified and all the missing values are filled, the extraction and classification steps are applied:

- Last Line Check Method: This method notices the variation in the height of the vehicle passing under the scanner. Once the object has completely passed through, the height drops below a threshold and the object is segmented.
- Two different classifiers are applied to the extracted object: an SVM and a KNN. An SVM is used because it is a binary classifier and is the most suitable for classification when the learning data base is not large. A KNN is one of the simplest classifiers, efficient if the value of  $K$  is high. As soon as the object is extracted and classified, it is counted. The counter takes the unique id of the classified vehicles.

At the end of this chapter, a demonstration was given to explain the results obtained after each step from processing the raw data until the vehicle was extracted and classified. In the next chapter the global results are shown after this proposed method has been applied on the entire database. These results are given along with explanations and interpretations.





## CHAPTER 4: Results and discussions

---

Introduction .....	91
4.1. Controlled site.....	91
4.2. Real Site SUDIII.....	96
4.2.1. SVM Results .....	96
4.2.2. KNN Results .....	102
4.3. Real Site Motor way A13 .....	107
4.3.1. SVM.....	108
4.3.2. KNN.....	108
Conclusion .....	110

---



## Introduction

The system processes the laser scanner's raw signal to detect, extract and count the vehicles that travel under the unit. Before presenting the results, here is a summary of the procedure:

The laser scanner is mounted on a gantry of a certain height above the inter-lane to cover a certain number of lanes (maximum 3 and ideally 2). The optimal position of the laser scanner with respect to the road profile is estimated and validated through the simulator. Once the position is defined, the site parameters i.e. the road verges and the height of the unit from the ground are calculated by data coherence method. The system is now ready for the laser scanner data processing.

For the pre-processing step, the data is in polar coordinates. There are some missing values (or non-observed values), usually due to the absorption of laser rays by dark or black objects. Similar behaviour is observed for the windshields. The 'fill' filter is applied to fill these non-observed values found in the scan. Once filled, the polar coordinates are converted to Cartesian coordinates and then these scans are accumulated (spatial information) during a certain period of time (temporal) to obtain the information in the spatio-temporal domain.

An extraction method; the Last Line Check (LLC) method, is applied to this information. Once the object is extracted, it is classified using either an SVM or a KNN. For the data collected at the controlled site just a SVM is applied, while on the real site both SVM and KNN are applied in order to compare their performances. Once the vehicle is classified, it can be counted.

The process summarized above has been applied to two different sites with two completely different conditions (Controlled and Real site) as discussed in Chapter Data Acquisition. The results are presented below.

### 4.1. Controlled site

Two different types of database were constructed by varying height of the laser scanner between 5 to 6 metres from the ground and at a distance of 3 metres perpendicular from the left edge of the road.

Different categories of vehicles passed at speeds varying from 20km/h to 120km/h, following all the safety standards. Here are a few cases presented constructed: A PTW passing alone, an LV passing alone, a PTW travelling in front of an LV, a PTW travelling behind an LV, a PTW travelling in between two LVs, an LV overtaking 2 LVs at the same time, a PTW travelling alone with a rider and a passenger; a PTW with a rider and a passenger overtaking an LV.

Figures 67 and 68 present the results with colour maps representing height.

Two types of vehicles are represented in terms of scans points on the  $X_{axis}$  and number of scans on the  $Y_{axis}$ . All this information is shown in semi-Cartesian coordinates.

The road is represented in blue while the PTW helmet and car roof are in red. A PTW correctly detected is put in a green boundary box, while the other categories of vehicles are in red.

It is to be noted that in the following Figures (67 and 68), the webcam was placed with a slight angle towards the environment, while the laser scanner was placed completely vertically to the ground. This slight angle of the webcam gave a larger field of view for the environment i.e. the passing vehicles.

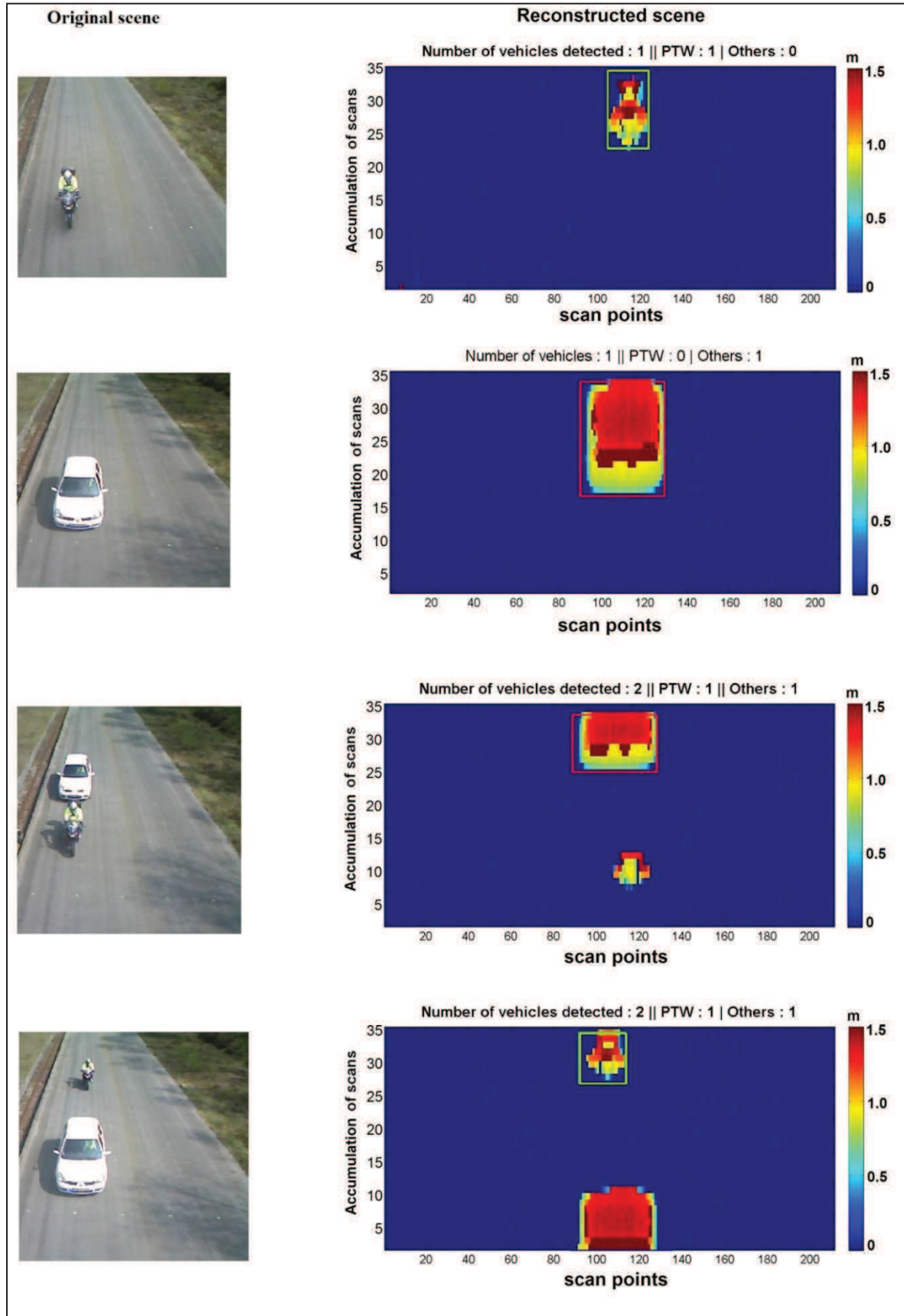
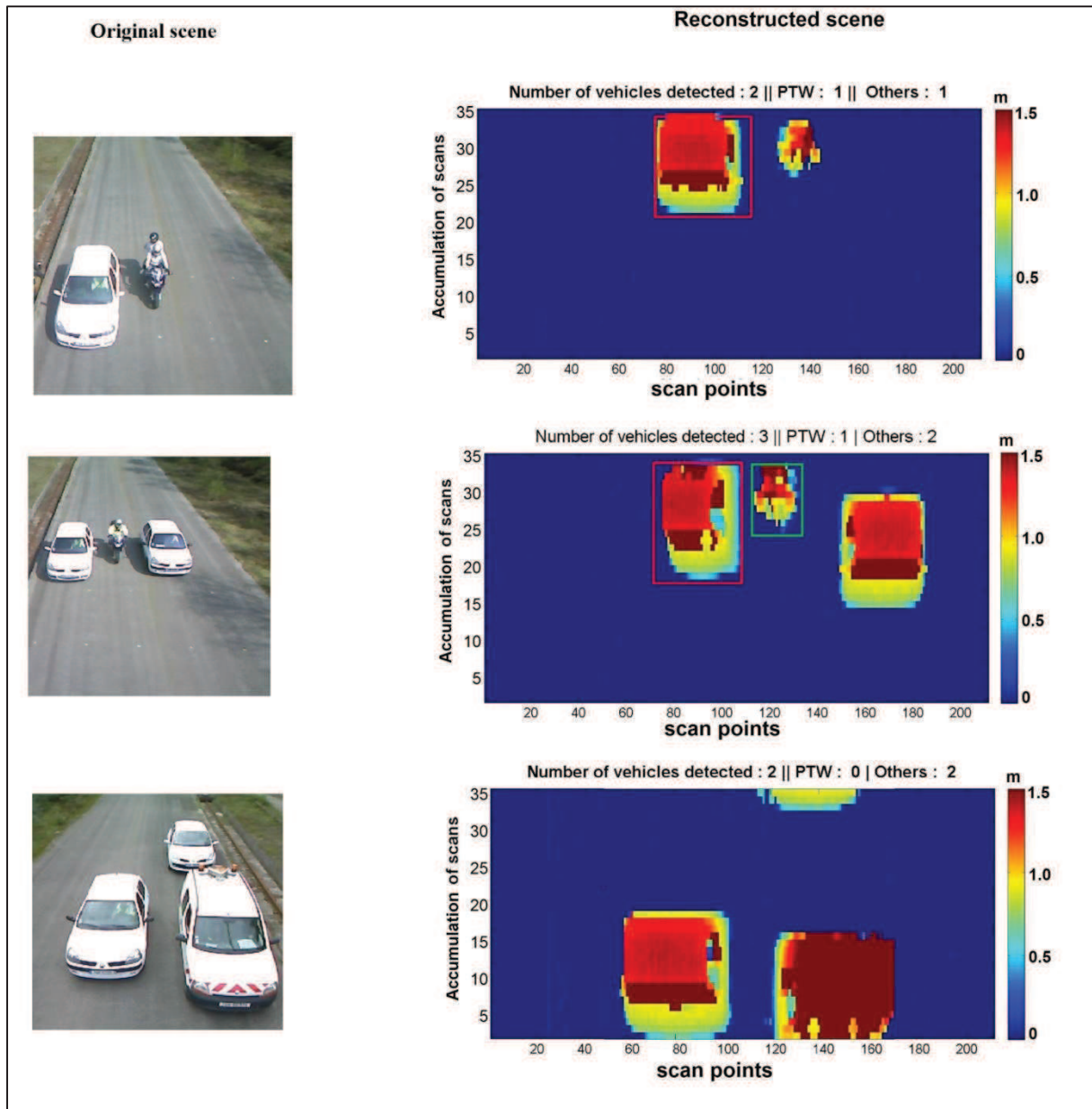


Figure 67: Scenes recorded with a camera installed next to the laser scanner, and results obtained after application of our method to these different scenes.



**Figure 68:** Scenes recorded with a camera installed next to the laser scanner, and results obtained after application of our method to these different scenes

A few examples of reconstructed traffic scenes are shown in Figures 67 and 68. On the left are the images of the scenes and on the right are the corresponding laser scanner images. The first image in Figure 68 shows a PTW with two passengers. The method was tested on the controlled site, with data represented in two different coordinate systems: semi-Cartesian coordinates and Cartesian coordinates. The results obtained after the application of the LLC method were more interesting with the Cartesian coordinates.

In the semi-Cartesian coordinate system, the distance ( $\rho$ ) was transformed into the height of the vehicle in metres and is plotted against the angle in degrees ( $\theta$ ), thus giving a semi-Cartesian coordinate system. Below is a table of the laser data acquired at the controlled site (Table 20).

	h=5m	h=6m	Total
PTW	52	25	77
LV	61	30	91
Van	0	0	0
Total	113	55	168

**Table 20: Controlled site database**

Of these 168 vehicles, 52 vehicles (28 PTWs and 24 LVs), were used in the training base. Table 21 shows the results when the LLC was applied with SVM.

LLC Method	Global	PTW
Correct detection rate	99.0%	98.6%
False detection rate	0.0%	0.0%
Non detected	1.0%	1.4%

**Table 21: Results of our method: semi-Cartesian coordinate system [120 samples]**

Table 21 presents the results applied to the controlled traffic for the LLC method developed. The result shows the detection rate for the global traffic and uniquely of PTWs in the semi-Cartesian coordinates.

The LLC method has a high overall detection rate of 99%; for PTWs the detection rate is 98.6%. This method is rapid as it is based on the intensity change of the last scan at each instant. Once the vehicle is detected and classified, it is counted.

In the results presented above (Table 21); there is no false detection as the conditions were controlled in terms of site and traffic i.e. a fixed number of vehicles (all white) in the constructed traffic. We do have one case where 1 PTW was not detected (which corresponds to 1% and 1.4% of non detected in table 21). This was when a van and a PTW were moving parallel to each other, with the van towards the laser scanner as shown in Figure 69.

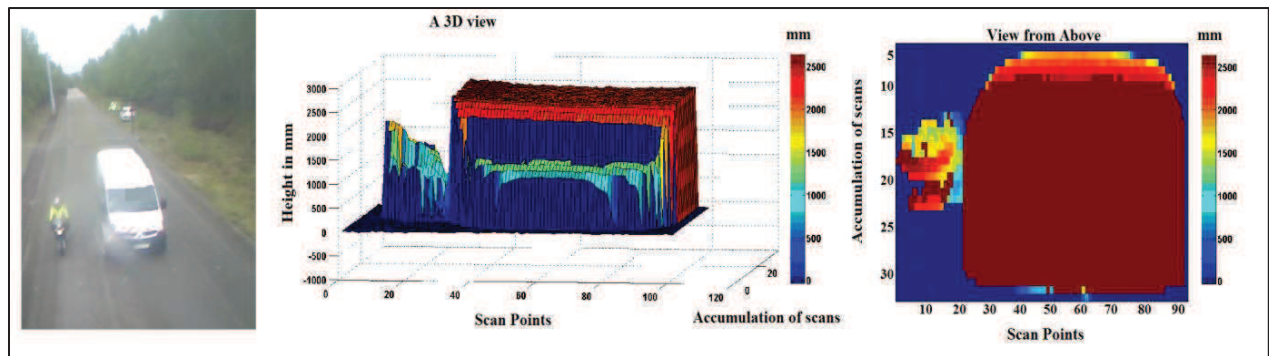


**Figure 69: 3D and 2D views of the semi-Cartesian coordinates**

Figure 69 represents a PTW travelling next to an HV. In the reconstructed 3D scene the ‘combination effect’ of the PTW and HV can be observed and hence, they are read as one vehicle by the system. This corresponds to the non-detected PTW.

The same type of problem was reported by [RIPO12] during the processing of traffic data in the city. But no solution was proposed for the problem.



So, to rectify this problem, the coordinates were completely changed to a Cartesian coordinate system thus giving a complete 3D view of the vehicle. This coordinate system change also takes into consideration the ‘slope’ effect. All these values that corresponded to blind spots are defined to zero in order to get a separate the combined vehicle as discussed in the previous chapter. So, after changing the coordinates the resulting image is shown in Figure 70.

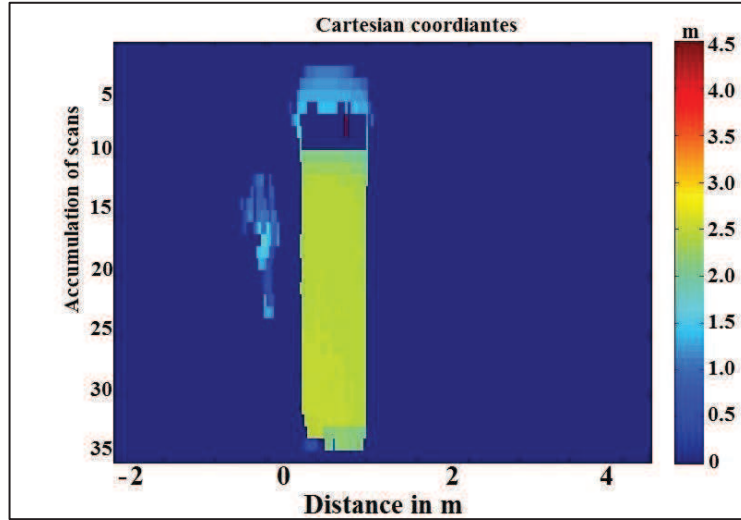


Figure 70: Cartesian coordinates

In Figure 70 the vehicles above are separated completely. The scene above is displayed with accumulation of scans on the  $Y_{axis}$  and distance in metres on the  $X_{axis}$ . The value of width calculated in the metric system helps us to validate our calculations by comparing them with the ground truth.

After processing, the results are as follows:

PTW detection rate	LLC
Correct detection rate	100.0%
False detection rate	0.0%
Non detected	0.0%

Table 22: Cartesian: Result of PTW detection

Table 22 shows a very encouraging result. It is to be noted, however, in the testing database, only one PTW was driven with different speeds and the learning set was constructed by taking a few samples from the database. This work was demonstrated at the mid-term METRAMOTO seminar organized on May 11<sup>th</sup> 2012 at CETE NC. For one scan, the average calculation time of the method, (conversion spatio temporal, LLC algorithm and classification) run with Matlab and on a normal machine, is 36ms. The method can thus work correctly in real-time if integrated in a real-time system deployed on a road. The seminar was open to the public and all the road administrators. This step validated our method and hence encouraged us to move to a real site.



## 4.2. Real Site SUDIII

Experimentations were conducted in the month of December 2012 on the site of SUDIII also known as RN338 consisting three lanes as shown below:

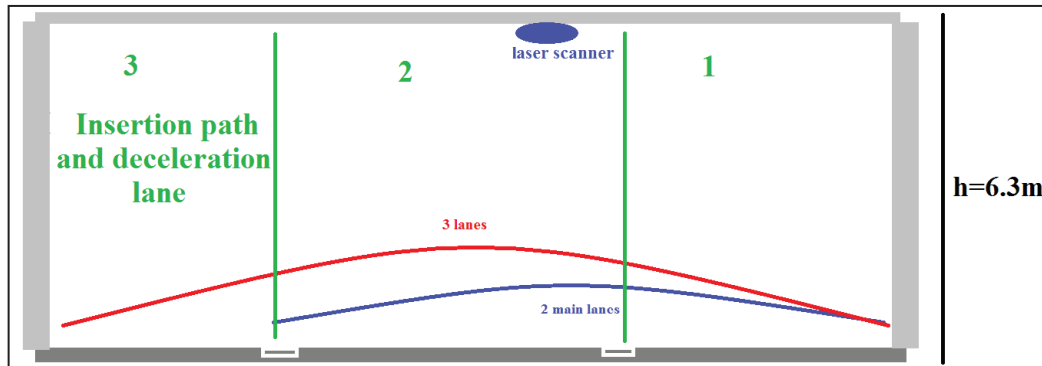


Figure 71: Site SUDIII

As shown in Figure 71, the third lane is an acceleration or insertion lane. This third lane must, therefore, share the traffic of the second lane (middle). The main problem in such a set-up is that one cannot just take two lanes and forget the third lane. Many vehicles move in between the second and the third lane, thus creating great confusion.

The laser scanner is placed at a height of 6.3 metres and not far from the exact middle of the first two lanes. As the three-lane traffic cannot be completely cut into two-lane traffic, a confidence range is defined. It corresponds to a width of 1m that is added to the second lane from the third lane so that a possible inter-lane vehicle case will be taken into account.

The learning database consists of 132 vehicles by taking the values of the base constructed from the controlled site at CETE NC and the first 2 minutes of the laser scanner data of the SUDIII. (Chapter: Data Acquisition). All these data were tested with two classifiers: SVM and KNN.

To make our system more precise, we add the notion of height of the vehicles classified as non PTW. The only way to distinguish between an HV and an LV is the height of the vehicle. An HV has a height of more than 4 metres, while an LV has an average height of nearly 2 metres. In other words, an HV is an LV with a height of more than 4 metres and a width more than 2m. Table 23 below gives the number of vehicles in the training database.

	PTW	LV	HV	Total
Controlled Site	28	24	0	52
Real Site	4	70	6	80
Total	32	94	6	132

Table 23: Training database (Controlled site + Real site)

### 4.2.1. SVM Results

As SVM is a linear and binary classifier, it is suited to our classification problem (PTW or non PTW). This three-lane data registered one hour of traffic (63 minutes) with a total of 2135 vehicles on 3 lanes. The traffic contained PTWs, LVs (cars, SUVs, etc), HVs (Trucks, Lorries, Busses, etc).

For a three lane classification problem, two parameters are used:  $W$  and the  $H\_Nbx$ .

		What the system detected			
Category of vehicle (GT)		PTW	LV	HV	Missed
	PTW	12	0	0	1
	LV	23	1878	0	7
	HV	0	0	214	0

**Table 24: Confusion matrix of vehicles: Real site**

Table 24 above presents the detection rate for the 63 minutes of traffic registered on SUDIII. There are 23 LVs that are misclassified as PTWs and there are 8 missed vehicles (1 PTW and 7 LVs). The number of vehicles misclassified as PTWs is nearly twice the number of PTWs classified correctly. Here are the explanations for the cases where the algorithm failed.

**Missing vehicles:** All the 7 missing LVs were observed in the third lane. These missing vehicles were due to the occlusion created by the HVs travelling in the second lane. The only missing PTW was not read by the system due to its high speed (145km/h or above). The exact value of this speed is unknown as no radar was installed next to the unit to calculate the speed of the passing vehicles. Figure 72 shows the example. Here are a few examples of occlusion.

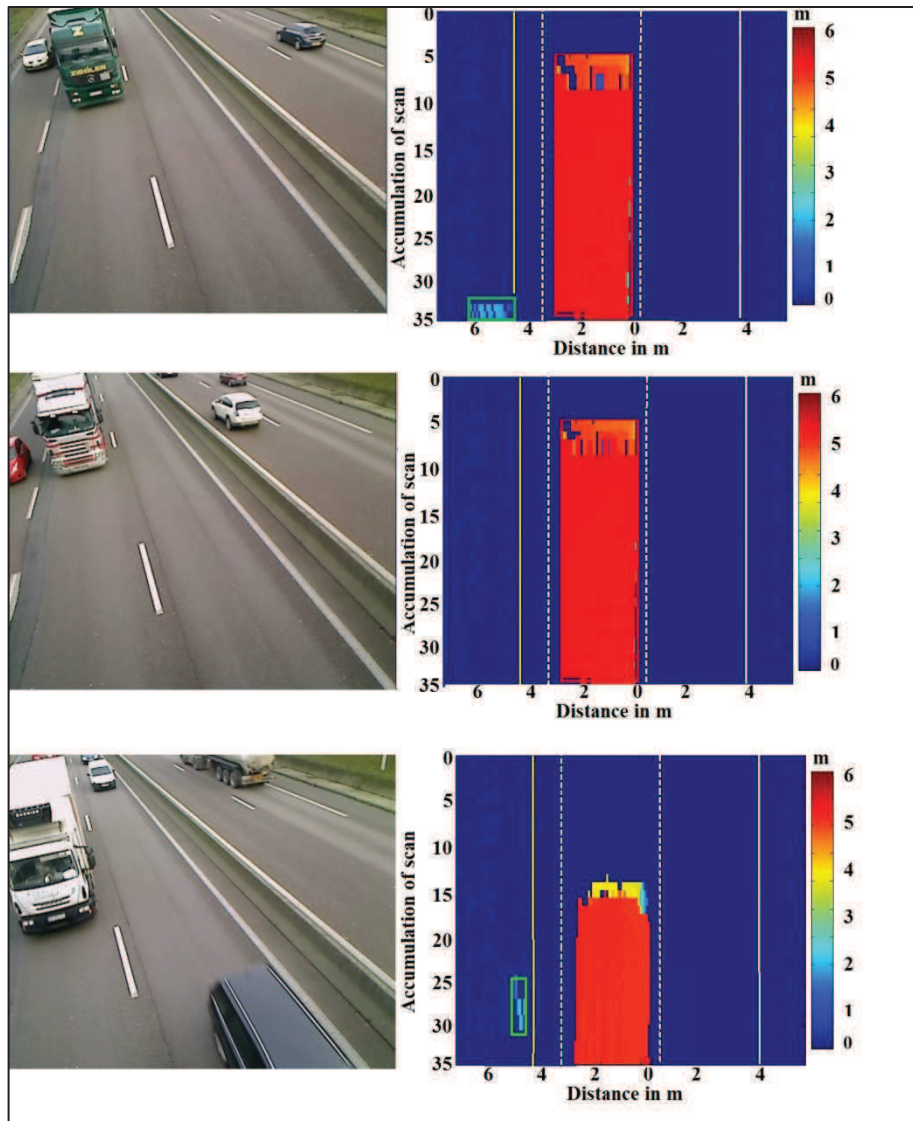


**Figure 72: Missed LVs due to occlusion**

The Figure 72 shows a few examples of occlusion observed on the RN338. The case where semi occlusion was observed, the classifier got confused and classified an LV as a PTW. Here are the detailed results for the 63 minutes data:

Lane number	Lane3	Lane2	Lane1
PTW	5	5	2
Others	390	997	705
Global classification %	95.1%	99.5%	99.1%

**Table 25: Vehicles detected on real site (1 hour data)**

Table 25 shows the correct classification rate of the overall traffic per lane. For 63 minutes an overall 98.5% correct classification rate was obtained, while for PTWs the correct classification rate was 91.7%. The detection rate is the least for the third lane which is explained by the missed vehicles and the LVs misclassified as PTWs. The first two lanes, however, have a higher detection rate. This is the detail of the result:

All vehicles (Others +PTW)		Lane2	Lane1	Total	Percentage
Correctly detected	ALL	979	699	1678	98.5%
	PTW	5	2	7	
Wrongly detected	ALL	17	6	23	1.3%
	PTW	0	0	0	
False Alarm		8	3	11	0.6%
Missed	ALL	1	0	1	0.1%
	PTW	1	0	1	
Total		997	705	1702	100

**Table 26: All vehicles detected on real site (2 lanes)**

Table 26 shows the global traffic of the first two lanes. It can be clearly seen that if only 2 lanes are taken, the risk of occlusion becomes minimum. Seven PTWs out of 8 were detected and correctly classified, thus giving a correct classification rate of 87.5% for the PTWs. This justifies the choice of scanning two lanes instead of three when using a single laser scanner. The proposition done has been explained in detail and is presented in Chapter 2 (Data Acquisition).

For the three-lane data, choosing two lanes increases the difficulty of the situation. In Table 26, several false alarms and wrong detection cases can be noticed for Lane 2. Taking just two lanes increases the wrong detection rate, as sometimes a vehicle changing lanes might just be cut into two, thus leading the extractor and classifier to treat the passing vehicle as a PTW. Hence the line of a line of tolerance has been introduced on the Lane 3 at a distance of 1 metre from the inter-lane of Lane 2 and Lane 3. The zone inside this line of tolerance is hereby called zone of confidence.

In order to verify the results obtained with the ground truth, it takes a lot a time as the verification has to be done manually to validate the presence of vehicles in the inter-lane.

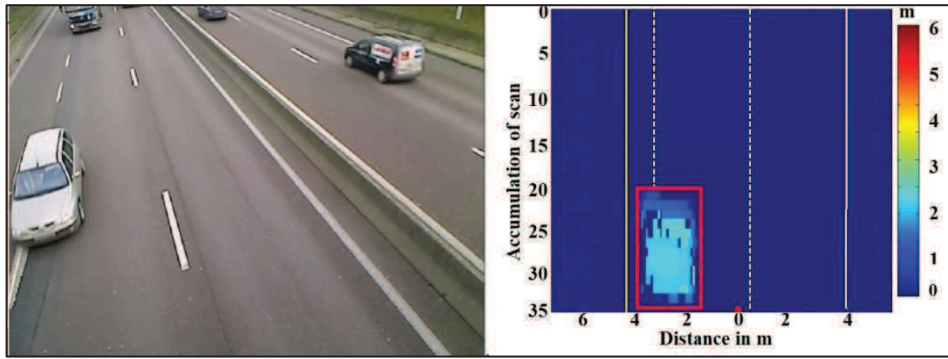


Figure 73: The original scene and the vehicle passed under the scanner. The red dot is where the laser scanner is placed. Yellow line is the line of tolerance.

On the right in Figure 73, the yellow line corresponds to the line of tolerance. As the vehicles were coming in and getting out of the third lane, so many times the vehicles were found at the inter-lane of second and third lane under the laser scanner. Brutally cutting three lanes into two may cut all these vehicles as well. To avoid this loss at maximum, a line of tolerance has been introduced on the Lane 3 at a distance of 1 metre from the inter-lane of Lane 2 and Lane 3. This distance of 1 metre corresponds to the width of the hard shoulder. For this two-lane problem, two SVMs and KNN are used with different parameters. To each of these classifiers, a mono parameter ( $W$ ) and the double parameters ( $W$  and  $H\_Nbx$ ) are used. This would help to see if a single classification parameter is able to classify this complex problem. Table 27 shows the traffic per category of vehicle per lane.

Type of Vehicle		Lane 2	Lane 1	Total per category
PTW		21	9	30
Others	LV	3190	1749	4939
	HV	1104	801	1905
Total		4315	2559	6874
Share / Lane %		62.8	37.2	100.0

Table 27: Traffic per lane (per category).

#### 4.2.1.1. SVM1

As the title suggests, here only one parameter is used to classify a vehicle i.e.  $W$ . This parameter was chosen as the width normally remains the same irrespective of the speed of the vehicle (except when the laser scanner rays fall on a PTW travelling at a very high speed). This was explained previously in detail in chapter 3 Extraction and Classification. Figure 74 shows the plot of different widths for different categories of vehicle (PTW and Non-PTW).

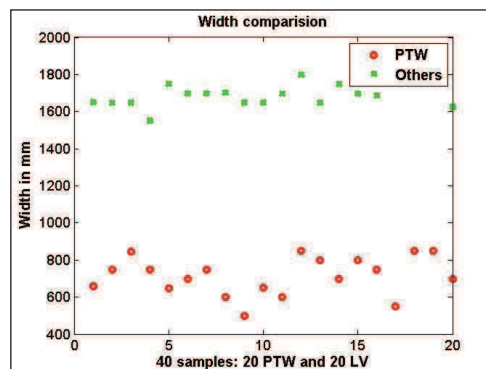


Figure 74: Width

Here is the classification result using  $W$  as the only parameter for the SVM:

		What is detected			
Ground Truth		PTW	LV	HV	Missed
	PTW	28	0	0	2
	LV	69	4870	0	0
	HV	0	0	1905	0

Table 28: SVM single parameter results

Table 28 above presents the classification results with the  $W$  as the only feature used to separate three classes. The table shows three classes PTW, LV and HV. It is to be noted that 69 LVs are misclassified as PTWs, which is due to the introduction of the line of tolerance. A total of 98.9% correct detection rate is obtained. Below is a table with more detailed results showing the detection rate per lane.

All Vehicles	Lane2	Lane1	Total	Percentage
Correctly detected	4260	2543	6803	98.9%
Wrongly detected	54	15	69	1.0%
Missed	1	1	2	0.0%
Total	4315	2559	6874	100%
Percentage/ lane	98.7%	99.3%	98.9%	
False alarm	61	3	64	0.9%

Table 29: Per lane detection rate using SVM (Width)

In table 29, a lower detection rate is observed for the second lane. This is due to the fact that the second lane carries traffic that depends upon the third lane traffic. All the vehicles entering and exiting the expressway are somehow at the middle of second and third lane. So most of the time, the vehicles taken into account are not completely in the zone of confidence as shown in Figure 75. So,  $W$  is sometimes a non-robust parameter for the correct classification of vehicles.

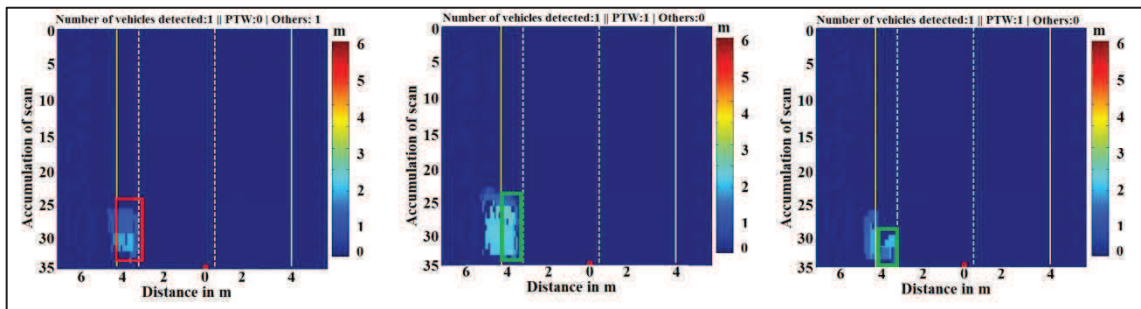


Figure 75: Vehicles passing through the zone of confidence (SVM (width)).

Figure 75 shows different cases when different vehicles are changing lanes, so they are cut by the line of tolerance. At the extreme left, a vehicle is observed which is correctly classified by the method, whereas in the other two cases, we have vehicles confused as PTWs. The vehicle inside the zone of confidence is not wide enough, hence confusing the classifier.

Tables 28 and 29 show the result. A total of 69 LVs were detected as PTWs: As many as 54 out of 69 LVs were misclassified in the second lane. These were mostly cut by the margin created that corresponds to the zone of confidence as can be seen in Figure 76. The first lane had fifteen LVs misclassified as PTWs. These cases correspond to small LVs travelling at high speed.

False alarms: There are nearly as many false alarms as there are misclassified PTWs. This number is twice the number of PTWs present in the database. The false alarms are explained in the general explanation section at the end of all the results (Figure 79).

Missed vehicles: The two PTWs that were not detected passed at a very high speed and the laser scanner did not have enough time to retrieve the information.

#### 4.2.1.2. SVM2

This SVM uses two parameters,  $W$  and  $H\_Nbx$ , in order to separate PTW class and non PTW class by a hyperplane. A combination of these two parameters might result in a classifier robust enough for the maximum real-time urban traffic classification problems.

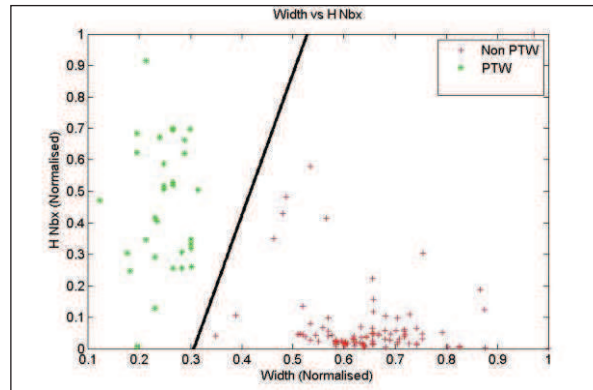


Figure 76: Linear separation: Width to Height to number of scans. PTW in green and others in Red.

The classification results are shown in the Table 30.

		What is detected			
Ground Truth		PTW	LV	HV	Missed
	PTW	28	0	0	2
	LV	42	4897	0	0
	HV	0	0	1905	0

Table 30: Confusion matrix SVM2

By using two features, the results have improved with a correct classification rate of 99.3% for global traffic and 93% for the PTWs. The results are better than SVM1 but still we have 42 LVs misclassified as PTWs.

Global		Lane2	Lane1	Total	Percentage
Correctly detected	ALL	4279	2551	6830	99.3%
	PTW	22	6	28	93.3%
Wrongly detected	ALL	35	7	42	0.6%
	PTW	0	0	0	0%
Missed	ALL	1	1	2	0.0%
	PTW	1	1	2	0.0%
Total		4315	2559	6874	100%
Percentage/ lane		99.1%	99.6%	99.3%	
False alarm		61	3	64	0.9%

Table 31: Per lane detection rate using SVM2 ( $W + H\_Nbx$ )



Table 31 presents the global results for all vehicles (including PTWs) and PTWs alone using two features, thus demonstrating that the classifier becomes more robust. For cases where the  $W$  alone fails to classify; the feature  $H\_Nbx$  helps by adding the notion of density to most of the vehicles half cut while passing through the zone of confidence. This can be seen in Figure 77.

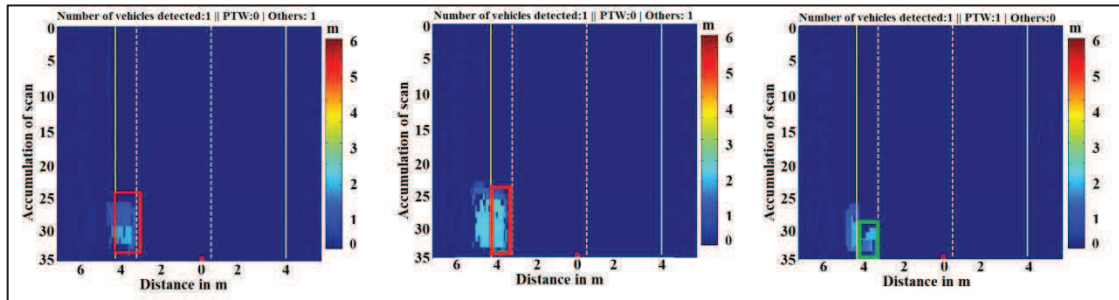


Figure 77: Vehicles passing through the zone of confidence (SVM2 ( $W+H\_Nbx$ )).

The Figure 77 shows relatively better results than the results for SVM1. For the first two cases, the vehicles are correctly classified. In the third case, the height representing the vehicle in the zone of confidence is too low for the classifier to correctly classify the vehicle.

A total of 42 LVs were detected as PTWs. In the second lane 35 out of 42 LVs were misclassified as PTWs. These were mostly cut by the margin created that corresponds to the line of tolerance (Figure 77). This number of misclassified vehicles is relatively lower than in SVM1. The improved detection rate is thanks to the addition of the notion of  $H\_Nbx$ .

#### 4.2.2. KNN Results

For this part three different values of  $K$  have been chosen,  $K=5$ ,  $K=10$  and  $K=20$  in order to understand, how the classification results evolve with the increase in the value of  $K$ . Two classification cases have been defined, KNN1 uses  $W$  as the only parameter of classification while  $W + H\_Nbx$  are taken as the parameters for KNN2. The KNN results for  $K=5$  are shown in the Table 32.

K=5	KNN1			KNN2			Missed
	PTW	LV	HV	PTW	LV	HV	
PTW	28	0	0	28	0	0	2
LV	105	4834	0	74	4865	0	0
HV	0	0	1905	0	0	1905	0

Table 32: KNN results ( $K=5$ )

With five neighbours, when  $W$  is used as a single feature for the classifier, a global classification rate of 98.4% is obtained whereas the classification performance increases to 98.8% for KNN2 for all vehicles. The reason behind this low detection rate is lower number of neighbours ( $K$ ). As this classifier is biased by the value of  $K$ , it does not have enough neighbours to compare the testing base. Thus the risk of false detection increases. The KNN results for  $K=10$  are shown in the Table 33.

K=10	KNN1			KNN2			Missed
	PTW	LV	HV	PTW	LV	HV	
PTW	28	0	0	28	0	0	2
LV	56	4883	0	46	4893	0	0
HV	0	0	1905	0	0	1905	0

Table 33: KNN results  $K=10$



When the number of neighbours is increased to 10, a relatively higher classification rate of 99% is obtained for a single feature ( $W$ : KNN1), while for the two features; KNN2, this rate increases to 99.3%. It must be noted that the percentage of misclassification decreases almost by a factor of 2.

The misclassified vehicles correspond to the LVs that are smaller in size and travel at a high speed. As discussed in Chapter 3, the value of  $K$  can be calculated using the rule of thumb, i.e. by taking the square root value of the size of the learning set which is 132 vehicles in our case. So, taking 12 as the value of  $K$  may give us a reliable classification result. The KNN results for  $K=20$  are shown in the Table 34.

K=20	KNN1			KNN2			Missed
	PTW	LV	HV	PTW	LV	HV	
PTW	28	0	0	28	0	0	2
LV	42	4897	0	36	4903	0	0
HV	0	0	1905	0	0	1905	0

Table 34: KNN results  $K=20$

At  $K=20$ , a global classification rate of 99.3% is obtained for KNN1 which is very encouraging result whereas with two features the correct global classification rate increases to 99.4% for all vehicles. No significant improvement in the results can be seen when the value of  $K$  exceeds 20 neighbourhoods. The overall results obtained are nearly the same as were obtained applying SVM2.

The PTWs were detected at a rate of 93.3% for the nearest neighbour value at 20. The 2 non-detected PTWs were travelling high speed and so the laser scanner did not have enough time to read them. An analysis of the rate of misclassification of LVs as PTWs shows that for  $K=5$  to  $K=20$ , the misclassification rate decreased by a factor of 3 for KNN1 and 2 for KNN2. This demonstrates that when the number of neighbourhood members increases, the classification results become more reliable. There are twice as many false detections as the number of PTWs detected. This can be explained by the reflections generated by windshields, oil tankers, trailers and by the fact that cutting the road sections in two cuts the vehicles as well.

KNN is a simple classifier but its processing speed is directly proportional to the size of database (number of calculations) and the value of  $K$  chosen.

Overall, a correct detection rate of 99.4% is obtained for the global traffic. The remaining 0.6% is shared by the wrongly detected vehicles and the missed vehicles. In the traffic of 6874 vehicles, there were 30 PTWs of which 28 were detected and correctly classified. The other two were among the missed vehicles. Figure 78 shows the two cases where the PTWs were not detected.

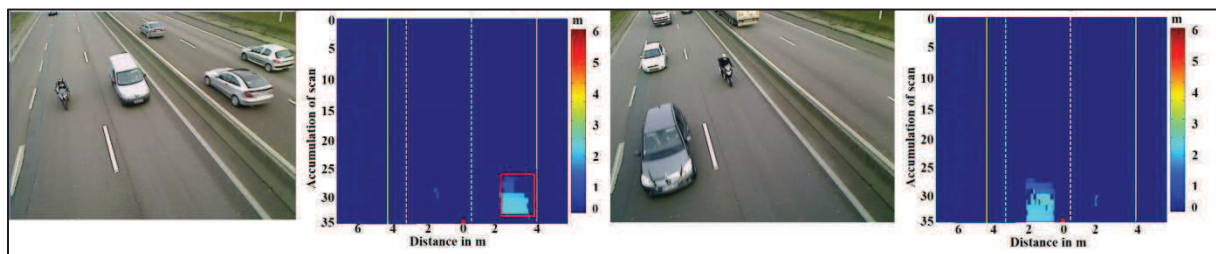
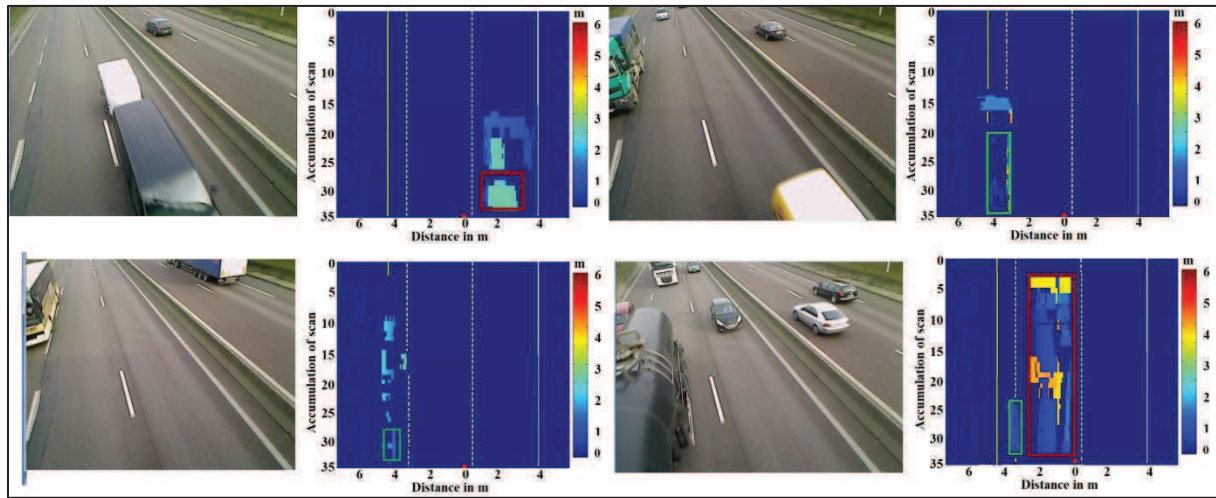


Figure 78: Case when the PTW is not detected

Figure 78 presents the case where our method was not able to detect the PTWs in the traffic. In both cases the speed of the PTW was high (145km/h or more) and hence the number of scans i.e. information that the system was able to retrieve, was insufficient for the algorithm to process. One of

the most important parts in the results is the false alarm case. In our case there are around 1.0 % of cases where a false alarm occurs.



**Figure 79: False alarm cases**

Figure 79 shows all the false alarm cases, not all of which are for PTWs; sometimes they are for an LV. The problem is mostly due to the refraction or high scattering of the laser scanner beams caused by different materials, trailers, etc. Here are a few examples of such cases:

The first case, top left, is quite common and can be seen often on the highways. There is a trailer behind an LV and it is detected as a separate vehicle. This does not happen every time. When the speed of the vehicle is high, the system may not have enough time to read the connector between the LV and trailer so the system detects two different vehicles.

The second case, top right, is the metallic bordered truck covered with a piece of leather / fabric. The front part of the truck is detected whereas the system is able to read just its metallic border and not the rest of the structure, so scattered data is observed and detected as a PTW. This might be similar to when the PTW is moving very slowly below the laser scanner.

The third case, bottom left, is when the laser scanner beams hit the window of the bus which are quite large in size. A refraction effect is observed and the beam is scattered, thus creating several small scattered information. The system takes these reflected parts as independent bodies and classifies them separately.

The fourth case, bottom right, involves an oil tanker. The laser beam tends to scatter when it touches the tanker, hence projecting a false alarm for the system.

There are a very few exceptions, which may be metallic objects of unknown shapes. Figure 80 shows the case where a ‘racing car’ shaped vehicle can be seen. These types of cars are not common but might sometimes generate false detections.

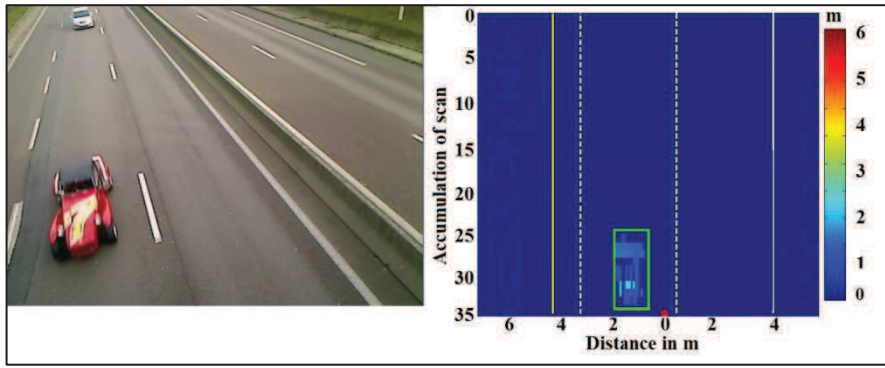


Figure 80: Exceptions

There are a few problems with that hinder the fair detection of the PTWs. For example, the air turbulence caused by an HV passing with a high speed next to the sensor, thereby oscillating or creating a lateral moment of the system. Hence it creates an effect of a curtain like noise that appears in the scene. This is shown in Figure 81. This curtain like noise is not important below the sensor (in light blue) and becomes significant as it moves away from the sensor (like an arc).

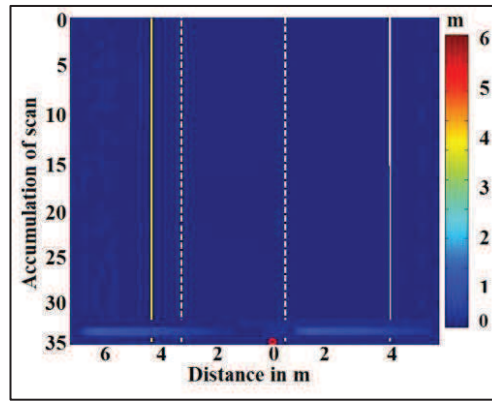


Figure 81: Sensor noise

A working example of our method is shown at the beginning of the section 4.2, that gives a practical validation to the choice of reading 2 lanes instead of 3 lanes. With 3 lanes, the problem of occlusion is often noticed. This can be more easily observed with very heavy traffic when most of the LVs or PTWs are occluded by the HVs. However, with 2 lanes, all the vehicles at the inter-lane of the second and third lane will be cut, and will thus generate false alarms and false detection.

All the results above show only 30 PTWs out of 6874 vehicles (LV+HV+PTW). The traffic of PTWs in this database represent around 0.4% of the total traffic which is a very low share and hence cannot be presented separately in a table.

A few examples of the PTWs detected are shown in Figure 82.

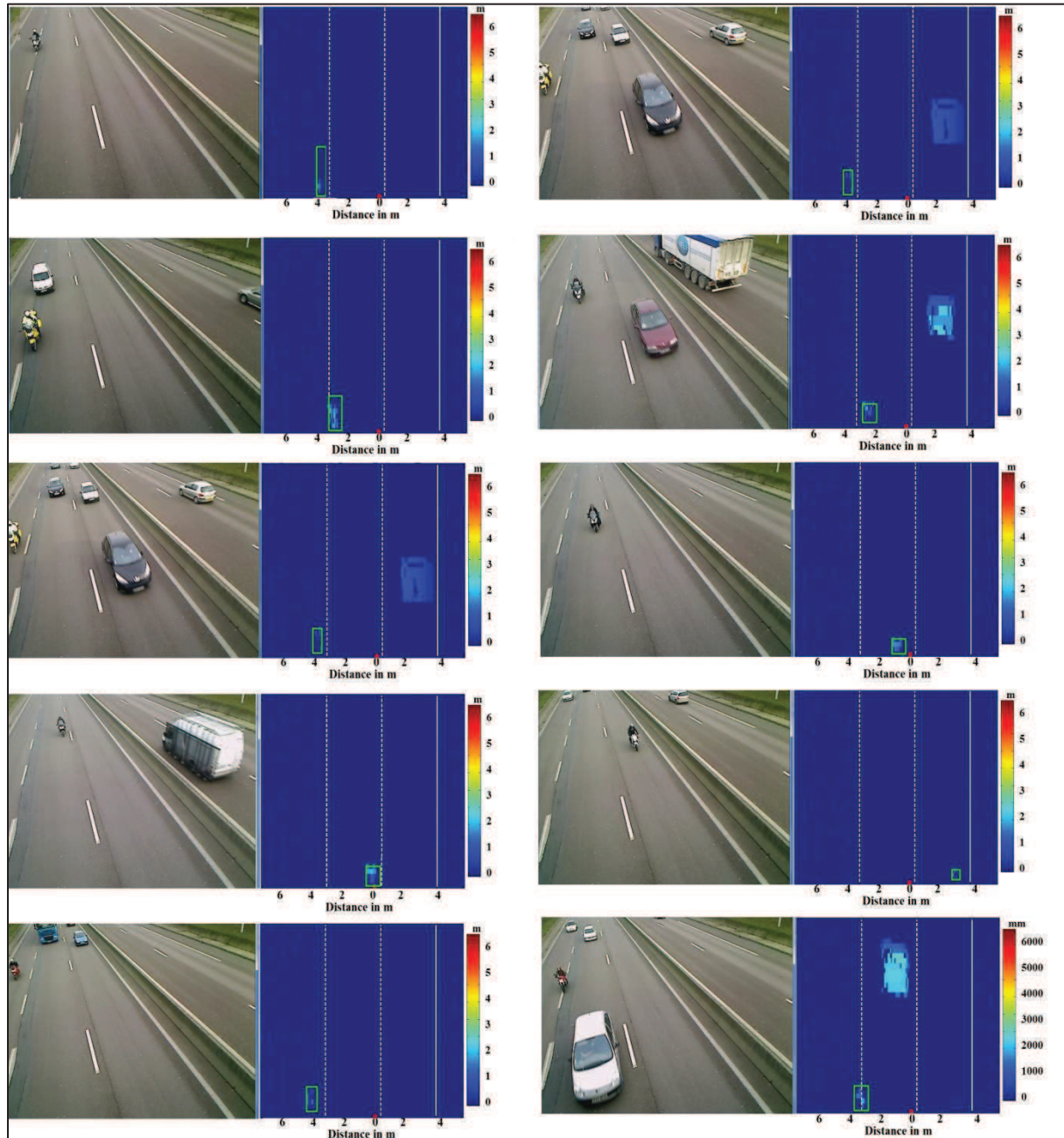


Figure 82: Different PTWs detected

Table 35 compares SVM and KNN performance on RN338 data:

Comparative table of classifiers (All vehicles)	KNN						SVM	
	K=5		K=10		K=20		SVM1	SVM2
	KNN1	KNN2	KNN1	KNN2	KNN1	KNN2		
Correct detection rate (%)	98.4	98.8	99.0	99.3	99.3	99.4	98.9	99.3
False detection (%)	1.5	1.1	0.8	0.7	0.6	0.5	1.0	0.6
Missed (%)	0	0	0	0	0	0	0	0

Table 35: Comparative KNN and SVM performance table P1: single parameter and P2: two parameters



Table 35 compares the performance of both the classifiers KNN and SVM. KNN gives nearly the same performance as SVM2. A KNN becomes slower with the increase in the number of K. Here is a table with the confusion matrix for the KNN and SVM

		What is detected											
Ground truth	KNN	K=5				K=10				K=20			
	PTW Alone	KNN1		KNN2		KNN1		KNN2		KNN1		KNN2	
		PTW	Other	PTW	Other	PTW	Other	PTW	Other	PTW	Other	PTW	Other
	PTW	28	0	28	0	28	0	28	0	28	0	28	0
	Other	105	6739	74	6770	56	6788	46	6898	42	6802	36	6808

**Table 36: KNN: Confusion matrix for PTW**

Table 36 shows a comparison of the confusion matrices obtained by varying different values of K and with a single parameter (KNN1) and two parameters (KNN2).

Ground truth	SVM	What is detected				
	PTW Alone	SVM1		SVM2		
		PTW	Other	PTW	Other	
		PTW	28	0	28	0
		Other	69	6775	42	6802

**Table 37: SVM: Confusion matrix for PTW**

The two comparative tables 36 and 37, show the results of each classifier. The method was able to attain a detection rate as high as 93% for the PTWs. The two non-detected PTWs were travelling at high speed (>144km/h).

If the evolution of the misclassification rate of LVs as PTWs is seen, for K=5 to K=20, the rate decreased by a factor of 3 for KNN1 and by a factor of 2 for KNN2. This shows that if the number of neighbourhood members increase; the classification results become more reliable. There is twice as much false detections as the number PTWs detected. This can be explained by the reflections generated by the windshields, the oil tankers, the trailers and fact of cutting a 3 lane carriageway in a 2 lane carriageway thereby cutting the vehicles present on them as well.

However, the number of PTWs present in the testing database, i.e. 30 are not sufficient to judge a true performance of our method and hence it would not be legitimate to compare the performance with SVM and KNN as they both are giving the same results for PTW i.e. 28 PTWs out of 30. This conclusion led us to test our algorithm on the site of A13 where the number of PTWs is relatively higher and they share a higher percentage of traffic as well.

### 4.3. Real Site Motor way A13

The experiment was conducted in June 2013. The laser scanner is 6.5 metres above the centre point between the first two lanes. For this experimentation, the same learning data base is used as in the previous part (SUDIII). Table 38 details the global traffic on the Parisian motor way (A13) which is a 3-lane problem.

Overall traffic/ Lane	Lane 3	Interlane (3-2)	Lane 2	Interlane (2-1)	Lane1	Total
PTW	0	0	3	43	8	54
Others	177	1	163	2	187	530
Total	177	1	166	45	195	584
Percentage	30.3%	0.1%	28.4%	7.7%	33.4%	100%

**Table 38: Parisian traffic (Motorway A13)**

As shown in the previous section, SVM and KNN classifiers were also applied to this database.

#### 4.3.1. SVM

As discussed in the last section, two different types of parameters are used for the SVM classification. In the first case, the  $W$  of the vehicle is used as the only parameter to separate classes. This is called as svm1 whereas in the second case,  $W$  and  $H\_Nbx$  are used as the parameter of separation. This second case is called SVM2.

Table 39 shows the comparative results obtained on the A13 data after applying SVM1 and SVM2:

SVM	SVM1		SVM2		Missed
	PTW	LV	PTW	LV	
PTW	54	0	54	0	0
LV	12	514	4	520	6

**Table 39: SVM classification results on A13**

A global detection rate of 97.2% is obtained for SVM1 while for SVM2 this rate increases to 98.2%. A rate of 100% was obtained for the PTWs and only 2 false alarms were registered. Out of these false alarms, there was only one false alarm for a PTW. These two cases are presented at the end of the KNN section (Figure 84).

The number of false detections has decreased by a factor of 3 for SVM2. These false detections were most commonly observed in the third lane where the  $W$  of vehicle is not always significant due to partial occlusions by the vehicles travelling in the middle lane. The six non-detected or missed vehicles correspond to the LVs that were occluded by HVs in the third lane.

#### 4.3.2. KNN

For this part three different values of  $K$  have been taken, as in the previous section,  $K=5$ ,  $K=10$  and  $K=20$ . The classification part has been sub divided into two cases. The first case uses  $W$  as the unique parameter and is called KNN1, whereas for the other case, the parameters taken are  $W$  and  $H\_Nbx$  and is called KNN2. Table 40 compares the performances of KNN1 and KNN2 for  $K=5$ .

K=5	KNN1		KNN2		Missed
	PTW	LV	PTW	LV	
PTW	54	0	54	0	0
LV	14	510	11	513	6

**Table 40: KNN results for Paris A13 (K=5)**

With five nearest neighbours, the global classification rate using the  $W$  alone (KNN1) is 96.5% while the global classification performance increases to 97.1% for KNN2. The reason for this low detection rate is a low value of the nearest neighbour, as in the previous section. The classifier becomes less efficient if the number of nearest neighbours is low. However, the detection rate for PTWs remains at 100% with two false alarms.

When the value of  $K$  is doubled, i.e.  $K=10$ ; the results are shown in table 41.

K=10	K1		K2		Missed
	PTW	LV	PTW	LV	
PTW	54	0	54	0	0
LV	12	512	7	517	6

**Table 41: KNN results for Paris A13 (K=10)**

When the number of neighbours is increased to 10, a relatively higher classification rate of 97% is obtained for a single feature ( $W$ ) while for the two features, this rate increases to 97.7% for KNN2.

Table 42 shows the classification results for the value of  $K$  as 20.

K=20	K1		K2		Missed
	PTW	LV	PTW	LV	
PTW	54	0	54	0	0
LV	11	513	3	521	6

**Table 42: KNN results for Paris A13 (K=20)**

At  $K=20$ , the encouraging results at 97.1% for all vehicles were obtained by using  $W$  (KNN1) as the only parameter whereas with two features (KNN2) the correct classification rate increased to 98.5% for all vehicles. The classification performance starts to stabilize when the value of  $K$  exceeds 20 neighbourhoods. The results obtained are nearly the same as were obtained by applying SVM2.

Discussion: For all these cases, there were 6 missed vehicles. All these vehicles were travelling in the right-most lane (third lane) and were occluded by the heavy vehicles. All 54 PTWs were detected and only 3 LVs were misclassified as PTWs. These three misclassified vehicles correspond to either small cars that moved at high speed in the left-most lane or the vehicles that were semi occluded by the heavy vehicles.

However, there were just two false alarms. One false alarm corresponded to a trailer car while the second one corresponded to the reflection of an HV. The number of false alarms found in this experimentation is not as high as in the experimentation carried out on SUDIII. This can be explained by understanding the difference between the two sites, the type of traffic present and the density of the traffic.

Here are a few differences between the nature of data obtained from the two real experimental sites (SUDIII and A13):

- Traffic on SUDIII was free flowing traffic, whereas on the Paris A13 it was congested.
- Most of reflections that generated the false alarms were due to oil tankers. For the Paris A13 data, no oil tankers passed through.
- The laser scanner was placed on a bridge which was not perpendicular to the SUDIII road. This gave a deformed shape of LVs and PTWs passing under the laser scanner.



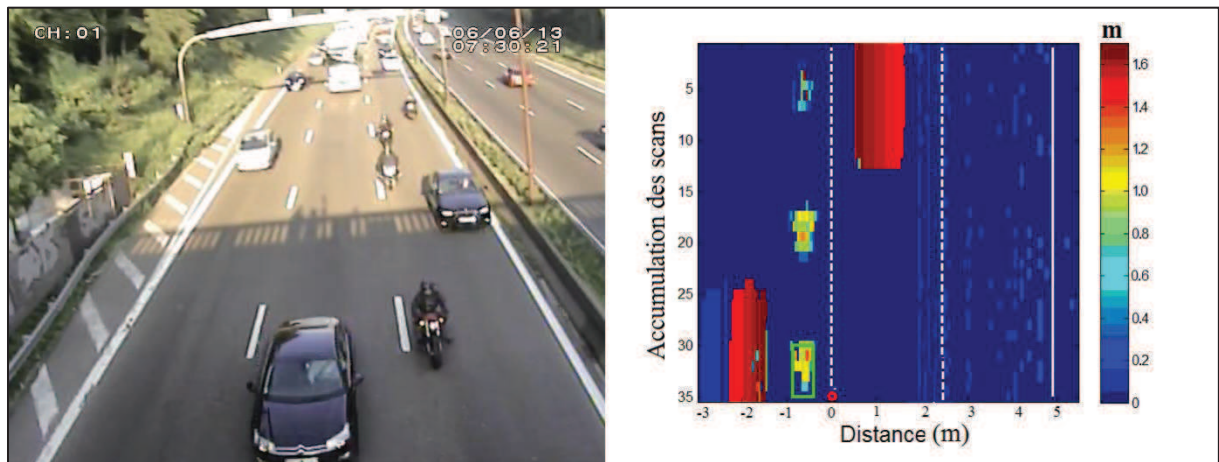


Figure 83: Inter-lane practice A13

Figure 83 shows an example of the practice of inter-lane riding, which can be easily seen in Parisian traffic. Our algorithm is able to correctly extract and classify PTWs moving close to LVs even in congested traffic. The only two cases where a false alarm was generated are shown in Figure 84.

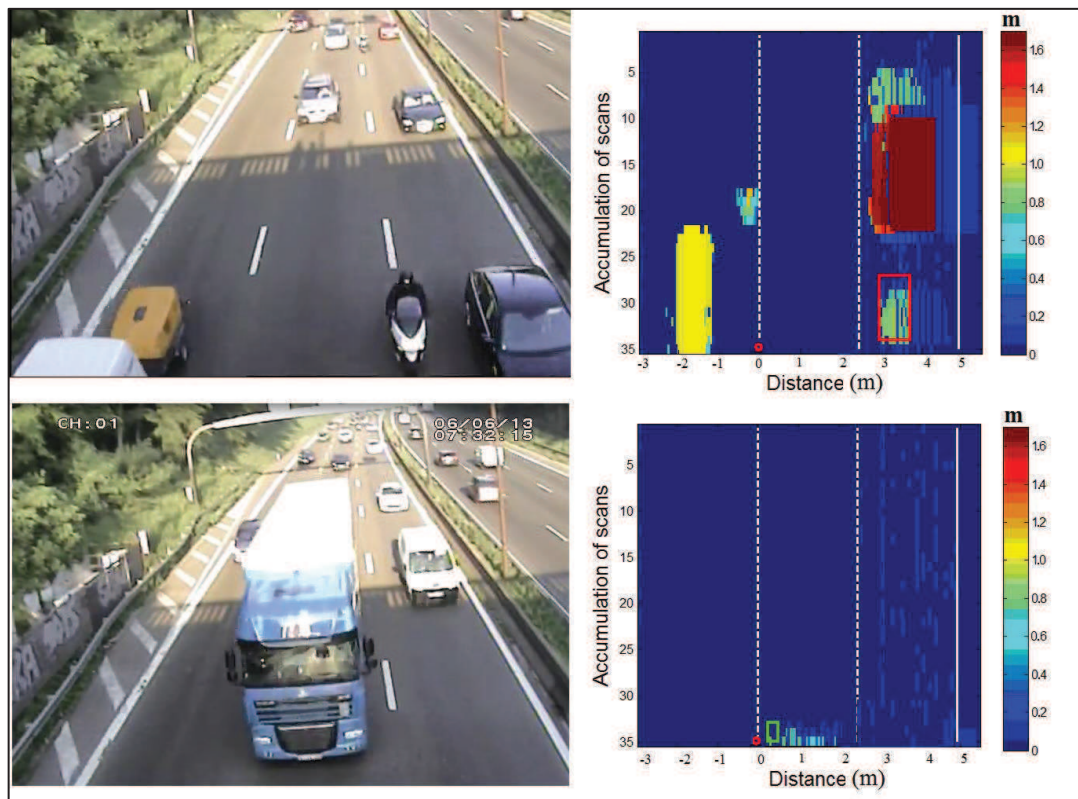


Figure 84: The false alarm cases (A13)

In the first case, in the presence of a trailer, our algorithm got confused and took it as another vehicle. In the second case, the reflection caused by the windshield of an HV created this confusion.

## Conclusion

In this chapter the overall results of the solution proposed for detecting and counting PTWs in traffic are given. Our method was first tested on the data constructed at the controlled site where the traffic, speed, behaviour, inter vehicle distance etc were respected. For the classification an SVM was used as it is a binary classifier and we have either a PTW or a non-PTW in the traffic, since PTW is the

category of vehicle that interests us. The experimental results gave us a 96.8% correct detection rate for PTWs at the controlled site. The non-detection was due to the fact that semi-Cartesian coordinates were used i.e. the values were plotted with height in metres and angles in degrees. The data was therefore converted into Cartesian coordinates keeping the inclination angle in mind. This gave a full detection score for the controlled site thus validating our method on the controlled site.

After validating the method on the controlled site, we moved further on the real sites. The data was acquired in December 2012 for a period of 3.5 hours with a total of 6874 vehicles including 30 PTWs. Two classifiers, SVM and KNN, were applied to the database. An encouraging result of 99% of correct classifications for all vehicles on RN338 (SUDIII) was obtained. For the A13, where traffic is heavier, 98.5% of the total vehicles were correctly classified. But at the same time there was nearly 1.0% of false alarms, caused by various factors such as refractions or reflection of laser rays.

For PTWs, on RN338, 28 PTWs out of 30 were correctly detected and classified. This gave a correct classification rate of 93%. However, the algorithm was used on a database with a higher percentage of PTWs on the A13, where the conditions are more challenging; all the PTWs were correctly detected and classified.

The reason for using only SVM on the data of the controlled site is that the database at the time of construction on this site was not big and SVM can be used begin such cases. This classifier helped us to validate our method on the controlled site, which encouraged us to move to the real site. On the real site a larger database was constructed, which gave us an opportunity to apply KNN as well on the laser scanner data.

- The system is capable of classifying several vehicles entering in the scene at the same time and is invariant to the direction of traffic.

What makes the proposed method different from the one proposed by [RIPO12]:

- [RIPO12] presented a general traffic counter and the focus was not put on the PTWs in traffic whereas our aim is to classify the PTWs in urban, suburban or motorways.
- The laser scanner of [RIPO12] is installed mast-mounted on a traffic light. The traffic lights helped to decrease the speed of vehicles present in the scene. The threshold to validate the presence of vehicles is a minimum of 20 scans whereas our method needs a minimum of 2 scans to validate the presence of a vehicle.
- [RIPO12] presented the problem of occlusion. This problem corresponds to a ‘combined vehicle’ effect but no solution is proposed to overcome the problem. We also encountered this problem [Figure 69]. Our method proposes a solution that is able to separate vehicles correctly to overcome the combined effect.
- Our system is able to find its height and road verges by itself just by knowing the number of lanes to be scanned.

All information were not specified in detail by [RIPO12] in order to reproduce the method and compare it with our in on the same database.

For a scan containing vehicle information, in order to pre-process and process on Matlab with a machine at 2.27 Ghz, our method takes an average of 36ms. As the time taken by the laser scanner for a scan is 20 ms, so the proposed method can work in real time with a slight delay if installed on a road.

For better efficiency of the system:

- It should be deployed on a single or double lane and not on three or more lanes.
- The system should be placed above the centre point of the two lanes to be scanned.

However, the program may fail when

- A PTW travels above 144km/h. A PTW that is 2m long and moving at 144 km/h (40m/s), will take 1/20 second to pass under the laser scanner. At 50Hz, the laser scanner will have just enough time for two scans i.e. to attain the threshold condition. This will lead the algorithm to successfully extract the vehicle present in the scene. However, the classifier may not be able to correctly classify the vehicle extracted due to lack of information.
- The climatic conditions are not ideal. It means that during rain, the process of reflections and refractions can be more easily seen and thus may confuse the algorithm.

## Conclusion and Perspectives

The safety of Powered Two Wheelers (PTWs) is an issue of concern for public authorities and road administrators around the world. In 2011, the official figures show that the PTW is estimated to represent only 2% of the total traffic, but represents 30% of the deaths on the roads in France [ONSIR11]. The ambiguity in values is due to the fact that the PTWs are particularly difficult to detect because of their unknown interactions with the other vehicles on the road. To date, there is no overall definite solution to this problem that uses a single sensor to detect and count this category of vehicle on a highway. Hence the project ANR METRAMOTO was launched. This project aims not only to detect PTWs in traffic but also to identify the trajectory of PTWs. This would help the road administrators to understand the behaviour and interaction of this category of vehicle with other road users.

In this applied and technical research work a single plane laser scanner was used to detect and count PTWs in traffic. Our research statement is: Detection and counting of PTWs in traffic using a single-plane scanner. In other words, a solution is needed that uses a single-laser scanner, has an affordable price and is robust to a maximum of artefacts such as climatic conditions etc. This research work is aimed to be integrated in the near future into a system that can be easily installed on a highway and can count PTWs in real time with a good autonomy.

During these three years (October 2010 till September 2013) of research work, the solution was attained by the following steps:

The state-of-the-art in the detection and counting of PTWs on the road was investigated, but very little research work was found in this domain. The existing solutions are either expensive to deploy on the road or are limited to certain traffic conditions. In Europe there are several recent projects that deal with PTW safety but none of the projects involve the detection and counting of PTWs. This shows the originality of the present research work, which has been carried out as follows:

A simulator has been developed to find how the laser scanner can be installed on the road so that the risk of occlusion is minimised. Installing a laser scanner on a real site in order to analyse different traffic scenes is not easy, but thanks to this simulator, different scenarios with different possible laser scanner positions are simulated to visualise the effects of occlusion, thus giving the road administrators an idea about the position to opt for before going to the site.

Once the position of the scanner was found, it was installed on the real site. It is important to understand the problems that can be encountered while installing the sensor on the road. The place where the laser scanner will be installed is not pre-defined. Hence no information, such as the height of the laser scanner, its exact position with respect to the gantry or pole on which it is installed; the profile of the road (inclination angle of the road, number of lanes, etc) can be known beforehand. Moreover, the laser scanner may also have an error of inclination due to human error while installing it.

To minimise these problems; a data coherence method is proposed. This means that once the laser scanner is installed on the road, it should be capable of finding its own height above the road and the verges of the road. The user only needs to place the system on the gantry at a given position and indicate the exact number of lanes to be scanned. Once these basic parameters are found, the method is able to automatically correct the transversal inclination error and eliminate a maximum number of artefacts.

A ‘fill’ filter is introduced in order to increase the quality of the data. This filter is able to adapt itself according to the nature of the missing values, which can be due to the vehicles with dark colours (Black) or due to high reflection (windshield).

An extraction method, called the Last Line Check (LLC) method, is applied to the rectified data. This method estimates the presence of the vehicle by verifying the presence of a height above the threshold value in the very last scan done. This variation is taken into consideration with the help of a threshold. Once noted, it is kept in memory along with the area where the change occurs. As soon as the value becomes normal (less than the threshold), the object is extracted.

Once the objects are extracted, they are classified using two different classifiers: a linear SVM and a KNN. For both classifiers, two different parameters were chosen; Width ( $W$ ) and ratio of the Height of vehicle ( $H\_Nb\%$ ) with respect to the number of points representing this value.

The scanned length of the vehicle was not taken into account as it depends on the speed of the vehicle and hence varies as the speed varies. Our basic goal is to single out the PTW from the traffic, and both of the classifiers gave an optimal result.

When compared with the corresponding Ground Truth (GT), the width values of the extracted vehicles showed an accuracy of 99%. This demonstrates the precision with which our method can calculate values.

The method was first employed and tested in real-time conditions in controlled traffic, which helped in the construction of the first learning database set where the traffic was limited (just one PTW moving under the scanner at different speeds). All the conditions created during the construction of this database were audited by Ms. Christina BURAGA of CETE Mediterranean. These conditions were all inspired from the real-time traffic seen in typical Parisian traffic.

The proposed method can achieve a correct detection rate of 99% for all vehicles in normal traffic on a real site where the traffic conditions are very random. This loss of 1% is due to the occlusion that occurred when an HV hides the LVs or PTWs to the sensor eye. This loss cannot be recovered by means of any sensor.

On 11<sup>th</sup> May 2012, this method was demonstrated in front of the public and road administrators, when it was able to correctly detect, classify and count the vehicles in quasi real time.

For future work, we need to:

- implement our method on a database with several PTWs (both two-wheelers and three-wheelers) in the same scene under the laser scanner. This would give us a very rich database and hence help to increase the number of detectable classes (PTW, mopeds etc).
- construct a richer database with significantly larger data base that has a high number of PTWs. At present, there are only a few PTWs in the database (SUDIII). For this reason the system was installed in Paris on the A13. The database is 6 minutes long and has 10% of the PTWs traffic in the total traffic. This higher number of PTWs in traffic helped us to validate the proposed method.
- test this method on the 3 week long database constructed on the A13 which contains many challenging traffic situations such as congested traffic, free flow traffic, traffic jam, accident scene, etc.



- test this method in different types of weather conditions (fog, rain, smog etc), as the laser reacts differently according to the density of water droplets , the size of the water droplets etc. [DAHL06][TOTH03][GEBH05][BENJ08]. This is a major aspect which needs an in-depth study on the behaviour of the laser in fog when the water droplets are uniformly distributed and in rain when the droplets may be of variable size and direction (wind). As the method is intended to be used in real-time traffic, it should be robust to all these weather conditions.
- use multi layered laser scanners to obtain a result robust to reflections. One example of such a laser scanner is the LMS SICK 5xx. With its higher angular frequency, the performance of the method can increase.
- use several planer laser scanner which could help to estimate the speed and acceleration of the PTW can be estimated. This parameter of estimated speed can be used to find an invariant length and hence can be used as parameter for classification, thus obtaining results with a better precision.
- compare the results with a 3D camera or a stereo camera. This comparison can help to determine the point at which the laser scanner becomes less efficient than a camera. This would help to fusion the technologies of the laser scanner and the camera in order to obtain a robust solution.
- add the notion of time delay in the temporal domain to the traffic in order to correctly detect all the trailers. To the laser scanner eye, trailers sometimes are separated by a gap from the vehicle. Adding a time delay, that is making the algorithm wait for a few more scans before extracting which may help to solve this problem.
- improve the LLC method by using the Temporal Occupancy Grids (TOGs). By defining the sensor model, the probability of finding an activity in the region of interest could be interesting. This method can equally be interesting to study the regions non-read (shadow or can also be called hidden space).





## List of Publications

### International conferences

Y.Prabhakar, P.Subirats, C.Lecomte, D.Vivet, E.Violette, A.Bensrhair, Detection and counting of Powered Two Wheelers by laser scanner in real time on urban expressway, IEEE Conference on Intelligent Transportation Systems (ITSC '13), Hague Netherlands, 6-9 October 2013.

Y.Prabhakar, P.Subirats, C.Lecomte, E.Violette, A.Bensrhair, A Lidar-Based Method for the Detection and Counting of Powered Two Wheelers ,IEEE Intelligent Vehicles Symposium (IV '13), Gold Coast Australia, Pages 1167-1172, 24-26 June 2013.

Y.Prabhakar, P.Subirats, C.Lecomte, A new method for the detection of motorbikes by laser rangefinder, IEEE International Conference on Communications and Signal Processing (ICCSP '11), Calicut India, Pages 246-249, 10-12 February 2011.

### National Conference

Y.Prabhakar, P.Subirats, C.Lecomte, E.Violette, A.Bensrhair, Détection des deux roues motorisés par télémétrie laser à balayage, GDR ONDES, Rennes, 27-28 Octobre 2010.

### International Journal

D. Vivet ; Y. Prabhakar ; P. Subirats ; C. Lecomte ; E. Violette ; A. Bensrhair, Laser-scanner-based powered two-wheeler traffic monitoring , Journal of Electronics Letters (EL'13), Volume 49, Issue 25, 05 December 2013, p. 1620 – 1622, 2013.



## ANNEX 1

Different types of laser scanners that exist in the market. Source: [w7]

Manufacturer		Software	Horizontal FOV	Min Range	Max Range	Distance Resolution	Scan Rate	Interface	Angular Resolution	Vertical FOV	Power	Voltage	Mass	Size	Tracking Targets	Sensor Fusion/Custom Options
	IIEO Automotive	Features: Long Range, Multi Echo, Embedded Object Tracking/Classification, Automotive quality, IP69K, Custom sensor, "Tusor" systems are available.														
		LUX 2010 Standard 4 Layer	110°	<0.3m	200m (90%)	4cm	11.5Hz	2.5Hz	Ethernet, CAN, RS232	up to 125°	3.2°	8w (Avg) <10w (Max)	9v-27v	approx 1kg	W164.5 x D93.2 x H88 mm	up to 64 objects
	IIEO Automotive	Features: Long Range, Multi Echo, Embedded Object Tracking/Classification, Automotive quality, IP69K, Custom sensor, "Tusor" systems are available.														
		Ibeo LUX HD	110°	<0.3m	90m (90%)	4cm	12.5Hz	2.5Hz	Ethernet, CAN, RS232	up to 125°	3.2°	8w (Avg) <10w (Max)	9v-27v	approx 1kg	W164.5 x D93.2 x H88 mm	up to 64 objects at 11.5Hz
	IIEO Automotive	Features: Long Range, Multi Echo, Embedded Object Tracking/Classification, Automotive quality, IP69K, Custom sensor, "Tusor" systems are available.														
		Ibeo LUX 8 Layer	110°	<0.3m	200m (90%)	4cm	6.25Hz	12.5Hz	Ethernet, CAN, RS232	up to 25°	6.4°	8w (Avg) <10w (Max)	9v-27v	approx 1kg	W164.5 x D93.2 x H88 mm	up to 64 objects at 6.25Hz (up to 4 layers only)
Automotive LIDAR coming soon!																
	Hokuyo	Features: Long Distance Laser Range Finder, Available for outdoor use because of 100,000lux for ambient illuminance and IP64 for protective structure.														
		UTM-30LX	Setup/Viewing Software	270°	0.1m	30m (90%) up to 60m	1.30m (+/-30mm) 10-30m +/-50mm	25ms scan speed	USB 2.0	0.25°	N/A	700mA	13v +/-10%	370g	W60 x D60 x H87mm	N/A
	Hokuyo	Features: Laser Range Finder, Multi-Echo Detection Ideal for outdoor applications. Performs well in rain, snow, mist, and dust. IP67														
		UTM-30LX-EW	Setup/Viewing Software	270°	0.1m	30m (90%) up to 60m	1.30m (+/-30mm) 10-30m +/-50mm	25ms scan speed	Ethernet	0.25°	N/A	700mA	12v +/-10%	370g	W62 x D62 x H87mm	N/A
	Hokuyo	Features: Laser Range Finder, Multi-Echo Detection Ideal for outdoor applications. Performs well in rain, snow, mist, and dust. IP67														
		UMX-30LX-EW	Setup/Viewing Software	190°	0.1m	30m (10%) up to 50m	1.30m +/-50mm 10-30m +/-100mm	50ms scan speed	Ethernet	0.25°	N/A	500mA	10v-30v	800g	W124 x D125.5 x H150mm	N/A
	Hokuyo	Features: Laser Range Finder, Compact and powerful environment detection sensor for intelligent robots. IP64														
		UHG-04LX	Setup/Viewing Software	270°	0.3m	11m (90%)	1.3m (+/-30mm) 1.8m (+/-3% of distance)	67ms scan speed	USB 2.0	0.36°	N/A	3.6w	12v +/-10%	500g	W83 x D83 x H86.4mm	N/A
	Hokuyo	Features: Compact Laser Range Finder, Low-power consumption (2.5W) for longer working hours. Optical Surface: IP64.														
		URG-04LX	Setup/Viewing Software	240°	0.2m	5.6m (90%)	6.1m (+/-30mm) 1.4m (+/-1% of distance)	100ms scan speed	USB 2.0	0.36°	N/A	2.5w	5v +/-5%	160g	W50 x D50 x H70mm	N/A
	Hokuyo	Features: "Simple URG-04LX" ideal solution for academic and R&D start-up applications. Compact Laser Range Finder, Low-power consumption (2.5W) for longer working hours. Optical Surface: IP64.														
		URG-04LX-U001	Setup/Viewing Software	240°	0.2m	5.6m (90%)	6.1m (+/-30mm) 1.4m (+/-3% of distance)	100ms scan speed	USB 2.0	0.36°	N/A	2.5w	5v +/-5%	160g	W50 x D50 x H70mm	N/A
	Hokuyo	Features: LED Obstacle Detection Sensor, Compact size. Used in Automated Guided Vehicle (AGV). 3 direction areas can be set by PC(RS-232C). Chargeover for Max. 15 kinds of detection area. IP64														
		PBS-03N	Setup/Viewing Software	180°	0.2m	3m	280ms or less scan speed	USB 2.0	1.8°	N/A	250ms or less	18v-30v	500g	W70 x D70 x H70mm	N/A	no
	Naptec	Features: OPAL-360SP Standard Performance. 15400mm, 360°, Long Range, Outdoor, IP67. Also available in many configurations including High Performance (OPAL-360HP) and Extreme Performance (OPAL-360EP).														
		OPAL 360-SP	360° System Manager with API	360°	0.3m	390m (120m) (90%)	contact us	30 revolutions per second	100 Mbps Ethernet, PS/2, RS-232	0.06°-300m (RS-232)	N/A	<120w	9v-32v	<50 lbs	61cm x 23cm x 36cm	N/A
	SICK	Features: Short Range, Indoor, 20m, IP65														
		SICK LMS100	SOPAS ET	270°	0.3m	20m (90%) 18m (10%)	+/- 12mm (+/-30mm)	≥ 20 ms	Ethernet, RS232	0.25°-0.5°	N/A	20w	10.8v-30v	1.1kg	105mm x 102mm x 162mm	N/A
	SICK	Features: Short Range, Outdoor, 20m, IP67														
		SICK LMS111	SOPAS ET	270°	0.5m	20m (90%) 18m (10%)	+/- 12mm (+/-30mm)	≥ 20 ms	Ethernet, RS232	0.25°-0.5°	N/A	60w	10.8v-30v	1.1kg	105mm x 102mm x 162mm	N/A
	SICK	Features: Short Range, Outdoor, 30m, IP67														
		SICK LMS151	SOPAS ET	270°	0.2m	50m (90%) 27.5m (10%)	+/- 12mm (+/-30mm)	≥ 20 ms	Ethernet, RS232	0.25°-0.5°	N/A	60w	10.8v-30v	1.1kg	105mm x 102mm x 162mm	N/A
	SICK	Features: Short Range, Indoor, 20m, IP65														
		SICK TMA310	SOPAS ET	270°	0.05m	4m (90%) 2m (10%)	+/- 30mm (+/-40mm)	Typ. 134 ms	micro USB	0.25°-0.5°	N/A	Typ. 3w	10v-28v	150g	60mm x 60mm x 79mm	N/A

**Figure 85: Different types of laser scanner in the market**



## Bibliography

- [ABDE01] Hossam M.Abdelbaki, Khaled Hussain and Erol Gelenbe, A Laser intensity image based automatic vehicle classification system, IEEE Intelligent Transportation System, Page 460-465, 2001.
- [ADEC12] ADEC Technologies, ADEC TDC3 Classification performance, Press release: Road traffic technology, 2012.
- [ALME05] A. Almeida, J. Almeida, and R. Araujo, "Real-time tracking of moving objects using particle filters, Pages 1327-1332, 2005.
- [ARRA07] Kai O.Arras, Oscar Martinez Mozos, Woldram Burgard, Using boosted features for the detection of people in 2D Range Data, IEEE Robotics and Automation, Pages 3402-3407, 2007.
- [AUPE11] S. Aupetit, Etudes des comportements spontanés de conduite des usagers de 2RM dans le trafic urbain et péri urbain, IFSTTAR, 2011.
- [AYCA11] O. Aycard, Q. Baig, S.Bota, F.Nashashibi, S.Nedevschi, C.Pantilie, M.Parent, P. Resende, Trung-Dung Vu, Intersection safety using lidar and stereovision sensors, IEEE Intelligent Vehicle Symposium, Pages 863-869, 2011.
- [BARG08] A Bargeton, F. Nashashibi, Laser-based vehicles tracking and classification using occlusion reasoning and confidence estimation, IEEE Intelligent Vehicle Symposium, Pages 847-852, 2008.
- [BEDK08] J. Bedkowski, M.Kretkiewicz, 3D laser range finder simulation based on rotated LMS SICK 200, RISE 2008
- [BENJ08] M. Benjamaa, C. Rozé, JL. Meyzonnette, C. Lavegne, Digital image computation of scenes during daytime fog, Journal Optical engineering Vol. 47, Pages 037401-1 : 037401-10, 2008.
- [BERG04] Flavien Bergonnier, Projet technique : Le télémètre Laser, 2004.
- [BORG04] G. A. Borges and M.-J. Aldon, Line extraction in 2D range images for mobile robotics, Journal of Intelligent and Robotic Systems: Theory and Applications, vol. 40, Pages 267-297, 2004.
- [BRUN07] X. Brun, JE. Deschaud and F. Goulette, On the way city mobile mapping using laser range scanner and fisheye camera, International Symposium on Mobile Mapping Technology, Pages 29-31, , Padoue Italy, 2007.
- [BURA13] C. BURAGA, P. SUBIRATS, Protocole d'évaluation des technologies de détection des deux roues motorisés, dans le cadre du projet Metramoto (MEsure du TRAfic des 2 roues MOTOrisés pour l'évaluation des risques et la mobilité) Congres ATEC, 2013.
- [CHAL97] J Chalidabhongse, Kuo, Fast motion vector estimation using multiresolution-spatio-temporal correlations, IEEE CirSysVideo, No.3, Pages 477-488. 1997.
- [CHEC08] Paul Checchin, Samuel Gidel, Christophe Blanc, Système de détection de piétons à bord de véhicules : approche par télémétrie laser, (Coloc Nationale de Recherche des IUT), CNRIUT 2008.

- [CHEU05] S. Cheung and C/ Kamath, Robust background subtraction with foreground validation for urban traffic video, *Journal on Applied Signal Processing*, Pages 2330–2340, 2005.
- [COIF10] H.Lee, B. Coifman, Side Fire LIDAR based Vehicle Classification, *Transportation Research Board*, 2010.
- [CONG10] Y Cong, Jun-jian Peng, Jing Sun, L Zhu, Y. Tang, V-disparity Based UGV Obstacle Detection in Rough Outdoor Terrain, *Journal Acta Automatica Sinica*, volume 36, Issue 6, Pages 667-673, 2010.
- [CONS06] K.Constantikes, Second generation laser rangefinder design and preliminary tests, *Precision Telescope Control System (PTCS) Project Note 48.1*, 2006.
- [COLV11] JT. Colvin, Path Planning Algorithms used in Autonomous Ground Vehicles with Visual Sensors for Dynamic Environments, *ADFA Journal of Undergraduate Engineering*, Final Project Report, Vol4, 2011.
- [CRAN06] C. D. Crane III, D. G. Armstrong II, R. Touchton, T. Galluzzo, S. Solanki, J. Lee, D. Kent, M. Ahmed, R. Montane, S. Ridgeway, S. Velat, G. Garcia, M. Griffis, S.Gray, J. Washburn, and G. Routson, "Field report: Team CIMAR's NaviGATOR: An unmanned ground vehicle for the 2005 DARPA Grand Challenge," *Journal of Field Robotics*, vol. 23, Pages 599-623, 2006.
- [DAHL06] H.Dahlkamp, A.Kaehler, D.Stavens, S.Thrun, and G.Bradski , Self-supervised Monocular Road Detection in desert terrain, *Journal of Robotics Sciences and Systems* , Vol 38, 2006.
- [DEME02] Daniel DeMenthon and Remi Megret, Spatio-temporal segmentation of video by hierarchical mean shift analysis, *Statistical Methods in Video Processing Workshop*, University of Maryland, 2002.
- [DIET01] Klaus C.J.Dietmayer, Jan Sparbert, Daniel Streller , Model based Object Classification and object Tracking in Traffic Scenes from Range Images, *IEEE IV*, Pages 2-1, 2001.
- [DIEW11] Fabien Diewald, Jens Klappstein, Frederik Sarholz, Juergen Dickmann and Klaus Dietmayer, Radar-interference-based bridge identification for collision avoidance systems, *IEEE Intelligent Vehicle Symposium*, Pages 113-118, 2011.
- [DIOS04] A. Diosi and L. Kleeman, Advanced sonar and laser range finder fusion for simultaneous localization and mapping, *Sendai, Japan*, Pages 1854-1859, 2004.
- [DOMI04] Antonio Domingues, Système embarqué multi-capteurs pour la détection d'obstacles routiers-Développement du prototype et réglage automatique de la chaîne de traitement d'images, *PhD Thesis-University of Orléans*, 2004.
- [DUCH12]. F. Duchon, M. Dekan, L. Jurisica, A. Vitko, Some Application of Laser Rangefinder in Mobile Robotics, *Journal of Controlled Engineering and Applied Informatics (CEAI)*, Vol. 14, Pages 50-55, 2012.
- [ERSO11] A report on European Road Safety Observatory (ERSO), 2011.

- [FAYA08] Fadi Fayad and Véronique Cherfaoui, Object-level fusion and confidence management in a multi-sensor pedestrian tracking system, *Multisensor Fusion and Integration for Intelligent Systems*, Pages 58-63, 2008.
- [FERN12-F] Christine Fernandez-Maloigne, Frédérique Robert-Inacio, Ludovic Macaire, *Couleur numérique: Acquisition, perception, codage et rendu*, Editions Hermès Science, Collection IC2, *Traité Signal et Image*, ISBN 2-7462-2555-7, June 2012.
- [FERN12-E] Christine Fernandez-Maloigne, Frédérique Robert-Inacio, Ludovic Macaire (Ed), *Acquisition and Coding of Digital Color*, Publisher : ISTE Ltd/John Wiley & Sons, ISBN 9781848213470, April 2012.
- [FLAM11] Remi Flamary, PhD report « Apprentissage statistique pour le signal », Laboratory Litis INSA Rouen, 2011.
- [FRAN05] J Franca, MA Gazziro, AN Ide. A 3D scanning system based on laser triangulation and variable field of view, *IEEE ICIP*, Pages 425-428, 2005.
- [FRER03] K.C. Frerstenberg, U. Lages, Pedestrian detection and classification by laser scanners, 9<sup>th</sup> European Engineers Cooperation International Congress, Paris 2003.
- [FURS00] K.Furstenberg, J.Hipp, A.Liebram, A laser scanner, for detailed traffic data collection and traffic control, *World congress on Intelligent Transport Systems*, Paper 2335, 2000.
- [FUER02] Kay Ch. Fuerstenberg , Multilayer Laserscanner for robust Object Tracking and Classification in Urban Traffic Scenes, 9th World Congress on Intelligent Transport Systems, ITS, Paper 2054, 2002.
- [FUMA11] Luca Fumagalli, Paolo Tomassini, Marco Zanatta, and Franco Docchio, A 400-kHz High-Accuracy Laser Telemeter for Distributed Measurements of 3-D Profiles, *Transactions on Instrumentation and Measurement*, Pages 1054-1060, 2011.
- [GATE08a] G. Gate and F. Nashashibi, Using Targets Appearance to improve pedestrian classification with a laser scanner, *Intelligent Vehicle Symposium*, Pages 1-6, Eindhoven June 2008.
- [GATE08b] G Gate and Fawzi Nashashibi, Targets Appearance to Improve Pedestrian Classification with a Laser scanner, *IEEE Intelligent Vehicle Symposium*, Page 571-576, Eindhoven, June 2008.
- [GEBH05] M.Gebhart, E.Leitgeb, S.Sheikh Muhammad, B.Flecker, C.Chlestil, Measurement of light attenuation in dense fog conditions for FSO applications, *SPIE*, Vol. 5891, Pages 58910K.1 – 58910K.11, 2005.
- [GEIG11] Andreas Geiger, Julius Ziegler and Christophe Stiller, StereoScan: Dense 3d Reconstruction in Real-time, *IEEE Intelligent Vehicle Symposium*, Pages 963-968, Kongresshaus Baden-Baden Germany, 2011.
- [GIBS10] David R.P. Gibson, Bo Ling, and Spandan Tiwari, Detecting Motorcyclists and Bicyclists at Intersections, *Journal of public roads*, May/June 2010 Vol. 73 · No. 6, 2010.



[GIDE08a] S. Gidel, P. Checchin, C. blanc, T. Chateau and L. Trassoudaine, Pedestrian Detection Method using a Multilayer Laser scanner: Application in Urban Environment, IEEE Intelligent Robots and Systems, Pages 173-178, 2008.

[GIDE08b] S. Gidel, P. Checchin, C. blanc, T. Chateau and L. Trassoudaine, Parzen method for fusion of laser scanner data: Application to pedestrian detection: Application in Urban Environment, IEEE Intelligent Vehicles Symposium, Pages 319-324, Eindhoven, 2008.

[GOUD11] D. Goudergues, Rapport classification des deux roues motorisés, CETE Méditerranée, 2011.

[GOUL06] F. Goulette , F. Nashashibi , I. Abuhadrous , S. Ammoun , C. Laugeau, An integrated on-board laser range sensing system for on-the-way city and road modelling, The International Archives of the Photogrammetry, Remote Sensing and Spatial Information Sciences, Vol. 34, 2006.

[GOYA08] Y.Goyat,T. Château, L. Malaterre and L. Trassoudaine, Estimation Précise de la Trajectoire d'un véhicule par Fusion Vision télémètre laser, 16e congrès francophone AFRIF-ARIA, Reconnaissance des Formes et Intelligence Artificielle, Amiens, 2008.

[GUYO08] Régis Guyot, Gisements de sécurité routière : les deux roues motorisés, ISBN : 978-2-11-006979-5, 2008.

[HERN09] Jorge Hernandez and Beatriz Marcotegui, Filtering of artifacts and pavement segmentation from mobile lidar data, F, Pierrot-Deseilligny M, Vosselman G (Eds) Laser scanning 2009, IAPRS, Vol. XXXVIII, Part 3, Pages 329-333, 2009.

[HIRA03] Kiyotaka Hirahara and Katsushi Ikeuchi ,Street-Parking Vehicle Detection from panoramic laser Range-Image, IEEE Intelligent Transportation Systems, Pages 41-48, 2003.

[HOFF86] R. Hoffman, A.K. Jain, Segmentation and classification of range data, computer vision and pattern recognition, Page 242-426, 1986.

[HOMM11] Florian Homm, Nico Kaempchen, Darius Burschka, Fusion of Laser scanner and Video Based Lane marking Detection for Robust Lateral Vehicle Control and Lane Change Maneuvers, IEEE Intelligent Vehicle Symposium, Pages 969 – 975, Kongresshaus Baden-Baden Germany, 2011.

[HONG01] T. Hong, R. Bostelman, and R. Madhavan, Obstacle Detection using a TOF Range Camera for Indoor AGV Navigation, PerMIS, 2004 .

[HOSS01] M. Abdelbaki Hossam, Khaled Hussain and Erol Gelende, A Laser Intensity Image Based Automatic Vehicle Classification System, IEEE ITS, Pages 460-465, 2001.

[IZRI04] Sonia Izri, Eric Brassart, Arnaud Cleretin, Détection de véhicules dans un environnement autoroutier à l'aide de données télémétriques et visuelles, International Journal on Info and com Sciences for Decision Making (ISDM), pages 12-22, 2004.

[JEAN13] Jean-philippe Roberge, Conception et intégration d'un capteur lidar 3D pour la navigation autonome des robots mobiles en terrain inconnu, Mémoire de master, Ecole polytechnique de Montréal, April 2013.

- [JOHN10] Nicholas Mckinley Johnson, simultaneous localization, mapping and object tracking in an urban environment using multiple 2d laser scanners, PhD. thesis, University of Florida, 2010.
- [KANH10] Neeraj K. Kanhere, Stanley T. Birchfield, Sara Khoeini, Traffic Monitoring of Motorcycles during Special Events Using Video Detection, Transportation Research Record: Journal of Transportation Research Board, Pages 69-76, 2010.
- [KAST11] Robert Kastner, Tobias Kuhn, Jannik Fritsch, Christian Goerick, Detection and motion estimation of moving objects based on 3D-Warping, IEEE Intelligent Vehicle Symposium, Pages 48-53, Kongresshaus Baden-Baden Germany, 2011.
- [KLUG01] B. Kluge, C. Kohler, and E. Prassler, Fast and robust tracking of multiple moving objects with a laser range finder, IEEE ICRA, Page 1683-1688, 2001.
- [KU08] Min-Yu Ku, Chung-Cheng Chiu, Hung-Tsung Chen and Shun-Huang Hong, Visual Motorcycle Detection and Tracking Algorithms, WSEAS transaction on Electronics, Page 121-131, 2008.
- [LABA05] R. Labayrade, C. Royere, D. Gruyer, and D. Aubert, Cooperative fusion for multi-obstacles detection with use of stereovision and laser scanner, Autonomous Robots, vol. 19, Pages 117-140, 2005.
- [LARA08] C. Lara, L. Romero, and F. Calderon, A robust iterative closest point algorithm with augmented features, Mexican International conference on Artificial intelligence, Pages 605-614, 2008.
- [LEE10] Yung-Chou Lee, Object tracking via the probability-based segmentation using Laser range images, Intelligent Vehicles Symposium, Page 197-202, San Diego, 2010.
- [LEFA02] Gildas Lefaix, Eric Marchand, Patrick Bouthemy, Motion based obstacle and tracking for car driving assistance, Page 74-77, International Conference on Pattern Recognition, 2002.
- [LEMONITEUR13] Journal Le moniteur, A Vancouver, Sanef exploite le plus grand péage sans barrière du monde, numéro 5701, Page 40, Edition march 2013.
- [LING12] Bo Ling, David Gibson, Standalone Motorcycle Detection and Counting System Using Microphone Array, Stereo and Infrared Cameras, Transportation Research Board, Washington DC, 2012.
- [LING13] Bo Ling, David Gibson and Dan Middleton, Motorcycle detection and counting using stereo camera, IR camera and microphone array, Proceedings of SPIE 8663, Video Surveillance and Transportation Imaging Applications, California, USA, March 2013.
- [LU97] F. Lu and E. Milios, Robot pose estimation in unknown environments by matching 2D range scans, Journal of Intelligent and Robotic Systems: Theory and Applications, vol. 18, Pages 249-275, 1997.
- [MA01] Yu-Fei Ma, Hong-Jiang Zhang, Detecting motion object by spatio-temporal entropy, IEEE International Conference on Multimedia and Expo (ICME), Pages 265-268, 2001.

- [MAAT93] K. Maata, J. Kostamovaara, R. Myllyla, Profiling of hot surfaces by pulsed time-of-flight laser range finder techniques, *Journal of applied optics*, Pages 5334-5347, 1993.
- [MACL06] R. A. MacLachlan and C. Mertz, Tracking of moving objects from a moving vehicle using a scanning laser rangefinder, Pages 301-306, 2006.
- [MANZ07] Antoine Manzanera, Julien Richefeu., A new motion detection algorithm based on  $\Sigma$ - $\Delta$  background estimation, *Journal Pattern Recognition Letters*, Volume 28, Issue 3, Pages 320-328, 2007.
- [MARQ94] Lino Marques, Fernando, Urbano Nunes and A. traca de Almeida, 3D Laser based Sensor for robotics, *IEEE Electrotechnical Conference*, Pages 1328-1348, 1994.
- [MATH12] T.V Mathew, Course Traffic Engineering and Management, Indian Institute of Bombay, 2012.
- [MEND04a] A. Mendes, L. C. Bento, and U. Nunes, Multi-target detection and tracking with a laser scanner, Pages 796-801, 2004.
- [MEND04b] Abel Mendes and Urbano Nunes, Situation-based Multi-target detection and tracking with laser scanner in outdoor semi-structured environment, *IEEE IROS*, Pages 88-93, 2004.
- [MIDD12] Dan Middleton and H. Charara, Improving the Quality of Motorcycle Travel Data Collection, *Transportation Research Board Conference*, Washington DC, 2012.
- [MING10] Erik Minge, Evaluation of Non-Intrusive Technologies for Traffic Detection, Report Minnesota department of transportation, 2010.
- [MONT06] Goncalo Monteiro, Cristiano Premebida, Paulo Peixoto and Urbano Nunes ,Tracking and Classification of Dynamic Obstacles using Laser Range Finder and Vision, *IROS Workshop*, Beijing China, 2006.
- [MONT07] Goncalo Monteiro, Cristiano Premebida, Paulo Peixoto and Urbano Nunes, A lidar and vision based Approach for pedestrian and vehicle detection and tracking, *ITSC*, Pages 1044-1049, Seattle Washington, 2007.
- [NEJA06] S M Nejad, S Olyaei, Comparison of TOF, FMCW and Phase Shift Laser Range Finding Methods by Simulation and Measurement, *Quarterly Journal of Technology & Education*, vol 1, Pages 11-18, 2006.
- [NIKI12] V.N. Nikias, V.lahogianni, E.I. Tzu-Chang Lee, Determinants of powered two-wheelers virtual lane width in urban arterials, *IEEE Intelligent Transportation Systems Conference*, Pages 1205 - 1210, 2012.
- [NIKN11] Hossein Tehrani niknejad, Koji Takahashi, Seiichi Mita, David McAllester, Embedded multi-sensors objects detection and tracking for urban autonomous driving, *IEEE Intelligent Vehicle Symposium*, Pages 1126-1133, Kongresshaus Baden-Baden Germany, 2011.
- [OHTA04] K Ohtani, M baba, A new laser rangefinder for measuring 3-D shapes of specular objects in a real environment, *IEEE SICE Vol. 2*, Pages 1223-1226, 2004.

- [OLIV86] J.L. Olivier, F. Ozguner, A navigation algorithm for an intelligent vehicle with a laser range finder, Pages 1145-1150, IEEE ICRA, 1986.
- [ONISR11] Sécurité routière – Chiffres clés: La mortalité routière en France, (Recueil statistique) Observatoire Nationale Interministérielle de Sécurité Routière (ONISR) 2011.
- [PAGO11] Vassillios Pagounis, Maria Tsakiri, Spiridon Palaskas, Barbara Biza and Elizabeth Zaloumi, 3D laser scanning for road safety and accident reconstruction, Engineering surveys for construction works 1, Page 15, 2006.
- [PAUN10] Chirag N. Paunwala and Suprava Patnaik, A Novel Multiple License Plate Extraction Technique for Complex Background in Indian Traffic Conditions, International Journal of Image Processing (IJIP) Volume 4, Issue 2, Page 106, 2010.
- [PFAF07] Patrick Pfaff, Christian Plagemann, and Wolfram Burgard, Improved Likelihood Models for Probabilistic Localization based on Range Scans, IEEE IROS, Pages 2192-2197, 2007.
- [PFEI07] N. Pfeifer and C.Briese, Laser scanning–principles and applications. 3<sup>rd</sup> International Exhibition & Scientific Congress on Geodesy, Mapping, Geology, Geophysics, Cadaster GEO-SIBERIA. 2007.
- [PFEI08] N. Pfeifer, B.Hofle, C.Briese, M.Rutzing and A. Haring, Analysis of the backscattered energy in terrestrial laser scanner data, The international archives of the photogrammetry, remote sensing and spatial information sciences, Pages 1045-1051, 2008.
- [PHAT09] Wiwat Phatanasrirat, Suebskul Phiphobmongkol, Motorcycle and License Plate Detection Using Fixed-Size Vertical Projection and Multi-Part Mean Analysis, IEEE International Conference on Computer Engineering and Technology, Pages 43-47, 2009.
- [PRAS00] E. Prassler, J. Scholz, and A. Elfes, Tracking multiple moving objects for realtime robot navigation, Autonomous Robots, Pages 105-116, 2000.
- [PREM05] C. Premebida and U. Nunes, Segmentation and geometric primitives extraction from 2D laser range data for mobile robot applications, Robotica- Scientific meeting of robotic festival, Coimbra, 2005.
- [REID95] I.D. Reid, J.M. Brady, Recognition of object classes from range data, Journal Artificial intelligence, Vol. 78, Pages 289-326, 1995.
- [RIPO12] Nieves Gallego Ripoll, Chapter 4: Laser scanner: eSafety and ITS Applications, book edited by J. Apolinar Munoz Rodriguez, ISBN 978-953-51-0280-9, March 28, 2012.
- [ROBE00] J. Roberts and P. Corke, Obstacle Detection for a Mining Vehicle using a 2D Laser , Australian Conference on Robotics and Automation, Pages 185-190, 2000.
- [SALO11] M. Salot and V. Cahill, A reliable membership service for vehicular safety applications, IEEE Intelligent Vehicle Symposium, Pages 1161-1167, 2011.
- [SCHA07] H. Schafer, M. Proetzsch, K. Berns, Obstacle detection in mobile outdoor robots - a short-term memory for the mobile outdoor platform raven. Proc. Inter. Conf. on Informatics in Control, Autom. and Robotics, Pages 141-148, 2007.

- [SCAR07] D. Scaramuzza, A. Harati, R. Siegwart, Extrinsic self calibration of a camera and a 3 D laser range finder from natural Scenes, IEEE IROS, Pages 4164-4169, San Diego California, 2007.
- [SCHI94] B. Schiele and J. L. Crowley, A comparison of position estimation techniques using occupancy grids, IEEE International Conference on Robotics and Automation, Pages 1628-1634, San Diego California, 1994.
- [SCHL11] Marc Schlopsing, Jakob Schepanek, Jan Salmen, Video-based roll angle estimation for two-wheeled vehicles, IEEE Intelligent Vehicle Symposium, Pages 876-881, Kongresshaus Baden-Baden, Germany, 2011.
- [SECK01] Andrew Secker and David Taubman, Motion-compensated highly scalable video compression using an adaptive 3-D wavelet transform based on lifting, IEEE Conference on Image Processing, Pages 1029-1032, Thessaloniki, Greece, 2001.
- [SETRA12] Draft rapport panorama capteurs systemes trafic, Service d'études sur les transports, les routes et leurs aménagements, 2012.
- [SIAD97] A. Siadat, A. Kaske, S. Klausmann, M. Dufaut, and R. Husson, An Optimized Segmentation Method For A 2D Laser-Scanner Applied To Mobile Robot Navigation, IFAC Symposium in Intelligent Components and Instruments for Control Applications, Pages 153-158, 1997.
- [SICK08] Data sheet, SICK Linear Measurement Systems 1xx, SICK AG- Division, site: [www.sick.com](http://www.sick.com), 2008.
- [SITH05] George Sithole, Segmentation and classification of airborne laser scanner data, PhD Thesis: Science integrated Geo-information and Map Production, ITC-Enschede, Netherland, 2005.
- [SPAR01] Jan Sparbert, Klaus Dietmayer, Daniel Streller, Lane detection and street type classification using laser range images, IEEE Intelligent Transportation Systems, Pages 454-459, Oakland California, 2001.
- [SPIN07] Luciano Spinello and Roland Siegwart, Unsupervised detection of artificial objects in outdoor environments, International conference of Field and Service Robotics (FSR) , Pages 401-410, Springer Berlin Heidelberg Germany, 2007.
- [STIL00] C. Stiller, J. Hipp, C. Rossig, and A. Ewald, Multisensor obstacle detection and tracking, Image and Vision Computing, Vol. 18, Pages 389-396, 2000.
- [STRE01] D. Streller, K. Dietmayer, J. Sparbert, Object Tracking in Traffic Scenes With Multi-Hypothesis Approach using Laser Range Images, IEEE Intelligent Transport Systems, Sydney, Australia, 2001.
- [STRE04] D. Streller and K. Dietmayer, Object tracking and classification using a multiple hypothesis Approach, IEEE ICRA, Pages 2424-2430, 2004.
- [SUBI09] P. Subirats and F. Rosey, La détection des 2RM: quels systèmes, quels outils? : Report CETE/CERTU, 2009.

- [SURM01] H. Surmann, K. Lingemann, A. Nuchter and J. Hertzberg, A 3D laser range finder for autonomous mobile robots, International Symposium on Robotics (ISR), Pages 153-158, Seoul, Korea, 2001.
- [TANA10] M.Tanaka, Development of traffic counters by laser range scanners, IEEE Annual Conference SICE, Pages 3128-3134, Taiwan, 2010.
- [TARE12] Jean-Philippe Tarel, Pierre Charbonnier, Francois Goulette , Jean-Emmanuel Deschaud, 3D Road Environment Modeling Applied to Visibility Mapping: An Experimental Comparison, IEEE/ACM 16th International Symposium on Distributed Simulation and Real Time Applications, Pages 19-26, Dublin Ireland, 2012.
- [TOTH03] C.K.Toth, A.Barsi, T Lovas, Vehicle recognition from Lidar data, International Archives of Photogrammetry and remote sensing, Vol. XXXIV, Pages 163-166, 2003.
- [TOTH07] Charles K.Toth and A. Grejner-Brzezinska, Vehicle classification from Lidar data to support traffic flow estimates, Advances in Mobile mapping technology, Pages 119-127, 2007.
- [TYPI08] Andrzej Typiak, Use of laser rangefinder to detecting in surroundings of mobile robot the obstacles, Symposium on automation and robotics in construction, Pages 246-251, Vilnius Lithuania, 2008.
- [VAND96] J. Vandorpe, H. Van Brussel, and H. Xu, Exact dynamic map building for a mobile robot using geometrical primitives produced by a 2D range finder, IEEE International Conference on Robotics and Automation, Pages 901-908, Minneapolis USA, 1996.
- [VAND10] A. Vandervalk, Counting motorcycles, Final report, Transportation Research Board, Washington DC, 2010.
- [VASC10] J.F. Vasconcelos, C. Silvestre, P. Oliveria and B. Guerreiro, Embedded UAV model and LASER aiding techniques for inertial navigation systems, Journal Control Engineering Practice, Pages 262-278, 2010.
- [VEIC11] A. Veichtbauer, P. Dorfinger and U. Schritterser, Live data acquisition for situation awareness in traffic management systems using laser sensors, International Conference on Sensor Technologies and Applications (Sensorcomm), Pages 268-273, 2011.
- [WANG94] John Y.A. Wang and Edward H. Adelson, Spatio-Temporal Segmentation of Video Data, SPIE: Image and Video Processing II, Vol. 2182, Pages 120-131, 1994.
- [WU96] Yong-Ge Wu, Jing-Yu Yang and Ke Liu, Obstacle detection and environment modeling based on multisensor fusion for robot navigation, Artificial intelligence in engineering, Vol. 10, Pages 323-333, 1996.
- [XAVI05] J. Xavier, M. Pacheco, D. Castro, A. Ruano and U. Nunes, Fast line, Arc/circle and a leg detection from laser scan data in a player driver, IEEE ICRA, Pages 3930-3935, Barcelona Spain, 2005.
- [XIAN01] Zhi-yu Xiang, Liu Ji-lin, Gu Wei-kang and Tian Yuan, Obstacle detection by ALV using two 2D laser range finders, Journal of Zhejiang University SCIENCE, Pages 388-394, 2001.



[YANO09] H. Yano, Y. Miyamoto and H. Iwata, Haptic Interface for Perceiving Remote Object Using a Laser Range Finder, EuroHaptics conference, 2009 and Symposium on Haptic Interfaces for Virtual Environment and Teleoperator Systems. World Haptics Conference, Pages 196-201, 2009.

[YGUE08] M. Yguel, O. Aycard and C. Laugier, Efficient GPU-based Construction of Occupancy Grids Using several Laser Range-finders, International Journal of Vehicle Autonomous Systems (IJVAS), Pages 48-83, 2008.

[YU08] Jin-Xia Yu, C. Zi-Xing, and D. Zhuo-Hua, Detection and tracking of moving object with a mobile robot using laser scanner, International Conference in Machine Learning and Cybernetics, Pages 1947-1952, Kunming China, 2008.

[YU10] Xin YU, Evaluation of Non-intrusive Sensors for Vehicle Classification on Freeways, International Symposium on Freeway and Toll way Operations, Honolulu Hawaii, 2010.

[ZHAN03] S. Zhang, M. Adams, F. Tang, and L. Xie, Geometrical Feature Extraction Using 2D Range Scanner, IEEE ICRA, Pages 901-905, Taipei Taiwan, 2003.

[ZHAO11] Yipu Zhao, Huijing Zhao, Jie Sha, and Hongbing Zha, Moving Object Trajectory Processing based on Multi-Laser Sensing, IEEE Intelligent Transportation Systems, Pages 550-558, Washington DC, 2011.

[w1] [blogs.wsj.com](http://blogs.wsj.com)

[w2] [www.sick.com](http://www.sick.com)

[w3] [www.its.com](http://www.its.com)

[w4] [www.projet-metramoto.fr](http://www.projet-metramoto.fr)

[w5] [www.sdelectronique.com](http://www.sdelectronique.com)

[w6] [www.lecia.com](http://www.lecia.com)

[w7] [www.autonomoustuff.com](http://www.autonomoustuff.com)

[w8] [www.scholarpedia.org/article/K-nearest\\_neighbor](http://www.scholarpedia.org/article/K-nearest_neighbor)









Présent  
pour  
l'avenir

CETE Normandie Centre  
IFSTTAR Equipe de Recherche Associée 34  
Accidentologie, Trajectographie et Risques routiers  
10, chemin de la Poudrière BP 90245  
76121 Le Grand-Quevilly cedex  
téléphone : 02 35 68 81 69  
télécopie 02 35 68 81 23  
[www.cete-normandie-centre.developpement-durable.gouv.fr](http://www.cete-normandie-centre.developpement-durable.gouv.fr)

